INVESTIGATING THE ROLE OF THE MAPK PROTEINS ERK1 AND ERK2 ON MAMMALIAN GAMETOGENESIS

A Dissertation

Presented to The Faculty of the Graduate School

of Cornell University

In Partial Fulfillment Of The Requirements For The Degree of

Doctor of Philosophy

By

Swapna Mohan

January 2014

INVESTIGATING THE ROLE OF THE MAPK PROTEINS ERK1 AND ERK2 ON MAMMALIAN GAMETOGENESIS

Swapna Mohan, PhD

Cornell University, 2014

Gametogenesis is one of the most important biological processes in the life of an organism because it results in the production of gametes, haploid cells that pass on the organism's genetic material to its offspring. However, it a very complicated, intricate process that demands a very high level of regulation. This regulation is to ensure error free meiotic and post-meiotic divisions resulting in a haploid gamete. Errors during the meiotic process can result in defective embryos or fetal demise. Among mammals, humans exhibit a very high rate of gamete defects (~25%) leading to high rates of early embryo loss.

Stage-specific cell signaling cascades such as the MAPK pathway regulate meiosis and germ-cell development. In addition to this, MAPKs specifically ERKs, are thought to be involved in cellular division, cytoskeletal reorganization and segregation of genetic material. So far pharmacological approaches have been used to study the action of ERKs in oocytes *in vitro* using inhibitors of the ERK pathway. However, these are not truly reflective of the physiological environment of the ovary. Hence, in order to better understand the mechanism of action of ERKs

on oocyte division, I have generated an *Erk2* conditional deletion system driven by an oocyte specific Cre on an *Erk1* null background. I hypothesized that deregulation of the MAPK pathway in oocytes will produce drastic changes in the cytokinesis and in chromosome segregation.

Mutant females were found to be infertile, with gross chromosome misalignment on metaphase spindles in oocytes, and severe early embryonic loss. This phenotype was accompanied by loss of phosphorylation of several downstream targets such as MSK1 and histone H3. Several possible new targets have also been identified in this study by comparing phosphrylation profiles of oocytes from various genotypes. Our results demonstrate that ERK activity specifically within the oocyte is essential for meiotic resumption and for normal pre-implantation development.

BIOGRAPHICAL SKETCH

Swapna Mohan was born on April 2nd 1980, to Dr Sarad Mohan and Mrs Sathi Mohan in Kerala, India. She grew up in New Delhi where she and her sister Sandhya spent happy childhood years exploring the local flora and fauna of the NISTADS (National Institute of Sc. Tech and Devt Studies) campus. After graduating from DTEA (Delhi Tamil Education Association) Senior Secondary School, Swapna joined the BSc program in Botanical Sciences at Miranda House, Delhi University. However, in her second year there, she was accepted into the College of Veterinary and Animal Sciences, Kerala for Bachelors in Veterinary Sciences (BVSc and AH). So, in 1998 she moved to Kerala where she spent the next six years studying veterinary medicine. It was here that she met her future best friend, Jackin Jayaram. After her BVSc she moved to the USA where she completed a Masters in Biology from Indiana State University studying the sleep waves of the North American bat population. She then worked at University of Pennsylvania for a year under the direction of Dr Ina Dobrinski, where she studies germ cell biology and transgenesis in porcines. In 2009 Swapna joined the Molecular and Integrative Physiology graduate program at Cornell University, College of Veterinary Medicine, in the lab of Dr Paula Cohen. For her PhD reseach, she has been studying the role of MAPK pathway in gametogenesis. Upon completion of her dissertation in January 2014, she plans to continue a career as a researcher in the field of mammalian reproductive biology.

DEDICATION

I would like to dedicate this work to my dearest ammamma, Anandavalliamma. I hope that this work makes you proud.

ACKNOWLEDGEMENTS

Completing my PhD was possibly one of the biggest challenges of my life and I would like to thank all the people whose support helped me achieve this goal.

My first note of gratitude must go to my advisors, Dr Paula Cohen and Dr Mark Roberson, whose patient encouragement and invaluable guidance made this work possible.

Special thanks to my committee Dr Scott Coonrod, Dr Pat Johnson and Dr Teresa Southard for their guidance, support and advice. I would like to express my heartfelt appreciation to them.

My sincerest thanks to current and past members of the Cohen lab, Dr Kim Holloway, Dr Andrew Modzelewski, Dr Xianfei Sun, Kadeine Peterson, Melissa Toledo and Peter Borst for their friendship and support all these years. From the Roberson lab I would like to thank Rachel Preston and Dr Jianjun Xie for all their help. I could not have asked for better colleagues and friends.

I would like to acknowledge the help extended by the various facilities at Cornell University: Dr Sheng Zhang and James McArdle at the Proteomics facility, Pat Fischer and Dr Lynn Dong at the Immunopathology Research and Development Core Laboratory, and all the wonderful staff at the ECRF animal facility.

I wish to thank my parents Dr Sarad Mohan, Mrs Sathi Mohan and my sister Sandhya Mohan for always believing in me. I would not have come this far in life if it hadn't been for you. And finally, I would like to thank my husband, Dr Jackin Jayaram without whose unconditional support and encouragement I would not even be in a PhD program, much less graduating from an ivy-league one. Thank you for being with me and helping me see light at the end of the tunnel.

TABLE OF CONTENTS

LIST OF FIGURES

LIST OF TABLES

CHAPTER 1

Germ cell development and gene networks

This work has been published as Chapter 3. Gene Networks in Oocyte Meiosis. In Alan Trounson, Roger Gosden, Ursula Eichenlaub-Ritter (2013) Biology and Pathology of the Oocyte: Role in Fertility, Medicine and Nuclear Reprogramming. 2nd Edition. Cambridge University Press. Sections marked with * are not included in the original book chapter.

1. Abstract

In the current era of the genome, the amount of information available about gene expression, protein products, their interactions and pathways in almost any physiological system has become quite overwhelming. The processes of mammalian meiosis and oocyte development are no exception. Most of these data have been generated using high throughput genomic and proteomic screening systems. However, various experimental approaches over several decades, such as targeted mutagenesis, modification/suppression of specific genes both *in vivo* and *in vitro*, have also contributed greatly to our understanding of the genetic basis for meiotic processes and oogenesis (Martin and Drubin 2003). Such studies have also been greatly enhanced using comparative analyses of these processes across the animal kingdom, allowing us to identify key genetic pathways that are functionally conserved in germ cells. With all the available

information from multiple online databases, gaining an understanding of a complex process like meiosis, that spans several years and involves numerous cellular pathways, is challenging. It is especially difficult when trying to obtain a view that encompasses both the cellular events of meiosis, yet also puts these processes in the context of the overall physiology and systems biology of the ovary. Representation of biological interactions within the cell in terms of gene networks provides an accurate and explanatory basis for studying cellular events. In addition, creating gene networks, by its very nature, helps us to define common processes amongst many different species, allowing us to appreciate both the similarities and the differences in these processes across the animal kingdom. At the same time, we can identify commonalities among cellular processes in terms of the networks that they utilize.

2. Introduction to gene networks

Gene networks are defined as graphs showing multiple genes as intersection points of lines that represent the interaction between these points (Rapaport, Zinovyev et al. 2007). These can represent direct gene product interactions, such as protein-protein interactions, or indirect interactions corresponding to successive steps of a metabolic pathway (Table 1). Interactions can also arise between genes themselves causing an up-regulation or suppression of activity (protein-DNA interaction). These interactions can be useful in predicting changes in expression patterns

and/ or change in metabolic pathways of other genes that are closer in the network to the gene of interest. This is extremely useful in creating a detailed biological model of cell-cell interactions, pathways and roles of genes in specific cellular pathways within a tissue without having to determine the action of each individual gene one-by-one (D'Haeseleer 2005). Networks can also be used to predict the function of previously unknown genes if they are identified to be a part of known gene clusters with high-confidence interconnections (Cohen and Holloway 2010).

A gene network is created by integrating many different criteria such as temporal gene expression, physical interaction of products, protein domains, comparative expression patterns in taxonomically close organisms (phylogeny), contribution to similar pathology and participation in connected biological processes (gene ontology) (Cohen and Holloway 2010). Some of these criteria are obtained by wet-bench experimentation (expression profiles etc.), while others can be obtained *in silico* (by computational means: gene similarities, common functional motifs etc.). Many databases are becoming available for collating such data across large gene sets, often linked to the genome browser sites (Table 2). Collectively, all these features are assigned quantitative values and their combined measurement gives an idea of the strength of functional association of a group of genes. Such data sets are then analyzed by different methods like cluster analysis, correlation analysis and analysis of mutual information (Hallinan, James et al.

2011). The resulting data is then used as a resource to highlight groups of genes over-represented in a particular cell type at specific times and subsequently to understand the mechanisms driving the development and function of that cell type/ tissue.

Table 1.1. Common interactions in a network

Physical interactions	
Interaction type	Example
• Between components found in the same cellular compartment	Membrane fusion proteins and cargo binding proteins in secretory vesicles
• Part of the same macromolecular structure	Structural proteins forming the meiotic spindle
• Produced at about the same time in the cell cycle	Proteins required for gap junction closure in cumulus-oocyte complex and proteins for phosphodiesterase activity in the oocyte

Functional interactions	
Interaction type	Example
• Found in the same cellular pathway	DNA repair proteins
• Genetic interactions	Proteins involved in of the epigenetic reprogramming oocyte during development
• Producing similar tissue expression patterns (in analogous processes across cell types or between species)	Retinoic acid response elements expression in testicular tissue

• Taking part in the same functional process	Chemotactic proteins and extracellular matrix proteins both regulating germ cell migration

Table 1.2: More commonly used databases for observing biological themes in expression patterns

Database	Description
Gene ontology http://www.geneontology.org/	Gene and gene product functions across species at biological, cellular and molecular levels
NCBI Gene Entrez http://www.ncbi.nlm.nih.gov/gene	Gene and protein sequences, structures, chromosome maps, references
Kyoto Encyclopdia of Genes and Genomes(KEGG) http://www.genome.jp/kegg/	Genomes, biological pathways, molecular interactions, diseases and drug development
OMIM http://www.ncbi.nlm.nih.gov/omim	Catalog of human diseases with known genetic components
UniProt database http://www.uniprot.org/	Protein function, cellular localization, interactions, expression patterns, domains

3. Germ cell development

The formation of germ cells and their commitment to either one of two sex-specific developmental pathways (oogenesis or spermatogenesis) occurs during fetal life in mammalian species. In the mouse and human, cells in the germ cell lineage arise from the epiblast region of the embryo, closest to the extra-embryonic ectoderm (Acevedo and Smith 2005). These cells acquire the competence to form primordial germ cells (PGCs) but only a subset of them actually go on to become PGCs (Ewen and Koopman 2010).

3.1 Competence to form PGCs

Competence to enter the PGC specification pathway occurs under the influence of factors such as BMP4 and BMP8b, which are expressed by cells of the surrounding extra-embryonic ectoderm (Amleh and Dean 2002; Acevedo and Smith 2005). These factors induce the expression of genes in the Fragilis family, such as *Ifitm3* (*Fragilis*), *Ifitm1*(*Fragilis2*) and *Ifitm2*(*Fragilis3*) in the PGC precursor cells, which may play a role in germ cell adhesion and specification (Ewen and Koopman 2010). A subset of the PGC precursor cells also begin expression of *Blimp1* (*Prdm1*). It is these cells specifically, that are destined for the PGC fate (Hayashi, de Sousa Lopes et al. 2007). BLIMP1 is a key factor in regulating PGC specification of cells characterized by the

repression of somatic genes and upregulation of germ cell specific genes like *Prdm14, Ssea1, Tnap* and *Tiar*.

Ifitm3 is responsible for the production of Fragilis protein in the mouse, which then induces the expression of a germ-cell specific gene *Stella*(*Dppa3*) that is involved in chromosome organization and RNA processing and allows the PGCs to retain pluripotency (Hayashi, de Sousa Lopes et al. 2007). Retention of pluripotency in the PGCs is accompanied by the expression of stem cell-associated markers including *Nanog, Oct4* and *Sox2*, which are initially seen only in the very early embryo, and which are then re-expressed in the mouse PGCs by Embryonic day 7.25 (E7.25) (Hayashi, de Sousa Lopes et al. 2007). However, transcripts of *Oct4* have been detected in the mouse epiblast as early as E6.5. *Oct4*, in addition to maintaining pluripotency, is needed for the survival of the PGCs, which may explain its relatively early expression (Oktem and Urman 2010). In addition to this *Blimp1* and *Smad1* expression has been implicated in suppression of genes required for setting up somatic cell lineage like *Hoxb*, *Fgf8* and *Snail* (Combes A 2010).

3.2 Migration and colonization of the fetal gonad

The PGCs migrate from the extra-embryonic mesoderm to the urogenital ridge of the embryo at E10 in mice and about third week of gestation in humans (Amleh and Dean 2002). This

migration is mediated by the interaction between c-kit, a tyrosine kinase receptor located on the surface of PGCs and its ligand, KitL, located on the somatic cells along the migratory pathway. The expression of *c-kit/W* in the PGCs and *Kitl* in the somatic cells therefore, is high at this time (Zheng and Dean 2007) as are several somatic cell signals necessary to regulate PGC motility like SDF1 and PECAM1 (Ewen and Koopman 2010). At the same time, the PGCs themselves express a variety of genes, including *Mvh*, *Dnd, Dazl1* and *Nanos3,* all of which assist in maintaining germ cell lineage during this migration (Oktem and Urman 2010; Wang, Kou et al. 2010).

After migration to, and colonization of, the genital ridges, new interactions with the surrounding somatic cells of the indifferent gonad induces expression of genes in the germ cells encoding adhesion molecules (ADAM family) (Combes A 2010). The PGCs proliferate rapidly under the influence of several proliferation signals from genes such as *Cxcr4, Pin1, Ssea1, Wt1, Nanos3* and LIF receptor (Ewen and Koopman 2010; Rolland, Lehmann et al. 2011). Surrounding somatic cells also initiate several paracrine mechanisms with factors such as TNFa, SDF1 FGF2, FGF4 and FGF8 to ensure the survival and proliferation of the PGCs in their new environment (Ewen and Koopman 2010). Expression of some germ cell markers decreases (*Tnap, Prdm1, Ssea1*) at this time, accompanied by a reduction in ability to form pluripotent stem cells, at least

in culture (Combes A 2010; Rolland, Lehmann et al. 2011). Concomitantly, expression analysis on fetal gonads in mice (E11-18) shows higher expression of a group of 37 genes, which include known pluripotency markers like *Dppa2, Nanog, Oct4* and *Sox2*, along with other genes that regulate meiotic entry and germ cell differentiation, including *Ddx4, Gcna1, Dazl* and *Gcl* (Rolland, Lehmann et al. 2011). These expression changes are accompanied by widespread epigenetic reprogramming in the form of genome demethylation and chromatin remodeling (Rolland, Lehmann et al. 2011), with some hundred or so genes undergoing this type of imprinting in the females. At this time the non-germ cell populations in the gonad have bipotential, having the ability to develop into Sertoli or granulosa cells (Combes A 2010).

The germ cells colonizing the female gonadal ridges (now known as the oogonia at around E9.5) are initially present as cell clusters connected by cytoplasmic bridges, which after complete cytokinesis become surrounded by pre-granulosa cells, thereby forming the first primordial follicles. *Figα* expression in the oogonia is shown to be required for this process (Combes A 2010). Gene network analysis of mouse oogonia showed overexpression of some 500 or so genes. GO annotation analysis revealed their involvement in biological processes such as germ cell development, DNA methylation, ovarian follicle development and meiosis (Rolland, Lehmann et al. 2011).

4. Sex determination

Mouse fetal gonads at E12 start showing sexual dimorphism, which is initiated by the somatic cell environment of the germ cells. Sexual differentiation of the somatic component of the gonad is followed by differentiation of the germ cells, which involves an upregulation of several genes in both the male and female gonad. About 250 of these genes are germ cell specific while close to 1700 genes are in the somatic cells. Of these genes, female bias is shown by group containing *Bmp2, Fst* and *Wnt4* genes whereas *Sox9, Amh* and *Cyp26b1* showed male-biased expression. After E12 some 60 genes have been shown to have female specific expression. Some of these are meiosis specific genes like *Dmc1* and *Spo11* indicating the achievement of meiotic competence in female germ cells immediately after colonizing the gonads (Combes A 2010). Furthermore, this same group of genes was highly expressed in post-natal testis only at the beginning of spermatogenesis although both XX and XY germ cells have been shown to be meiotically competent in culture at this stage (Combes A 2010; Rolland, Lehmann et al. 2011).

Figure 1.1. Genes expressed for primordial germ cell (PGC) development in the mouse

Gene names above the dotted line are expressed in the germ cell and below the dotted line are observed in the somatic cell population. Germ cell specification begins in the extra embryonic ectoderm when cells in the proximal epiblast acquire competence to form PGCs (PGC precursor cells). A subset of these cells then goes on to have PGC fate later on in development. Both these steps of specification are the effect of paracrine signals from the surrounding cells of the extra-embryonic ectoderm such as proteins from TGFβ, BMP and SMAD families. These signals induce the expression of genes involved in the germline fate allocation of the cells expressing them. Simultaneously, the PGCs also express genes required for maintaining the pluripotency potential and for suppression of a somatic cell fate. The next step in PGC development is their migration from the specification site along the hindgut through the dorsal mesentery to the genital ridges on either side. This process is mediated by somatic cell- derived signals for motility such as Kit-Ligand factor (encoded by *Steel*) and signals for chemotaxis such as SDF1 (encoded by *Sdf1*) and adhesion molecules such as those of the ADAM family. Colonization of the genital ridges is mediated by the expression of germ cell specific factors (Gcna1, Ddx4), which is followed by epigenetic reprogramming (Blimp1, Prmt5) which sends the germ cells to a fate of meiotic competence. The timescale is as per embryonic development in the female mouse.

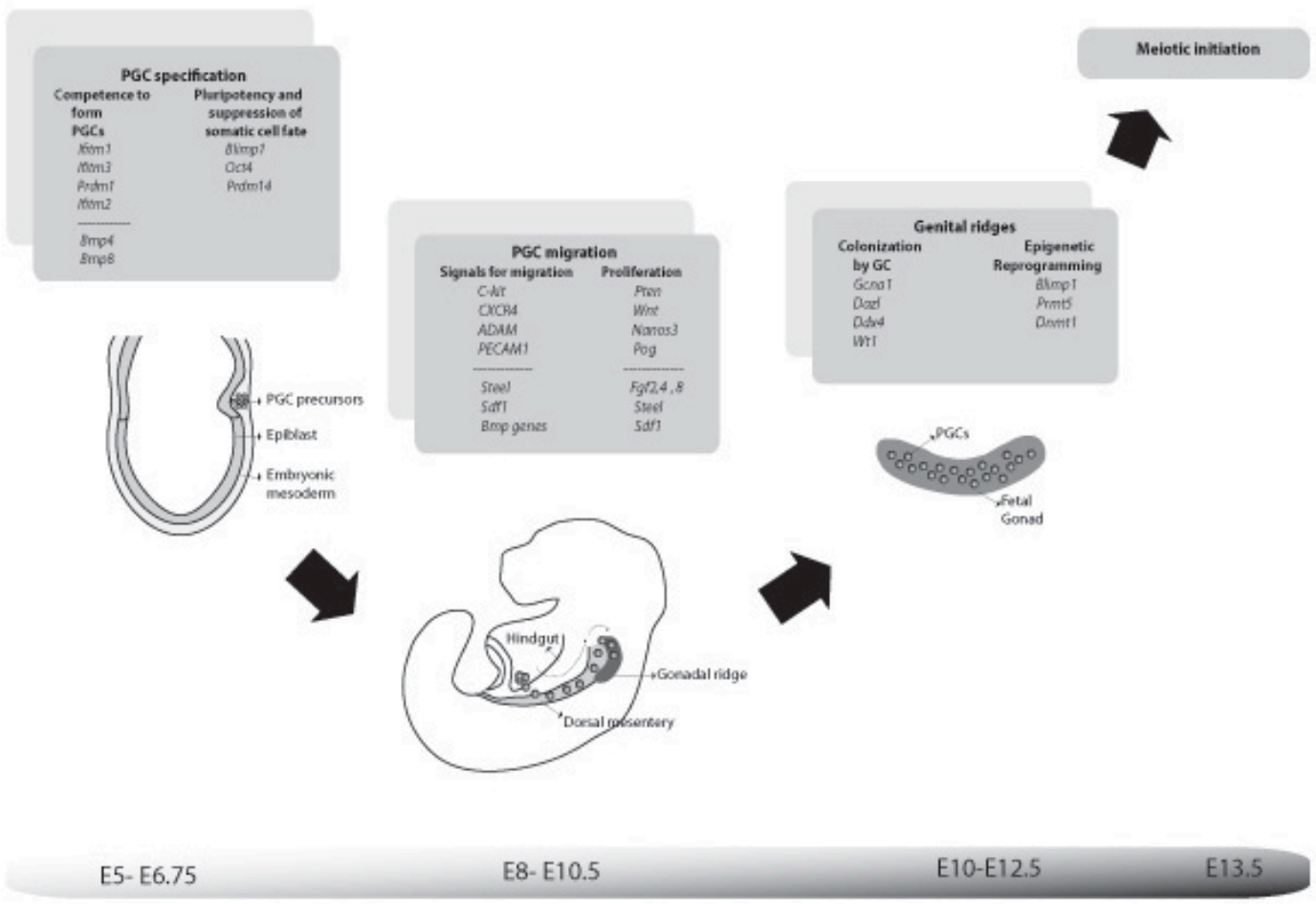
PGC specification
Competence to form PGCs
Pluripotency and suppression of somatic cell fate
Mitm1
Mtm3
Prdm1
Mtm2
Blimp1
Oct4
Prdm14
Bmp4
Bmp8
PGC migration
Signals for migration
Proliferation
C-kit
CXCR4
ADAM
PECAM1
Pten
Wnt
Nanos3
Pog
Steel
Sdf1
Bmp genes
Fgf2,4 ,8
Steel
Sdf1
Genital ridges
Colonization by GC
Epigenetic Reprogramming
Gcna1
Dazl
Ddx4
Wt1
Blimp1
Prmt5
Dnmt1
Meiotic initiation
PGC precursors
Epiblast
Embryonic mesoderm
Hindgut
Gonadal ridge
Dorsal mesentery
PGCs
Fetal Gonad
E5- E6.75
E8- E10.5
E10-E12.5
E13.5

5. Entry into, and progression through, Meiotic prophase I during fetal life

5.1 Entry into the meiotic pathway

In female embryos, entry into meiosis is marked by, and dependent on, up-regulation of retinoic acid (RA) response genes, including *Stra8* (Combes A 2010), while PGCs from male embryos express genes that are required for RA degradation, thus preventing meiotic entry at this time (Koubova, Menke et al. 2006). In females, germ cells at this stage are called primary oocytes. *Stra8* expression is required for pre-meiotic DNA replication, chromosome condensation and occurs at E12-13 in mice and 8-13 weeks of gestation in humans (Combes A 2010). At the same time, the RNA binding factor, *Dazl*, is also expressed, and this appears to be essential for germ cell specification of sexual fate in both males and females (Gill, Hu et al. 2011). *Dazl* expression is co-incident with expression of at least 13 other genes, including some that code for translation factors (*Eif3g, Eif4b, Eif4h*), and other RNA binding proteins (*Igf2bp1, Cpeb2*) (Zheng, Griswold et al. 2010), collectively suggesting a requirement for RNA involvement and/or control of translation in germ cell specification. Here, once again, gene ontology can provide vital clues as to the functional requirements for a given process.

RA is a metabolite of vitamin A, and is essential for the development of several tissues in the embryo (Griswold, Hogarth et al. 2012). RA is synthesized by the oxidative metabolism of

Retinol by retinaldehyde dehydrogenases. It acts through two nuclear receptors, RAR (Retinoic acid Receptor) and RXR (Retinoic X Receptor) to activate RA response elements (RARE) in target genes to modulate their transcriptional activity (Combes A 2010; Griswold, Hogarth et al. 2012). RA is degraded by enzymes in the cytochrome p-450 family (CYP26A1, CYP26B1, CYP26C1), which help to regulate RA levels within a tissue (Combes A 2010). One of the main gene targets of RA within the gonad is *Stra8*, which is expressed in the mouse fetal ovary as early as E12.5 whereas its expression in the testis is delayed until 10 dpp (10 days post-partum). Up until that time, endogenous RA is constantly degraded in the testis by CYP26B1 (Combes A 2010). Studies performed on embryonic mouse gonads show that both exogenous and endogenous RAs as well as several RARs (RARα, RARβ, RARγ) can induce *Stra8* expression in Vitamin A deficient mice, indicating the role of RA in regulating *Stra8* function (Koubova, Menke et al. 2006; Griswold, Hogarth et al. 2012).

Stra8 is upstream of pre-meiotic DNA replication, and analysis of *Stra8* null mice demonstrates its requirement in meiotic initiation during both spermatogenesis and oogenesis (Anderson, Baltus et al. 2008). However *Stra8* is only one of the genes in the transcriptome profile of RA response genes in mouse gonads. While this list contains genes known to be involved in meiosis, such as *Slc25a31*, *Tex15* and *Rad51*, other genes with as yet unknown functions in meiosis

(*Esco2*, *Setdb2*, *Uba6*) have been found to be highly up-regulated directly or indirectly in response to RA (Hogarth, Mitchell et al. 2011). ESCO2 is involved in sister chromatid cohesion, whereas SETDB2 and another SET family protein SUV39H2 have been implicated in chromatin remodeling in germ cells (Hogarth, Mitchell et al. 2011). UBA6 is a protein in the ubiquitylation pathway (Hogarth, Mitchell et al. 2011). These genes have been implicated in meiotic initiation only in the male germ cells so far and their functions in females are yet to be identified. However their presence downstream of RA in males, together with the timing of expression would, in predictive network analysis, make them solid candidates for oocyte RA responses too.

There appears to be some crosstalk between the RA response pathway and other pathways for meiotic initiation. Homeobox transcription factors *Msx1* and *Msx2* can be up-regulated by RA, as well as Bone Morphogenic Proteins BMP4 and BMP2, have been shown to regulate *Stra8* expression in mouse fetal ovary, but not the testis (Le Bouffant, Souquet et al. 2011). The DM domain gene *Dmrt1* known to be required for testicular differentiation is required for transcriptional activation of *Stra8* in the mouse fetal ovary, however, the process maybe independent of RA (Krentz, Murphy et al. 2011).

5.2 Initiation of meiosis and Prophase I

Meiosis initiates soon after DNA replication, with entry into prophase I. Prophase I is subdivided into five stages – Leptonema, Zygonema, Pachynema, Diplonema and Diakinesis. Prophase I encompasses all the defining features of meiosis, namely the pairing and physical association (or synapsis) of homologous chromosomes, formation of the synaptonemal complex and the initiation of recombination events between them (crossing over). In the perinatal female mouse, oocytes then enter a prolonged diakinesis state known as dictyate arrest, in which meiosis I halts, only to resume following puberty in response to the LH surge that triggers ovulation (Morelli and Cohen 2005; Handel and Schimenti 2010). The synaptonemal complex (SC), the most characteristic feature of prophase I, is a tripartite proteinaceous structure that binds homologous chromosomes together to aid recombination events between them (Handel and Schimenti 2010).

Prophase I begins with chromosomes searching for their homologous partner based on DNA sequence homology (Li and Ma 2006). While it is thought that synapsis of homologous chromosomes is brought about by formation of single strand overhangs that then find the homology sequence in the partner chromosome, it is believed that a physical congregation of chromosomes into a structure known as the "*telomere bouquet*", and the attachment of their telomeres to the nuclear envelope facilitates the initial alignment of homologous chromosomes

with each other (Handel and Schimenti 2010). In mammals, *Unc84a*/*Sun1* expression is believed to play a role in the formation of these telomeric clusters at the nuclear envelope, while other organisms express genes that are orthologous to these SUN/KASH domain genes (Hiraoka and Dernburg 2009).

The initial localization of synaptonemal complex proteins SYCP2 and SYCP3 to form axial elements of the SC also serves in bringing homologous chromosomes closer with their interactions (Handel and Schimenti 2010). These associations culminate in synapsis, where the two homologous chromosomes are physically held together along their entire lengths by means of the central element. The SC components assemble sequentially, starting with the axial elements, which form foci along each homologue, and these foci then coalesce to form a filament that eventually spans the entire length of the chromosome, with DNA loops extending perpendicularly from the core. The foci of axial elements are formed by grouping of SC specific proteins like SYCP2 and SYCP3. Cohesion proteins like SMC1B, REC8 and STAG3 localize to the axial elements and are believed to play a structural role in the assembly of the axial element (Handel and Schimenti 2010). Once pairing is established and confirmed, the central element then assembles, with appropriate density of DSB-induced DNA-DNA interactions between homologs. The central element of the SC is formed by SYCP1, SYCE1, SYCE2 and TEX12

which are also meiosis specific (Handel and Schimenti 2010). HORMAD1 and HORMAD2 are present in unsynapsed regions of axial element and may play a role in regulation of homolog interactions and synapsis (Handel and Schimenti 2010; Santucci-Darmanin 2010).

5.3 Meiotic recombination

Homolog pairing occurs around the same time as the formation of the double strand breaks (DSBs) that are of the precursors for meiotic recombination and which, in mammals at least, precede the process of synapsis (the physical tethering of paired homologous chromosomes). Recombination between homologs in a chromosome pair is under the control of several serially expressed genes responsible for specific events in the recombination pathway and, in its simplest form, represents a highly regulated DNA repair process involving many components of the DNA damage repair (DDR) machinery. Not surprisingly, therefore, genes that participate in DDR events are all expressed at high levels during prophase I, and many share overlapping functions with canonical repair events in somatic cells.

DSB formation is catalyzed by the highly conserved topoisomerase SPO11 (Santucci-Darmanin 2010). A SPO11 dimer creates DSBs in the two strands of DNA and each monomer then attaches

to the 5' terminus of each strand break from where it is cleaved away by endonucleases (Keeney 2008). SPO11 induced double strand break formation is found in almost all meiotic species studied to date. In *Saccharomyces cervisiae* Spo11 requires at least 9 other gene products in order to produce DSBs, only a handful of orthologs of which have been identified in mammals. These include components of the mammalian Mre11 complex (*Xrs2, Rad50, Mre11*), collectively known as the MRX/N complex, which tethers DNA to co-ordinate events at the two ends of the DSB (Keeney 2001; Santucci-Darmanin 2010). Apart from the MRX/N complex *Mei1* has also been implicated in DSB formation and interaction with SPO11 in the mouse (Munroe, Bergstrom et al. 2000; Kumar, Bourbon et al. 2010).

Following DSB formation in early leptonema, the breaks are then processed through several common precursor steps, for a number of possible recombination pathways. Firstly, 3' overhangs are generated following 5' end resection by an exonuclease whose identity is uncertain in mammals, but which appears to be primarily Exo1 in yeast (Neale, Pan et al. 2005). The RecA homologs, DMC1 and RAD51, bind to the single stranded overhangs and cause interaction between homologous chromosomes and facilitate strand invasion (Santucci-Darmanin 2010). In addition the protein BRCA2 is also known to be involved in DSB processing and strand invasion, perhaps by interacting with RAD51 and DMC1 and allow correct positioning of

RAD51-DMC1 foci (Li and Ma 2006). Other accessory proteins in mammals that assist the formation and function of RAD51-DMC1 foci are the HOP2-MND1 dimer that stabilizes these foci and promotes their ability to associate with DNA; and RAD54B which is thought to promote that strand invasion activity of DMC1 (Santucci-Darmanin 2010). In addition, mammals possess several *Rad51* paralogs that are expressed in cells exhibiting recombination such as *Rad51b, Rad51c, Rad51d, Xrcc2*, and *Xrcc3*. All these genes are expressed widely during homologous recombination (Masson, Tarsounas et al. 2001). *In vitro* these proteins for a complex known as the BCDX2 that binds to DSBs and are believed to aid RAD51 localization there (Masson, Tarsounas et al. 2001).

The next step in meiotic recombination is the processing of strand exchange by either CO (Crossover) or NCO (Non Crossover) pathways. Importantly, the number of CO events in mammals is about 10% of the number of initiating DSB events, suggesting that most of these DSBs are resolved by NCO, but that both CO and NCO events arise from common precursors. Briefly, following DSB formation and 3' overhang strand invasion, DNA synthesis takes place from this 3' end using the other chromatid as a template (Handel and Schimenti 2010). A double Holliday junction (dHJ) is formed as a result of ligation that are then resolved. The products can be either CO or NCO depending on how the Holliday junctions are resolved, but this process is

extremely biased towards CO fates, leading researchers to speculate on the existence of temporally and functionally distinct NCO pathways that can account for the over-abundance of NCO events. Evidence for this earlier NCO pathway, which utilizes a process known as synthesis-dependent strand annealing (SDSA), exists in *S. cerevisiae* (Ehmsen and Heyer 2008). CO events correspond to "*Chiasmata*", which physical tethers that are essential for holding the two homologous chromosomes together and ensure proper segregation during anaphase (Santucci-Darmanin 2010). The number and distribution of COs are strictly regulated by a process known as CO interference, hence only a fraction of DSBs are repaired to CO products (Ehmsen and Heyer 2008; Handel and Schimenti 2010). In *S.cerevisiae,* two components of the synaptonemal complex axial elements, Red1 and Hop1 are involved in prevention of crossovers between sister chromatids. The mammalian orthologs of these, HORMAD1 and HORMAD2 are also found in the axial region and are believed to perform the same function (Handel and Schimenti 2010).

Of the several gene products that are active in the crossover pathway in mammals, the mammalian orthologs of yeast ZMM proteins (a group of seven collaborating proteins) are involved in CO formation. MSH4 and MSH5 are proteins from this group that bind Holliday Junctions as a heterodimer, presumably encircling the DNA duplex and stabilizing them

(Santucci-Darmanin 2010). This heterodimer, named MutSg, is thought to participate in the CO bias for dHJ repair. However, the number of MSH4-MSH5 foci in the mouse exceeds the number of actual CO sites. Two other proteins that are downstream, MLH1 and MLH3, are recruited sequentially to MSH4-MSH5 foci for CO events (Kolas, Svetlanov et al. 2005). Only those foci that are stabilized by MLH1 and MLH3 go on to become crossovers, indicating that the interactions of these four proteins may influence CO interference (Ehmsen and Heyer 2008). The fate of the other foci is not known, but these could be processed through NCO pathways, or through a second pathway regulated by the MUS81-EME1 complex. More recently, ubiquitin ligase genes, such as *Rnf212* have been identified which determine recombination 'hotspots' in the genome (Holloway, Booth et al. 2008; Santucci-Darmanin 2010). The protein dimer XPF-ERCC1, supplement the action of mismatch repair components in the repair of insertions/deletions that are large in size (Ehmsen and Heyer 2008). Several gene products such as those of *Atr, Trip13,* and *Atm* are implicated in a checkpoint mechanism that monitors DSB repair and synapses of chromosomes at pachynema (Handel and Schimenti 2010).

Fig 1.2 Gene expression during meiosis in the mammalian fetal germ cell

In response to retinoic acid production from somatic cells in female embryonic gonad, there is an up-regulation of retinoic acid response genes in the germ cells, such as Stra8 and other related genes such as Msx1, Msx2 and Dmrt1, which facilitate the entry into meiosis in the germ cells. Other genes expressed at this time include Dazl as well as 13 other genes, which code for translation factors and RNA binding proteins. Genes expressed at this time are involved in pre-meiotic DNA replication, after which the germ cells enter Prophase I of meiosis. Homologous chromosomes are brought together by the action of Unc84a, which helps tether the chromosomes to the nuclear envelope. The products of genes such as Spo11, Xrs2(Nbs1), Rad50, Mre11, and Mei1 are involved in production of double strand breaks (DSBs). DMC1 and RAD51 proteins bind to the single stranded overhangs and cause interaction between homologous chromosomes and facilitate strand invasion alongwith several other proteins that aid RAD51 localization. These foci are processed through various crossover and non-crossover pathways involving protein products of genes such as Msh4, Msh5, Mlh1, Mlh3, Mus81, and Eme1. Several gene products such as those of Atr, Trip13, Atm, Ercc4 and Ercc1are implicated in pachytene checkpoint mechanism as well as supplementing the action of mismatch repair components in

the repair of insertions/deletions that are large in size. After completion of recombination events genes such as Nek1 and Ubb are involved in cohesin removal and exit from prophase I.

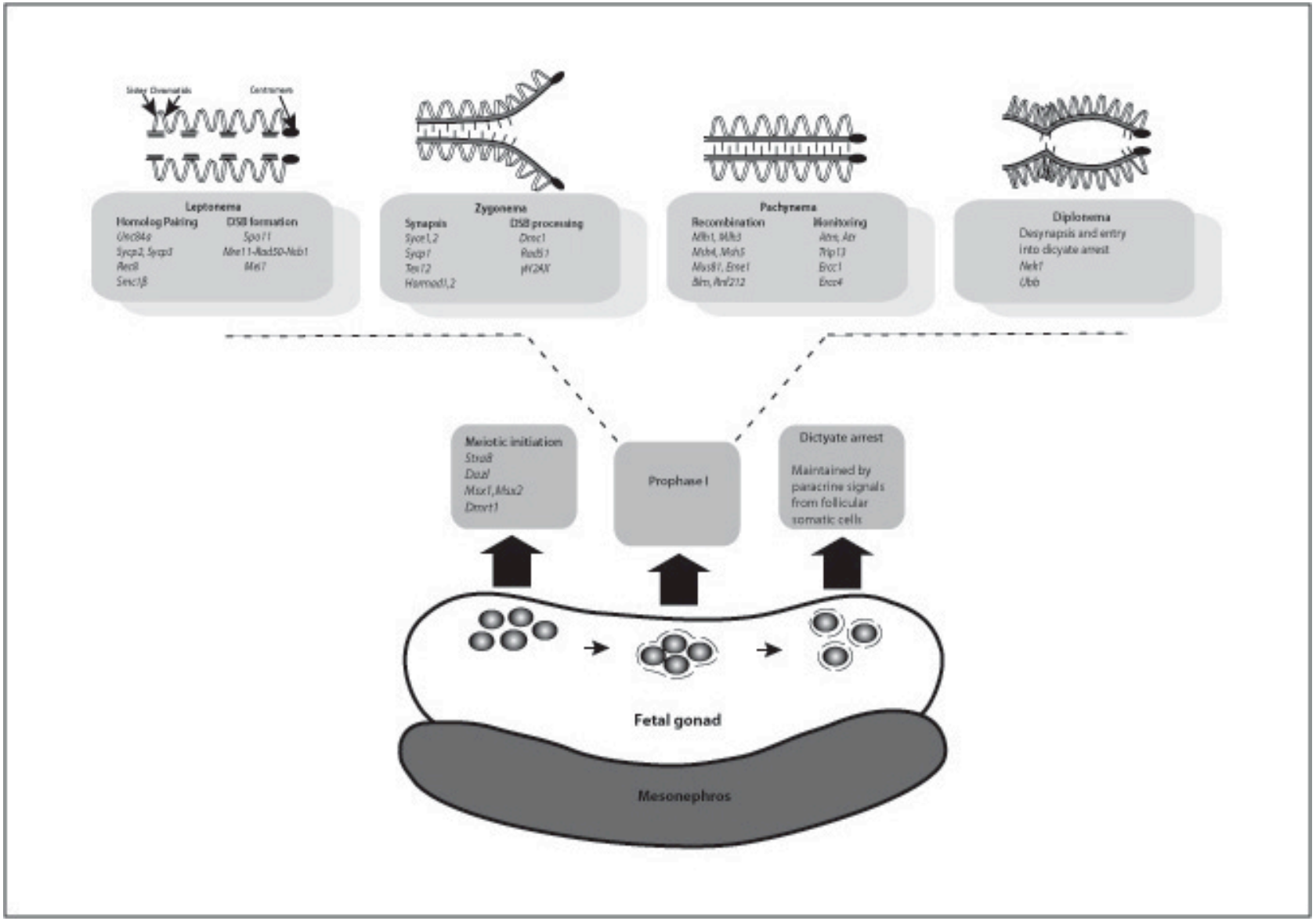
Sister Chromatids
Centromere
Leptonema
Homolog Pairing
Uxc84a
Sycp2, Sycp3
Rec8
Smc1β
DSB formation
Spo11
Mre11-Rad50-Nbs1
Mei1
Zygonema
Synapsis
Syce1,2
Sycp1
Tex12
Hormad1,2
DSB processing
Dmc1
Rad51
γH2AX
Pachynema
Recombination
Mlh1, Mlh3
Msh4, Msh5
Mus81, Ercc1
Slm, Rnf212
Monitoring
Atm, Atr
Trip13
Ercc1
Ercc4
Diplonema
Desynapsis and entry into dictyate arrest
Nek1
Ubb
Meiotic initiation
Stra8
Dazl
Msx1,Msx2
Dmrt1
Prophase I
Dictyate arrest
Maintained by paracrine signals from follicular somatic cells
Fetal gonad
Mesonephros

Much of our understanding of meiotic recombination comes from studies of yeast and other organisms. However, since many of the genes and their functions in prophase I are highly conserved, we can be confident that the pathways may be similar from yeast to human. In fact, gene co-expression networks constructed using gene profiles from meiotic prophase microarray data in yeast, mouse and humans show several conserved gene modules that fall into GO categories like recombination, cohesion, transcription, synaptonemal complex assembly and pachytene (Li, Lam et al. 2010). Also, not all genes forming a network in meiotic prophase are meiosis specific. Known non meiosis-specific genes like *Rad21, Smc3, Smc1, Mad2l1, Espl1, Ccna1* and *Rad51* are seen to be interacting with meiosis specific genes during several steps of the recombination pathway (Zheng, Griswold et al. 2010). *Rad21, Smc1a* and *Smc3* are involved in chromatin cohesion whereas *Mad2l1* participates in spindle assembly during both mitosis and meiosis (Zheng, Griswold et al. 2010). The rest are involved in homologous recombination and mismatch repair. In a network constructed of genes conserved between human and mouse, several connections are found with non-meiotic genes. For instance, *Sycp2* is shown to be connected with genes like *Tex11, Tex15, Hspa41, Hsf2bp* and *Hormad2(Su, Li et al. 2011)*. Of these *Hspa41* and *Hsf2bp* are heat-shock proteins while the others have unknown functions but have been shown to associate with unsynapsed chromosomes. Similarly, *Msh4* has been shown

to be connected with *Mtl5*, a gene encoding metallothionein protein, in this network(Su, Li et al. 2011). These observations underscore the importance of using gene regulatory networks in studying specifics of prophase I and also concomitant mechanisms like nuclear organization, DNA repair and so on.

5.4 Meiotic recombination and aneuploidy

In contrast to the high degree of conservation among species at the genetic and functional level, it is important to note that humans exhibit an unusually high (10-25%) rate of aneuploidy, resulting in high rates of embryonic defects and fetal demise. Unusual distribution of recombination events, such as formation of COs close to the telomere, presence of two or more COs in close proximity etc, have been associated with aneuploidy in human oocyte (Garcia-Cruz, Roig et al. 2009). The number of MLH1 and MLH3 foci is highly heterogeneous in human oocyte chromosomes as compared to the mouse, suggesting the natural occurrence of achiasmatic chromosomes (and therefore, aneuploidy) is more frequent (Lenzi, Smith et al. 2005). Maternal age has been the primary focus of studies on the risk of human aneuploidy along with environmental pollutants like bisphenol A (Hunt, Koehler et al. 2003; Garcia-Cruz, Roig et al. 2009). Both factors have been linked with heterogeneity of MLH1 foci as well. Studies on heat shock proteins like HSF1 and HSF2, whose activity is regulated by environmental stressors,

show that they are powerful transcriptional regulators of several gene networks in the meiotic pathway. This indicates that meiosis, through the action of HSFs, is heavily modulated by environmental conditions (Le Masson, Razak et al. 2011). Moreover, data from both mouse and humans indicate the involvement of less stringent checkpoint mechanisms in the female leading to a higher tolerance to errors (Nagaoka, Hodges et al. 2011). This implies that in humans, the already high tendency towards aneuploidy, combined with exposure to environmental risk factors and reduced regulational control, may all contribute to the high incidence of meiotic errors, thereby affecting the quality of reproductive health in women.

6. Meiotic resumption after birth

By the end of pachynema the SC begins to disassemble, allowing the homologs to move apart during diplonema. After this the oocytes enter what is known as the dictyate arrest (E20), which is a quiescent form of diplonema, and remain in this state until puberty when meiosis is resumed in cohorts of oocytes, under the influence of gonadotropins (Richards and Pangas 2010). Meiotic resumption is triggered by LH-induced EGFR pathway signals from cumulus cells resulting in Germinal Vesicle Breakdown (GVBD) in the oocytes followed by condensation of chromatin into chromosomes (Sun, Miao et al. 2009). GVBD marks the exit of the oocyte from the first meiotic arrest, which is then followed by completion of meiosis I, where asymmetric cytokinesis

after telophase I results in the formation of a small polar body that is then extruded (Sun, Miao et al. 2009). The oocyte then enters meiosis II, progresses to metaphase II (MII), where it is arrested a second time. Exit from this arrest occurs only after fertilization followed by completion of meiosis II and extrusion of a second polar body (Sun, Miao et al. 2009). These events are used to categorize oocytes into three important and physiologically distinct stages of post-prophase development namely, GV stage (prior to onset of meiotic resumption), MI (during completion of meiosis; "reactivated" oocytes) and MII (at arrest prior to fertilization) (Wang, Kou et al. 2010). Developing GV stage oocytes accumulate resources required for the resumption from dictyate arrest and completion of meiosis whereas the MII stage oocyte accumulates resources required for fertilization, oocyte to zygote transition and early cleavage divisions of the embryo. Transcriptome profiling of these different stages provide great insight into the processes regulating development of an immature oocyte and its transformation to an embryo (Zhang, Zucchelli et al. 2009).

Developing oocytes in growing follicles accumulate mRNA transcripts and proteins required for later functions during fertilization and first cleavage divisions. Transcriptional activity is lower in oocytes that have reached their maximum size and progressively decreases with each step of the oocyte maturation with the lowest gene expression in the MII oocyte (Assou, Anahory et al.

2006). Of the many genes in the same GO categories expressed in both GV and MII stages, such as metabolism and cell communication, the proportion of genes in individual categories is higher in GV stage (Assou, Anahory et al. 2006; Fair, Carter et al. 2007). However, oocytes undergoing meiotic resumption have been shown to have gene expression profiles that are stage-specific. A stage-by-stage analysis of human oocyte mRNA transcripts and their GO categorization showed the total number of expressed genes declined from 10869 in GV oocytes to 9682 in MI and 5633 in MII oocytes. While a large number of genes (444) were overexpressed in MII oocytes there was an increase in the number of genes that were under expressed (803) specifically at this stage. This demonstrates that the transcriptional activity is higher in oocytes earlier in meiotic resumption, leading to production and storage of transcripts required for completion of meiosis, fertilization and early cleavage divisions.

Similar global gene expression analysis from mRNA transcripts of bovine oocytes undergoing meiotic resumption and maturation showed over 800 genes that are differentially expressed between GV and MII oocytes out of a total of 8000 expressed genes (Fair, Carter et al. 2007). With mouse oocytes, the global gene expression patterns showed about 2000 genes differentially express between GV and MII (Cui, Li et al. 2007). While the differential expression between GV and MI oocytes is very minor in all mammalian species, a large amount of modifications to

mRNA transcripts occur after MI before entering MII and may be responsible for the widespread change in protein composition and abundance that accompany fertilization and transition from oocyte to embryo (Assou, Anahory et al. 2006). For example, genes that encode F-box family of proteins are overrepresented in oocytes at different stages, are involved in ubiquitin linked protein degradation pathway, and have been implicated in this extensive change in protein profile along with proteins involved in epigenetic modifications like methylases, demethylases and acetylases (Wang, Kou et al. 2010). PADI6, another well-known histone demethylase, is involved in ribosome storage and embryonic genome activation and its transcript is present in the oocyte after the MI stage (Yurttas, Vitale et al. 2008).

Human oocytes collected at different stages of maturation and analyzed for gene expression levels using microarray and cluster analysis of specific marker and related genes showed that GV oocytes have a higher expression of genes involved in protein formation and metabolism, cell cycle regulation, electron transport, and production of cytoskeletal elements whereas MII oocytes have an overrepresentation of genes involved in DNA replication and repair, cell proliferation, lipid and amino acid metabolism, formation of G-protein coupled receptors (GPCR) and other signaling molecules (Cui, Li et al. 2007; Gasca, Pellestor et al. 2007). Gene networks constructed from mouse oocytes using an IPA database (Ingenuity Pathway Analysis

http://www.ingenuity.com/products/pathways_analysis.html) of MII specific genes like *Plat, Gdp1, Ints9, Gdf9* and *Sic23a* revealed GO function categories of cellular movement cellular assembly and organization, cell cycle regulation, DNA replication, recombination and repair, lipid metabolism and apoptosis (Jincho 2008). In addition, genes upregulated in mammalian oocytes can be subdivided into various post-prophase I meiotic events, including those participating in MPF (*Ccnb1, Ccnb2, Cdc2, Cdc25A, Cdc25B, Cdc25C*), signaling (*Mos, Bmp6, Gdf9, Fgf9, Kit, GPR family, Zp1, Zp2, Zp3, Zp4*), spindle assembly (*Bub1, BubR1, CenpA, CenpE, CenpH, Mad2L1*), Anaphase-promoting Complex (*APC1, APC10, Stag3*), transcription factors (*Sox30, Sox15*) and cell cycle regulation (*Pttg1, Pttg3, Emi1*) (Assou, Anahory et al. 2006; Cui, Li et al. 2007; Fair, Carter et al. 2007; Wang, Kou et al. 2010). *Pttg1* and *Pttg3* encode Securin protein that, along with cohesions, regulate sister chromatid association during meiosis II (Assou, Anahory et al. 2006).

Results similar to the IPA were shown by proteome analysis of mouse oocytes (Wang, Kou et al. 2010). In general, proteome profiles give a more accurate representation of regulatory networks, as non-translation of transcripts and activation of proteins within the cell cannot be assessed by transcriptome profiles alone. In the oocyte proteome profile about 2800 GV specific proteins and 3000 MII specific proteins were identified and a GO annotation analysis showed that GV oocytes

specifically contain proteins related to metabolism, oocyte function and maturation (Wang, Kou et al. 2010). For example, several protein families involved in molecular transport across oocyte and cumulus cell membranes were found to be in abundance in the GV oocytes, such as the amino acid transporters of the SLC family, gap junction proteins and adhesion proteins (Wang, Kou et al. 2010). Proteins involved in DNA replication and recombination pathway are seen in MII oocytes in higher levels than the GV oocytes. MII oocytes in addition to possessing proteins for cell cycle regulation, show abundance of specific transcription factors such a SIN3a, TRIM28 that prevent stem cell differentiation and TCL family of proteins that are involved in reprogramming of cells to pluripotency. Both stages of oocytes (GV and MII) show high expression of protein families like ARF (ADP ribosylation factor) MATER (Maternal Antigen That Embryos Require), Tudor and Fbox family which are required for cell cycle regulation and self-renewal. ARF family of proteins is also involved in the asymmetric division of oocytes (Wang, Kou et al. 2010). Other over-represented genes in the MII oocytes are part of the MAPK pathway and TGFβ pathway, which are involved in oocyte activation, cell differentiation and cell proliferation respectively. For instance, *Map2k1* and *Pacsin2* are two genes whose products are involved in cell signaling pathways and are highly expressed after the GV stage. PACSIN2 belongs to a family of proteins known to participate in oocyte maturation, fertilization, and early

embryonic divisions (Cui, Li et al. 2007). Products of another gene *Adam1a* are expressed in MII and are known to play a role in fertilization. However, ZP proteins, also known to be required for fertilization, are formed as early as GV stage oocytes as seen by high expression of *Zp1*, *Zp2*, and *Zp3* genes in GV oocytes indicating a possible role of these proteins in interactions with cumulus cells(Cui, Li et al. 2007).

6.1 Role of cumulus cells in meiotic maturation

The role of cumulus cells in oocyte maturation and meiotic resumption have been further illuminated by gene expression analysis. Genome wide expression analysis in human oocytes using oligonucleotide based microarrays reveals significant differences in expression profiles for many genes between oocyte and cumulus cells. Some of these genes are known to be oocyte specific (*Zp1, Zp2, Zp3, Zp4, Gdf9*), and others are known to be specific to the meiotic pathway within the oocyte (*AurkC, Cdc25A, Cdc25B, Cdc25C*) (Assou, Anahory et al. 2006). Many genes involved in signaling pathways mediated by cumulus cells are over-expressed at all stages of development within the oocyte. For instance, genes encoding growth factor receptors (*Bmpr2, Kit, Erbb4*) and GPCRs (*Gpr37, Gpr39, Gpr51, Gpr126*) are over-expressed in oocytes, suggesting the role of their cumulus cell-derived ligands in regulating oocyte maturation (Assou, Anahory et al. 2006).

Figure 1.3.Genes expressed during different stages of mammalian oocyte development and function.

Genes above the dotted line are expressed in the oocyte and below the dotted line are observed in the somatic cell population of the follicle. Oocytes within primary follicles in the ovary have upregulation of specific transcription factors required for folliculogenesis (Figla, Nobox), zona pellucida formation (Zp1, Zp2, Zp3, Zp4) and post-fertilizational development (Zar1). In the pre-antral follicles, several oocyte expressed genes like Gdf9, Bmp15 etc are involved in regulation of follicle development, proliferation and differentiation of granulosa cells. Within the antral follicles several new genes are expressed in preparation for meiotic resumption (Cdk1, Mad2, Bub3), cell cycle progression (FMN2 required for polymerization of actin) and GVBD (Histone1a required for chromatin remodeling) are expressed in the oocyte. In the cumulus cells of the antral follicle, upregulation of genes required for hormone response (LHCGR, FSHR) and regulation of follicular atresia (Bcl2) is observed. Ovulation, being similar to an inflammatory response, shows an upregulation of mediators of inflammation such as NOS (Nitric oxide synthetase) and Cox (cyclo-oxygenases). Genes upregulated in GVBD and MI oocytes are required for participating in MPF (Ccnb1, Ccnb2, Cdc2, Cdc25A, Cdc25B, Cdc25C), signaling (Mos, Bmp6, Gdf9, Fgf9, Kit, GPR family, Zp1, Zp2, Zp3, Zp4), spindle assembly (Bub1,

BubR1, CenpA, CenpE, CenpH, Mad2L1), and Anaphase-promoting Complex (APC1, APC10, Stag3). In addition to these, MII oocytes show upregulation of genes that play a role in fertilization (Pttg1, Pttg3, Emi1, and Adam1a) and early cleavage divisions (MATER, Pacsin2).

Ovary
Ovidiuct

Of the genes that are over expressed in cumulus cells, 24 % are involved in extracellular signals and membrane structure indicating their highly supportive role that the cumulus cell play in oocyte development (Assou, Anahory et al. 2006).

Cumulus cells also play a major role in ovulation, and several gene networks spanning the entire cumulus-oocyte complex are involved in this process (Kim, Bagchi et al. 2009). Hormonal stimulation of the ovary sets in motion a series of events that lead to the expulsion of the now viable (and fertilization competent) oocyte from the follicle. Gene profiles from mature follicles reveal gene networks comprising of several progesterone-regulated genes like *Adamts1, Edn2, Pparγ, Il6* and *Ptgs2* which code for proteins like proteases, cell adhesion components, transcription factors, regulators of vascular activities and inflammation regulators (Kim, Bagchi et al. 2009). Each of these networks is involved in the damage and repair events that characterize the ovulation process (Kim, Bagchi et al. 2009).

Transcriptome profiles of human oocytes between MII (unfertilized) stage and the 4-cell embryo stage revealed that while a large number of transcripts show an overall decreasing expression, there is an increase in the expression of a specific set of genes encoding proteins localized in the nucleus and on ribosomes. GO analyses identified these proteins as being required for RNA processing and metabolism indicating that they are probably involved in the transition from

maternal to zygote genome. The overall reduction in transcripts at this stage could be due to degradation of maternal transcripts that accompany this transition (Zhang, Zucchelli et al. 2009). The oocyte-derived transcripts at this stage might be responsible for the extensive reprogramming of a terminally differentiated cell (the oocyte) to a pluripotent cell (the zygote). Study of gene networks involved in this unique process have great value in induced pluripotent stem cell (iPSC) research and therapy (Wang, Kou et al. 2010).

7. Role of the oocyte in ovarian development

While oocytes are progressing through prophase I of meiosis during fetal life, the somatic cells in the ovary surround the germ cell clusters and the whole gonad itself begins to be delineated into cortical and medullary regions due to differential gene expression in the cells (Combes A 2010). For instance, cortical cells showed a marked increase in *Bmp2* expression while medullary cells have higher *Wnt4*, *Fst* expression. While the exact function of *Bmp2* in the cortex cells is not known, Follistatin (the protein product of the *Fst* Gene) is known to be involved in activin-mediated regulation of ovary function. *Rspo1* expression activates the Wnt signaling pathway in the ovary which, in turn, suppresses both endothelial cell migration and the formation of testis-specific vasculature in the ovary (Yao, Matzuk et al. 2004; Combes A 2010). Not surprisingly, therefore, GO biological process analysis of *Wnt4* shows its involvement in commitment to cell

fate in primary germ layers and in branching and patterning of blood vessels (Yao, Matzuk et al. 2004; Combes A 2010).

Somatic cells, as expected, influence follicle formation greatly in the postnatal ovary. *Foxl2* is required for normal follicle formation and is expressed by pregranulosa cells in the gonad (E12.5), and then later on the granulosa cells of the early follicles (Combes A 2010). However, the oocytes themselves are also important for folliculogenesis, since loss of oogonia at different stages of development has been shown to disrupt follicle and ovarian development (Combes A 2010). In the absence of oogonia, somatic cells can still form clusters, however, they seem unable to form follicles and the cell clusters start regressing in a few days (Combes A 2010). Two oogonia specific genes, *Fig1a* and *Nobox,* have been implicated in the oocyte-driven control of folliculogenensis at this stage of development. Loss of oocytes in the meiotic stages of development produces a transdifferentiation of pre-granulosa cells of the early follicles to Sertoli-like cells indicating that oocytes play an important role in maintaining the female specific differentiation pathway at this stage. *Wnt4*, *Rspo1,* and *Amh* expressed in the oocyte have been implicated in this part of ovarian development (Acevedo and Smith 2005). Even in much later stages of the female reproductive life, loss of oocytes can be detrimental to ovarian function. For instance, oocyte loss from preovulatory follicles in the adult ovary causes leutinization of the

follicle. *Bmp15* and *Gdf9* expression in the oocyte have been shown to be responsible in preventing this disintegration and for maintaining proper follicle function prior to ovulation (Combes A 2010).

8. Conclusions

Our understanding of cellular processes has been aided greatly by a more complete picture of the genetic networks that regulate these events, and the oocyte is no exception. Indeed, the similarities in gene expression profiles between oocytes and somatic cells in terms of their proliferative and differentiation programs, and between oocytes during meiosis and the DDR program in somatic cells, such comparative genetic profiling will be useful in elucidating common mechanisms and in predicting genes that are likely to play important roles in one or both pathways. Indeed, as our ability to perform high throughput sequencing advances, and with the emergence of technologies capable of allowing transcriptome profiling of single oocytes, the scope and resolution of these gene networks is likely to improve dramatically.

9. References

Acevedo, N. and G. D. Smith (2005). "Oocyte-specific gene signaling and its regulation of mammalian reproductive potential." Frontiers in bioscience : a journal and virtual library **10**: 2335-2345.

Amleh, A. and J. Dean (2002). "Mouse genetics provides insight into folliculogenesis, fertilization and early embryonic development." Human reproduction update **8**(5): 395-403.

Anderson, E. L., A. E. Baltus, et al. (2008). "Stra8 and its inducer, retinoic acid, regulate meiotic initiation in both spermatogenesis and oogenesis in mice." Proceedings of the National Academy of Sciences of the United States of America **105**(39): 14976-14980.

Assou, S., T. Anahory, et al. (2006). "The human cumulus--oocyte complex gene-expression profile." Human reproduction **21**(7): 1705-1719.

Cohen, P. E. and J. K. Holloway (2010). "Predicting gene networks in human oocyte meiosis." Biology of reproduction **82**(3): 469-472.

Combes A, S. C., Koopman P (2010). Sex determination and gonadal development. Oogenesis: The universal process. V. A. Verlhac MH, John Wiley and Sons**:** 27-78.

Cui, X. S., X. Y. Li, et al. (2007). "Maternal gene transcription in mouse oocytes: genes implicated in oocyte maturation and fertilization." The Journal of reproduction and development **53**(2): 405-418.

D'Haeseleer, P. (2005). "How does gene expression clustering work?" Nature biotechnology **23**(12): 1499-1501.

Di Agostino, S., P. Rossi, et al. (2002). "The MAPK pathway triggers activation of Nek2 during chromosome condensation in mouse spermatocytes." Development **129**(7): 1715-1727.

Ehmsen, K. and W.-D. Heyer (2008). Biochemistry of Meiotic Recombination: Formation, Processing, and Resolution of Recombination Intermediates. Recombination and Meiosis. R. Egel and D.-H. Lankenau, Springer Berlin Heidelberg. **3:** 91-164.

Ewen, K., A. Jackson, et al. (2010). "A male-specific role for p38 mitogen-activated protein kinase in germ cell sex differentiation in mice." Biology of reproduction **83**(6): 1005-1014.

Ewen, K. A. and P. Koopman (2010). "Mouse germ cell development: from specification to sex determination." Molecular and cellular endocrinology **323**(1): 76-93.

Fair, T., F. Carter, et al. (2007). "Global gene expression analysis during bovine oocyte in vitro maturation." Theriogenology **68 Suppl 1**: S91-97.

Garcia-Cruz, R., I. Roig, et al. (2009). "Maternal origin of the human aneuploidies. Are homolog synapsis and recombination to blame? Notes (learned) from the underbelly." Genome dynamics **5**: 128-136.

Gasca, S., F. Pellestor, et al. (2007). "Identifying new human oocyte marker genes: a microarray approach." Reproductive biomedicine online **14**(2): 175-183.

Gill, M. E., Y. C. Hu, et al. (2011). "Licensing of gametogenesis, dependent on RNA binding protein DAZL, as a gateway to sexual differentiation of fetal germ cells." Proceedings of the National Academy of Sciences of the United States of America **108**(18): 7443-7448.

Griswold, M. D., C. A. Hogarth, et al. (2012). "Initiating meiosis: the case for retinoic acid." Biology of reproduction **86**(2): 35.

Hallinan, J. S., K. James, et al. (2011). "Network approaches to the functional analysis of microbial proteins." Advances in microbial physiology **59**: 101-133.

Handel, M. A. and J. C. Schimenti (2010). "Genetics of mammalian meiosis: regulation, dynamics and impact on fertility." Nature reviews. Genetics **11**(2): 124-136.

Hayashi, K., S. M. de Sousa Lopes, et al. (2007). "Germ cell specification in mice." Science **316**(5823): 394-396.

Hiraoka, Y. and A. F. Dernburg (2009). "The SUN rises on meiotic chromosome dynamics." Developmental cell **17**(5): 598-605.

Hogarth, C. A., D. Mitchell, et al. (2011). "Identification and expression of potential regulators of the mammalian mitotic-to-meiotic transition." Biology of reproduction **84**(1): 34-42.

Holloway, J. K., J. Booth, et al. (2008). "MUS81 generates a subset of MLH1-MLH3-independent crossovers in mammalian meiosis." PLoS genetics **4**(9): e1000186.

Hunt, P. A., K. E. Koehler, et al. (2003). "Bisphenol a exposure causes meiotic aneuploidy in the female mouse." Current biology : CB **13**(7): 546-553.

Jincho, Y. K., T. (2008). "Dynamism in the Gene Expression Profile after Oocyte Activation in Mice." Journal of Mammalian Ova Research **25**(3): 150-162.

Keeney, S. (2001). "Mechanism and control of meiotic recombination initiation." Current topics in developmental biology **52**: 1-53.

Keeney, S. (2008). "Spo11 and the Formation of DNA Double-Strand Breaks in Meiosis." Genome dynamics and stability **2**: 81-123.

Kim, J., I. C. Bagchi, et al. (2009). "Control of ovulation in mice by progesterone receptor-regulated gene networks." Molecular human reproduction **15**(12): 821-828.

Kolas, N. K., A. Svetlanov, et al. (2005). "Localization of MMR proteins on meiotic chromosomes in mice indicates distinct functions during prophase I." The Journal of cell biology **171**(3): 447-458.

Koubova, J., D. B. Menke, et al. (2006). "Retinoic acid regulates sex-specific timing of meiotic initiation in mice." Proceedings of the National Academy of Sciences of the United States of America **103**(8): 2474-2479.

Krentz, A. D., M. W. Murphy, et al. (2011). "DMRT1 promotes oogenesis by transcriptional activation of Stra8 in the mammalian fetal ovary." Developmental biology **356**(1): 63-70.

Kumar, R., H. M. Bourbon, et al. (2010). "Functional conservation of Mei4 for meiotic DNA double-strand break formation from yeasts to mice." Genes & development **24**(12): 1266-1280.

Le Bouffant, R., B. Souquet, et al. (2011). "Msx1 and Msx2 promote meiosis initiation." Development **138**(24): 5393-5402.

Le Masson, F., Z. Razak, et al. (2011). "Identification of heat shock factor 1 molecular and cellular targets during embryonic and adult female meiosis." Molecular and cellular biology **31**(16): 3410-3423.

Lee, H. S., E. Y. Kim, et al. (2010). "Obox4 critically regulates cAMP-dependent meiotic arrest and MI-MII transition in oocytes." FASEB journal : official publication of the Federation of American Societies for Experimental Biology **24**(7): 2314-2324.

Lee, H. S., E. Y. Kim, et al. (2011). "Changes in gene expression associated with oocyte meiosis after Obox4 RNAi." Clinical and experimental reproductive medicine **38**(2): 68-74.

Lenzi, M. L., J. Smith, et al. (2005). "Extreme heterogeneity in the molecular events leading to the establishment of chiasmata during meiosis i in human oocytes." American journal of human genetics **76**(1): 112-127.

Li, W. and H. Ma (2006). "Double-stranded DNA breaks and gene functions in recombination and meiosis." Cell research **16**(5): 402-412.

Li, Y., K. S. Lam, et al. (2010). "A yeast's eye view of mammalian reproduction: cross-species gene co-expression in meiotic prophase." BMC systems biology **4**: 125.

Martin, A. C. and D. G. Drubin (2003). "Impact of genome-wide functional analyses on cell biology research." Current opinion in cell biology **15**(1): 6-13.

Masson, J. Y., M. C. Tarsounas, et al. (2001). "Identification and purification of two distinct complexes containing the five RAD51 paralogs." Genes & development **15**(24): 3296-3307.

Morelli, M. A. and P. E. Cohen (2005). "Not all germ cells are created equal: aspects of sexual dimorphism in mammalian meiosis." Reproduction **130**(6): 761-781.

Munroe, R. J., R. A. Bergstrom, et al. (2000). "Mouse mutants from chemically mutagenized embryonic stem cells." Nature genetics **24**(3): 318-321.

Nagamatsu, G., T. Kosaka, et al. (2012). "Tracing the conversion process from primordial germ cells to pluripotent stem cells in mice." Biology of reproduction **86**(6): 182.

Nagaoka, S. I., C. A. Hodges, et al. (2011). "Oocyte-specific differences in cell-cycle control create an innate susceptibility to meiotic errors." Current biology : CB **21**(8): 651-657.

Neale, M. J., J. Pan, et al. (2005). "Endonucleolytic processing of covalent protein-linked DNA double-strand breaks." Nature **436**(7053): 1053-1057.

Oktem, O. and B. Urman (2010). "Understanding follicle growth in vivo." Human reproduction **25**(12): 2944-2954.

Pfeuty, B., J. F. Bodart, et al. (2012). "A dynamical model of oocyte maturation unveils precisely orchestrated meiotic decisions." PLoS computational biology **8**(1): e1002329.

Rajkovic, A., C. Yan, et al. (2002). "Obox, a family of homeobox genes preferentially expressed in germ cells." Genomics **79**(5): 711-717.

Rapaport, F., A. Zinovyev, et al. (2007). "Classification of microarray data using gene networks." BMC bioinformatics **8**: 35.

Richards, J. S. and S. A. Pangas (2010). "The ovary: basic biology and clinical implications." The Journal of clinical investigation **120**(4): 963-972.

Rolland, A. D., K. P. Lehmann, et al. (2011). "Uncovering gene regulatory networks during mouse fetal germ cell development." Biology of reproduction **84**(4): 790-800.

Roy Choudhury, D., C. Small, et al. (2010). "Microarray-based analysis of cell-cycle gene expression during spermatogenesis in the mouse." Biology of reproduction **83**(4): 663-675.

Santucci-Darmanin, S. a. B., F. (2010). Meiotic recombination in mammals. Oogenesis: The universal process. V. A. Verlhac MH, Wiley & Sons**:** 141-177.

Sonn, S., G. T. Oh, et al. (2011). "Nek2 and its substrate, centrobin/Nip2, are required for proper meiotic spindle formation of the mouse oocytes." Zygote **19**(1): 15-20.

Steuerwald, N., J. Cohen, et al. (2001). "Association between spindle assembly checkpoint expression and maternal age in human oocytes." Molecular human reproduction **7**(1): 49-55.

Su, Y., Y. Li, et al. (2011). "Mammalian meiosis is more conserved by sex than by species: conserved co-expression networks of meiotic prophase." Reproduction **142**(5): 675-687.

Sun, Q. Y., Y. L. Miao, et al. (2009). "Towards a new understanding on the regulation of mammalian oocyte meiosis resumption." Cell cycle **8**(17): 2741-2747.

Wang, S., Z. Kou, et al. (2010). "Proteome of mouse oocytes at different developmental stages." Proceedings of the National Academy of Sciences of the United States of America **107**(41): 17639-17644.

Yao, H. H., M. M. Matzuk, et al. (2004). "Follistatin operates downstream of Wnt4 in mammalian ovary organogenesis." Developmental dynamics : an official publication of the American Association of Anatomists **230**(2): 210-215.

Yurttas, P., A. M. Vitale, et al. (2008). "Role for PADI6 and the cytoplasmic lattices in ribosomal storage in oocytes and translational control in the early mouse embryo." Development **135**(15): 2627-2636.

Zhang, P., M. Zucchelli, et al. (2009). "Transcriptome profiling of human pre-implantation development." PloS one **4**(11): e7844.

Zheng, P., B. Baibakov, et al. (2013). "PtdIns(3,4,5)P3 is constitutively synthesized and required for spindle translocation during meiosis in mouse oocytes." Journal of cell science **126**(Pt 3): 715-721.

Zheng, P. and J. Dean (2007). "Oocyte-specific genes affect folliculogenesis, fertilization, and early development." Seminars in reproductive medicine **25**(4): 243-251.

Zheng, P., M. D. Griswold, et al. (2010). "Predicting meiotic pathways in human fetal oogenesis." Biology of reproduction **82**(3): 543-551.

CHAPTER 2

The Mitogen-Activated Protein Kinase (MAPK) pathway and its relation to oocyte biology.

1. Introduction

The MAPK pathway is a highly conserved signaling cascade that interacts very closely with various meiotic events such as meiotic initiation, prophase I, meiotic resumption, meiotic transition (MI to MII), maintenance of MII arrest, spindle assembly and checkpoint function (See also Chapter 3) (Pfeuty, Bodart et al. 2012). Several pre-meiotic events such as germ cell specification, sex differentiation and spermatogonial division also show the involvement of the MAPK pathway (Ewen, Jackson et al. 2010; Nagamatsu, Kosaka et al. 2012).

2. MAPKs and meiotic gene networks

MAPK pathway related gene expression during specific cell functions is a good indicator of the role of MAPK within that system. For instance, an expression study of cell cycle genes in male meiotic cells of the mouse showed about 550 differentially expressed cell-cycle genes during

various stages of spermatogenesis. Of these about 100 or more were known to be components of cell-cycle regulating pathways such as those for DNA repair, ubiquitination, cell signaling etc (Roy Choudhury, Small et al. 2010). Several of these genes have products that are known components of the MAPK pathway [MAPK1, MOS, MAPK4, MAPK6, MAPK7, MAPK13] and several others that are closely associated in the signaling cascade [JUN, RAF, RAS]. Several other genes that are regulated during meiosis have products that are known or putative interactors with components of the MAPK pathway [MAD2, MAD2L1, BUB1, BUB1B, BUB3, NEK2, WEE1, MPS1, CREB]. Of these, MAD and BUB protein complexes are known to be involved in spindle assembly checkpoint function for accurate assembly and maintenance of the bipolar spindle (Steuerwald, Cohen et al. 2001). NEK2 and CREB are involved in chromatin condensation for both spindle function as well as transcriptional regulation (Di Agostino, Rossi et al. 2002; Sonn, Oh et al. 2011).

2.1 Gene networks showing involvement of MAPKs in spindle configuration and function

Two oocyte specific proteins, OBOX4, a homeobox family member is known to be involved in meiotic development of mouse oocytes (Lee, Kim et al. 2011). OBOX (Oocyte specific Homeobox) is a family known to be expressed only in mammalian oocytes during folliculogenesis and meiotic resumption (Rajkovic, Yan et al. 2002). Of this group, OBOX4 is

thought to play a role in spindle configuration and chromosome segregation during MI to MII transition (Lee, Kim et al. 2010). An RNAi induced reduction in *Obox4* transcripts resulted in an MI arrest and differential expression of approximately 420 genes. KEGG groupings of these differentially expressed genes showed several pathways involved in metabolism, cell cycle regulation etc. The MAPK pathway was in the top 15 of the list generated by the KEGG analysis (Lee, Kim et al. 2011). Specifically, among the *Obox4* knockdown induced down-regulated gene clusters, were several genes whose products are components of the ERK/MAPK pathway [MEK2, MEK1, ERK2, ERK1] and genes whose products are involved in the cytoskeletal dynamics of oocyte division [Cdc42, Rac, F- Actin] (Zheng, Baibakov et al. 2013).

3. Conclusions

Stage-specific expression of gene networks regulate meiosis and germ-cell development. These gene networks include components of cell signaling cascades such as the MAPK pathway indicating their role in the regulation of meiotic events. Much of what is known about the MAPK signaling cascade is in relation to the transcriptional control brought about by the cascade in response to mitogenic signals. However, in addition to this, MAPKs specifically ERKs, are thought to be involved in cellular division, cytoskeletal reorganization and segregation of genetic

material. In investigating the role of ERKs and other regulators in cytoskeletal organization, chromosome segregation and ploidy, the oocyte has proved to be an excellent model.

So far pharmacological approaches have been used to study the action of ERKs in oocytes *in vitro* using inhibitors of the ERK pathway. However, these are not truly reflective of the physiological environment of the ovary. Also, while deletion of *Erk1* seems to have no effect on the viability of the mice, *Erk2* deletion causes embryonic lethality. Therefore it is impossible to study the effect of total ERK ablation in the oocyte and adult ovary. Hence, in order to better understand the mechanism of action of ERKs on oocyte division, we have generated an *Erk2* conditional deletion system driven by an oocyte specific Cre on an *Erk1* null background. This system proves to be an excellent model to study the roles of MAPK proteins ERK1 and ERK2 and their downstream signaling activity in meiotic cell cycle, oocyte division, chromosome segregation and early embryo development.

MAPKs are integral to meiotic regulation. Therefore, I hypothesize that deregulation of the MAPK pathway in oocytes will produce drastic changes in the spindle dynamics and in chromosome segregation. The above mentioned mouse model will be an excellent resource for delineating the exact mechanisms that bring about any such defects.

4. References

Di Agostino, S., P. Rossi, et al. (2002). "The MAPK pathway triggers activation of Nek2 during chromosome condensation in mouse spermatocytes." Development **129**(7): 1715-1727.

Ewen, K., A. Jackson, et al. (2010). "A male-specific role for p38 mitogen-activated protein kinase in germ cell sex differentiation in mice." Biology of reproduction **83**(6): 1005-1014.

Lee, H. S., E. Y. Kim, et al. (2010). "Obox4 critically regulates cAMP-dependent meiotic arrest and MI-MII transition in oocytes." FASEB journal : official publication of the Federation of American Societies for Experimental Biology **24**(7): 2314-2324.

Lee, H. S., E. Y. Kim, et al. (2011). "Changes in gene expression associated with oocyte meiosis after Obox4 RNAi." Clinical and experimental reproductive medicine **38**(2): 68-74.

Nagamatsu, G., T. Kosaka, et al. (2012). "Tracing the conversion process from primordial germ cells to pluripotent stem cells in mice." Biology of reproduction **86**(6): 182.

Pfeuty, B., J. F. Bodart, et al. (2012). "A dynamical model of oocyte maturation unveils precisely orchestrated meiotic decisions." PLoS computational biology **8**(1): e1002329.

Rajkovic, A., C. Yan, et al. (2002). "Obox, a family of homeobox genes preferentially expressed in germ cells." Genomics **79**(5): 711-717.

Roy Choudhury, D., C. Small, et al. (2010). "Microarray-based analysis of cell-cycle gene expression during spermatogenesis in the mouse." Biology of reproduction **83**(4): 663-675.

Sonn, S., G. T. Oh, et al. (2011). "Nek2 and its substrate, centrobin/Nip2, are required for proper meiotic spindle formation of the mouse oocytes." Zygote **19**(1): 15-20.

Steuerwald, N., J. Cohen, et al. (2001). "Association between spindle assembly checkpoint expression and maternal age in human oocytes." Molecular human reproduction **7**(1): 49-55.

Zheng, P., B. Baibakov, et al. (2013). "PtdIns(3,4,5)P3 is constitutively synthesized and required for spindle translocation during meiosis in mouse oocytes." Journal of cell science **126**(Pt 3): 715-721.

CHAPTER 3

Disruption of ERK activity in mouse oocytes results in infertility due to failed early embryonic development.

This chapter has been written as a manuscript for publication and is being submitted to scientific journals for peer review. Sections marked with * are not included in the original manuscript.

1. Abstract

The extracellular signal-regulated kinases, ERK1 and ERK2, are the major mitogen-activated protein kinases (MAPK) that respond to a variety of growth factors, hormones, and cytokines. In mammalian germ cells, ERK1 and ERK2 regulate G2/M transition, while phosphorylation-induced activation of ERKs in oocytes and granulosa (Fan et al., 2009) accompanies post-pubertal resumption of meiosis. Here we utilize a conditional approach to delete *Erk1* and *Erk2* specifically in mouse oocytes after birth, prior to germinal vesicle breakdown. Double mutant females are infertile, with gross chromosome misalignment on metaphase spindles in oocytes, and severe early embryonic loss. These changes coincide with a loss of ERK-dependent MSK1 phosphorylation and disruption of histone H3 phosphorylation on metaphase II spindles. In contrast, a major downstream target of ERK1 and ERK2 in somatic cells, RSK1, is unaffected by

the loss of ERK signaling in the oocyte. Our results demonstrate that ERK activity specifically within the oocyte is essential for meiotic resumption and for normal pre-implantation development.

2. Introduction

The MAP kinases are serine-threonine kinases that are part of a cascade that transduce a variety of extracellular signals (Raman, Chen et al. 2007), into a wide range of cellular effects including proliferation, apoptosis, cell movement and differentiation (Cargnello and Roux 2011). ERK1 and ERK2 (also known as MAPK3 and MAPK1, respectively) share approximately 83% similarity at the amino acid level, and both are expressed in a variety of tissues including those of the reproductive tract (Kang, Tai et al. 2000). In the ovary, pituitary gonadotropins activate the ERK1/ERK2 pathway in the granulosa cells mainly via the activation of epidermal growth factor receptor, leading to activation of the cRaf kinase (MAPKKK), and downstream activation of ERK1 and ERK2 (Cameron, Foster et al. 1996). This ERK-driven cascade is essential for ovulation, cumulus-oocyte complex expansion, oocyte maturation and follicle leutinization (Su, Wigglesworth et al. 2002; Richards and Pangas 2010). Studies in mammals and other vertebrate systems indicate that the ERK pathway also functions within the oocyte itself, participating in several post-prophase I events, including spindle formation (Yu, Xiong et al. 2007), maintaining spindle stability (Petrunewich, Trimarchi et al. 2009), the spindle assembly checkpoint (Cross and Smythe 1998; Schwab, Roberts et al. 2001), polar body extrusion (Choi, Fukasawa et al. 1996), metaphase II arrest (Phillips, Petrunewich et al. 2002) and fertilization (Fan and Sun

2004; Li, Lian et al. 2011). All of these studies have utilized pharmacological approaches involving the application of inhibitors such as U0126, which inhibits MAPK-ERK kinase or MEK, the upstream activator of ERKs. However, the granulosa cell-specific function for ERKs in oocyte maturation precludes the use of such inhibitors for understanding oocyte-intrinsic ERK function during meiotic resumption. Moreover, since processes such as oocyte development, ovulation and fertilization are best observed in a physiological milieu, the use of these pharmacological inhibitors on isolated oocytes *in vitro* is inadequate. Therefore, in order to understand the oocyte-intrinsic role of ERK1 and ERK2 during post-prophase I meiotic resumption and fertilization changes, we employed a very specific LoxP-Cre recombinase mediated conditional deletion of *Erk2* on an *Erk1* null background.

3. Materials and Methods

3.1 Generation of the *Erk2* $^{fl/fl}$ *Erk1* $^{-/-}$ mouse

Wildtype control mice and *Zp3-Cre* mice were obtained from Jackson Laboratories. The *Erk1* knockout strain (*Erk2*$^{fl/fl}$*Erk1*$^{-/-}$) have been reported in previous study (Bliss, Miller et al. 2009). Mice with ERK 1/2 double deletion in oocytes were generated by crossing *Zp3-cre* line

with the *Erk2*$^{fl/fl}$ *Erk1*$^{-/-}$ line. All the mice used in this study are on a C57BL/6 background. Animals were housed according to the Cornell University Institutional Animal Care and Use Committee regulations. For breeding studies 6-8 week old female mice were housed two at a time with a wildtype male of proven fertility and checked for vaginal plugs daily. On observation of a plug, the females were housed individually for duration of 21 days after which the litter size was noted.

3.2 Genotyping

Tail snips were used as a source of genomic DNA. PCR genotyping strategies for *Erk1* and *Erk2* were performed as described previously (Bliss, Miller et al. 2009). Cre PCR for confirming the recombination at *Erk2*$^{fl/fl}$ employed the following primers-

Forward: GTCGATGCAACGAGTGATGAGGTTCG and

Reverse: CCAGGCTAAGTGCCTTCTCTACACCTGC.

3.3 Oocyte retrieval and culture

For assessment of GVBD, MI and MII spindle structures, oocytes were collected from ovaries of 21-day-old mice by follicle puncture with a 26.5 gauge needle in M2 medium containing

hyaluronidase (MR 051F, EMD Millipore, Billerica, MA). For superovulation, 4 week old females were injected with PMSG (5 IU, i/p) followed by hCG (5IU, i/p), and oocytes were collected from oviducts the following morning. The oocytes were then transferred to M2 medium without hyaluronidase (MR 015D, EMD Millipore, Billerica, MA) and finally to KSOM medium (MR 020P, EMD Millipore, Billerica, MA) under oil in a 35 mm culture dish. The oocytes were then incubated in conditions of 5% O2 and 5% CO2 at 37C for specific time periods: GVBD (3hrs), MI (~8hrs) and MII (16hrs). MII stage was confirmed by the presence of a polar body.

3.4 Embryo collection and culture

For assessment of early embryo development, females were housed with proven wildtype males and checked for vaginal plugs daily. Upon observation of a plug the female was euthanized and fertilized oocytes were collected from the oviduct in M2 medium with hyaluronidase. Fertilization was confirmed by the presence of two polar bodies. About 10 fertilized oocytes were cultured in a 26 μl droplet of KSOM under oil under conditions of 5% O2 and 5% CO2 at 37C with change of media every 24 hours for 6.5 days.

3.5 Assessment of reproductive competence

Female mice were housed with proven wild type males for 6 days and were checked for copulation plugs daily. Pregnancy was assessed by regular monitoring of body weight and delivery of litters 20-21 days following copulation.

3.6 Vaginal cytology

Vaginal cytological examination was performed to assess the estrous cycles of the *Erk1* SKO and *Erk1/2* DKO animals. Briefly, cytological smears were made from vaginal swabs collected from mice at the same time each day. Slides were allowed to air dry and stained with Wright-Giemsa reagent (VWG-128, Volu-Sol, Sal Lake City, UT) and observed under the light microscope. Stages of the estrous cycle were differentiated based on the morphology and abundance of epithelial cells and leucocytes.

3.7 Detection of implantation

Mice were anesthetized 5.5 days after detection of vaginal plug with 0.5 ml of Avertin (T48402, Sigma-Aldrich, St Louis, MO) and the jugular artery was exposed by resecting skin. 0.1 ml of 1% Pontamine Blue solution in 0.9% saline (Product 34139, BDH Chemicals, Poole, England)

was very slowly injected into the jugular artery. The animals were then euthanized and the uteri were dissected.

3.8 Histology

For immunohistochemical labeling, ovaries were dissected out from 4-6 week old female mice. Tissues were fixed in 4% freshly prepared paraformaldehyde, embedded in paraffin and sectioned at 4 μm onto poly-L Lysine coated glass slides. Quality of sections was determined by hematoxylin and eosin staining as per standard procedure.

3.9 Immunohistochemistry

For immunostaining sections were deparaffinized, rehydrated and treated with 3% hydrogen peroxide. Antigen retrieval was done by boiling in 10mM sodium citrate buffer, pH 6.0. Sections were blocked in 1X TBST/ 5% NGS and incubated with rabbit anti-ERK1/2 antibody (4695, Cell Signaling Technology, Boston, MA) at 1:100 overnight at 4C. HRP conjugated goat anti-rabbit (31460, ThermoScientific, Rockford, IL) was used as secondary antibody. Color development was by Nova-Red (SK 4805, Vector labs, Burlingame, CA).

3.10 Immunofluorescent labeling

Immunofluorescent labeling of oocytes was performed as described previously (Mullen and Critser 2004). Briefly, oocytes were fixed in buffer containing 2% PFA, blocked for 1 hour at room temperature and incubated in primary antibody overnight at 4C. Oocytes were then washed, incubated in secondary antibody at room temperature for 1 hour and mounted in antifade containing DAPI. The cover glass was fixed over the slide using a 1:1 mixture of paraffin and petroleum jelly. Antibodies used were mouse anti-beta tubulin (T8328, Sigma-Aldrich, St Louis, MO), Rabbit anti-ERK 1/2 (4695, Cell Signaling Technology, Boston, MA), mouse anti-Gamma tubulin (ab27074, Abcam, Cambridge, MA), Rabbit anti-MSK1 (3489, Cell Signaling Technology, Boston, MA), Rabbit anti-pMSK1 Thr581(9595, Cell Signaling Technology, Boston, MA) and Rabbit anti-phospho histone H3 Ser10 (6570, EMD Millipore, Billerica, MA).

3.11 Western Blotting

For protein detection with western blot, oocytes were pooled from 4-6 week old superovulated female mice and lysed in 2X Laemelli buffer. Samples were immediately boiled at 95C and cooled on ice. Proteins were separated in an SDS-PAGE electrophoretic system and transferred

onto a Immuno-Blot PVDF membrane (162-0177, BioRad, Hercules, CA). Membranes were probed with mouse anti-beta tubulin (T8328, Sigma-Aldrich, St Louis, MO), Rabbit anti-ERK 1/2 (4695, Cell Signaling Technology, Boston, MA), mouse anti-Gamma tubulin (ab27074, Abcam, Cambridge, MA), Rabbit anti-MSK1 (3489, Cell Signaling Technology, Boston, MA), Rabbit anti-pMSK1 Thr581(9595, Cell Signaling Technology, Boston, MA) and Rabbit anti-phospho histone H3 Ser10 (6570, EMD Millipore, Billerica, MA) according to manufacturer instructions.

3.12 Statistical analysis

Statistical analysis of experiments was done by student t-test and analysis of variance as applicable. All statistical tests were performed using Prism 4.0 software (Graphpad).

3.13 Microscope image acquisition

Acquisition and processing of images was performed by microscope (Imager Z1; Carl Zeiss, Inc.) under a 10x eye-piece and 40× 0.5 NA ECPlan Neofluar air immersion (Carl Zeiss, Inc.) or 63× 1.4 NA Plan Apochromat oil immersion (Carl Zeiss, Inc.) magnifying objective at room temperature, cooled charged-coupled device camera (AxioCam MRm; Carl Zeiss, Inc.) and

AxioVision software (version 4.7.2; Carl Zeiss, Inc.). Images were analyzed using ImageJ program (ImageJ64.app, NIH).

4. Results and Discussion

In order to understand the oocyte-intrinsic role of ERK1 and ERK2 during post-prophase I meiotic resumption and following fertilization, we utilized oocyte-specific *Cre* recombinase mediated conditional deletion of *Erk2* on a background that is null for *Erk1* (Bliss, Miller et al. 2009). Ubiquitous *Erk2* deletion in the mouse results in embryonic lethality (Hatano, Mori et al. 2003; Saba-El-Leil, Vella et al. 2003), and thus we used a floxed allele of *Erk2* (*Erk2* $^{fl/fl}$) together with a null allele of *Erk1* (*Erk1*$^{-/-}$). *Erk1*$^{-/-}$ mice are viable and fertile (Pages, Guerin et al. 1999), while *Erk2* deletion was achieved through the use of a *Zp3-Cre* transgenic mouse in which *Cre* is expressed exclusively in the oocyte from postpartum Day1, prior to completion of the first meiotic division (Lewandoski, Wassarman et al. 1997). The resulting *Erk1*$^{-/-}$.*Erk2*$^{fl/fl}$ *Cre*$^{+}$ mice, hereafter referred to as the *Erk1/Erk2* double knockout or *Erk1/Erk2* DKO, were compared with *Erk1*$^{-/-}$.*Erk2*$^{fl/fl}$.*Cre*$^{-}$ (also known as *Erk1*$^{-/-}$ single nulls, *Erk1* SKO) littermates and wildtype C57 controls.

4.1 Total ERK proteins are absent in the DKO oocytes

ERK1 and ERK2 proteins localize to both the granulosa cell layers and the oocyte in the adult mouse ovary, the levels in the latter increasing upon follicular hormonal stimulation. Staining with anti-ERK antibodies on the *Erk1/Erk2* DKO mouse ovary sections confirmed the loss of ERK protein specifically in oocytes of the DKO mice, with normal ERK protein localization in the surrounding granulosa cell layers (Fig 1a). In *Erk1* SKO, however, ERK staining was still observed within the oocytes at all stages of development. When looking specifically at ERK localization within the oocyte, we observe ERK immunoreactivity on the metaphase I (MI) and metaphase II (MII) spindles in oocytes from wildtype control females (Fig 1B). Residual ERK immunoreactivity was observed in oocytes from *Erk1* SKO, indicating the persistence of ERK2 in these mice, while the total absence of ERK from *Erk1/Erk2* DKO mouse oocytes spindles confirmed the more extensive absence of both ERK1 and ERK2 (Fig 1). Protein detection by western blot on oocyte lysates corroborates the absence of both total ERK and phospho-ERK in the *Erk1/Erk2* DKO oocytes (Fig 1C).

Figure 3.1. Localization of total ERK protein in mouse oocytes.

(A) Total ERK immunoreactivity (red staining) was assessed in sections of adult ovary from wildtype (left panels), *Erk1* SKP (middle panels) and *Erk1/2* DKO females. Loss of the ERK was observed in *Erk1/2* DKO ovary sections, confirming the deletion of both genes in these mice. Scale bar 100 μm. (B) Localization of total ERK protein on meiotic spindles of MII arrested oocytes from wildtype control (Panel i), *Erk1*SKO (Panel ii) and ERK 1/2 DKO (Panel iii) animals with antibodies against ERK 1/2 (Texas-red conjugated) and b-tubulin (FITC conjugated). Panels show, from left to right, merged images from both flurochromes, total ERK 1/2 and chromatin. Total ERK signal is absent in the *Erk1/2* DKO oocytes. Scale bar 10 μm. (C) Absence of total ERK protein in oocyte lysates confirmed by western blot. Wildtype and *Erk1/2* DKO oocyte pools of 100 oocytes each in adjacent lanes, probed by Total ERK antibody and phospho-ERK antibody showing bands (~ 45kDa) in the wildtype lane and absence of bands in the *Erk1/2* DKO lanes. Tubulin used as loading control (~50kDa).

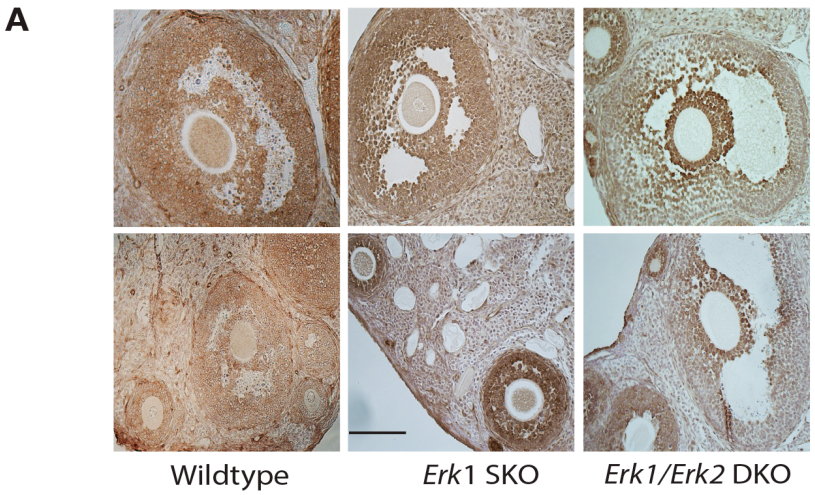
A
Wildtype
Erk1 SKO
Erk1/Erk2 DKO
B
Merge
Total ERK
DAPI
i
ii
iii
Wildtype
Erk1 SKO
Erk1/Erk2 DKO
C
Total ERK
Phospho-ERK
Loading control
(Tubulin)
Erk1 SKO
Erk1/Erk2
DKO

4.2 *Erk1/2* DKO animals have regular estrus cycles but are infertile

Reproductive performance and breeding efficiency were compared between wildtype females and those lacking either one *Erk* gene (*Erk1* SKO) or two (*Erk1/Erk2* DKO). *Erk1/Erk2* DKO mice do not produce any offspring, while *Erk1* SKO females had litter sizes comparable to wildtype controls (Fig 2A). However, *Erk1/Erk2* DKO females undergo normal estrous cycles (Fig S1A,B), mate with normal regularity (Fig S1C), and reach puberty at an equivalent age to that of *Erk1* SKO and wildtype littermate females (Fig 2B, Fig S1B). Thus, despite an apparently normal endocrine milieu in both *Erk1/Erk2* DKO and *Erk1* SKO adult females, the DKO mice fail to produce live offspring.

4.3 *Erk1/2* DKO animals fail to show implantation of embryos

To narrow down the timing of pregnancy failure in the *Erk1/Erk2* DKO females, we assessed implantation rates in the DKO strain using the extravasation of Pontamine blue. This macromolecular dye localizes to sites of high vascular permeability (Boshier 1970), thus allowing for the earliest possible detection of implantation within hours of initial implantation. Intravenous injection of Pontamine blue at day 4.5 after plug formation into *Erk1* SKO females showed normal appearance and frequency of blue bands across both uterine horns, each band corresponding to a single implanting embryo (Fig. 2C) at frequencies that were similar to that of

wildtype females. By contrast, Pontamine blue injection into *Erk1/Erk2* DKO females showed a complete absence of the blue banding across the uterus, indicative of no implantation-stage embryos or failed implantation at this stage.

4.4 *Erk1/2* DKO animals show normal folliculogenesis and ovulation rates

To differentiate between failed implantation, failed oogenesis/ovulation, and failed fertilization in *Erk1/Erk2* DKO females, we undertook a sequential analysis of female ovarian histology and folliculogenesis. Comparison of the ovarian histology between *Erk1* SKO, *Erk1/Erk2* DKO, and wildtype females revealed no gross morphological differences (Fig 2D). All stages of oocyte development were noted in ovarian sections from the DKO females. The appearance and abundance of ovarian follicles also appeared to be similar in mice of all three genotypes. The presence of numerous corpora lutea (CL) indicated that ovulation occurs in the single and double knockout mice. Indeed, treatment of *Erk1* SKO, *Erk1/Erk2* DKO, and wildtype females with exogenous gonadotropins to induce ovarian hyperstimulation resulted in the ovulation of similar numbers of oocytes in mice from all three genotypes (Fig 2E). Thus, folliculogenesis, ovulation, and post-ovulatory CL formation are not dependent on ERK activity within the oocyte.

Figure 3.2. Evaluation of reproductive phenotypes of the *Erk1/2* DKO females.

(A) Data from breeding studies conducted on age-matched wildtype, *Erk1* SKO and *Erk1/2* DKO females, mated to fertile wildtype males. Average litter size expressed as mean + standard error of the mean (SEM). (B) Results from vaginal cytology performed at 24 hour intervals in *Erk1* SKO (n=17) and *Erk1/2* DKO (n=23) animals are shown as mean + SEM of the number of estrous cycles reached in 26 days. P= 0.85. (C) Implantation rates were assessed in *Erk1* SKO and *Erk1/2* DKO animals at day 5.5 post-coitus by intravenous Pontamine Sky blue dye injection. (D) Histological assessment of ovaries from wildtype control, *Erk1* SKO and *Erk1/2* DKO was done on H&E stained sections. Scale bars for left hand three panels, 200 μm. Scale bars for middle and right hand panels (six panels in total), 50 μm. (E) Ovulation rates were assessed by superovulation with exogenous gonadotropin administration. Numbers indicate the number of ova collected per group.

A

	Wildtype	*Erk1* SKO	*Erk1/Erk2* DKO
Number of litters	9	15	15
Total pups born	50	82	0
Average litter size ±SD	5.55 ±0.58	5.46 ±0.45	0

B

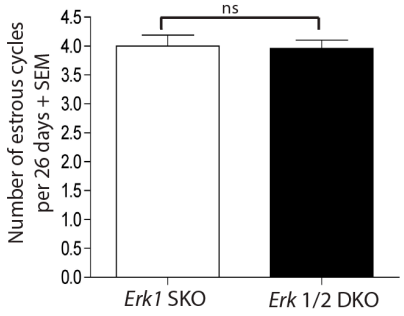

C

D

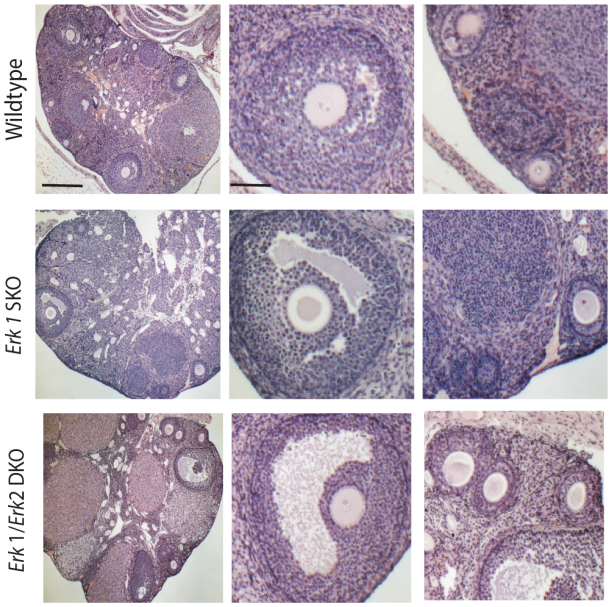

E

Wt (n=4)	*Erk1*$^{-/-}$ (n=4)	*Erk1/ Erk2* DKO (n=4)
51	43	46

4.5 *Erk1/2* DKO females show progressive embryo death following fertilization

Since ovulation was observed to be normal in the *Erk1/Erk2* DKO females, we next looked into development following fertilization in the *Erk1/Erk2* DKO oocytes. Females were mated with wildtype males, to produce heterozygous zygotes, which were then cultured *in vitro*. When cultured, fertilized oocytes from *Erk1/Erk2* DKO females showed significant death rate at each stage of development (Fig 3A,B) with a very small percentage (3%) of embryos reaching the blastocyst stage in the absence of both ERKs. *Erk1* SKO females also showed progressive loss of fertilized oocytes, though not to the same extent as that seen in *Erk1/Erk2* DKO females. This indicates that the functions of ERK1 and ERK2 in the oocyte may not be redundant. The gross morphology of one-cell and two-cell embryos from the *Erk1/Erk2* DKO mice did not differ from the embryos of *Erk1* SKO or wildtype females (Fig 3A). Clearly, the presence of paternally derived ERKs in one-cell and two-cell embryos is not sufficient to prevent the developmental defects that result in progressive loss of pre-implantation embryos, indicating strongly that the cause of the embryo loss lies with the loss of ERKs in the oocyte.

4.6 *Erk1/2* DKO oocytes show normal rates of meiotic resumption in culture

Meiotic resumption is initially marked by germinal vesicle breakdown (GVBD) in the oocyte, and is dependent on MAPK activity in surrounding granulosa cells (Abrieu, Doree et al. 2001;

Liang, Su et al. 2007; Fan, Liu et al. 2009). High levels of MAPK cause closure of gap junctions between granulosa cells and the oocyte by the phosphorylation of gap-junction protein Connexin 43 (Norris, Freudzon et al. 2008; Norris, Ratzan et al. 2009; Sun, Miao et al. 2009), thereby disrupting the supply of cAMP to the oocyte (Liang, Su et al. 2007; Norris, Ratzan et al. 2009; Tripathi, Kumar et al. 2010). This net reduction in cAMP causes inactivation of protein kinase A leading to the activation of Cyclin B-CDK1 complex (MPF) by dephosphorylation of CDK1 (Oh, Han et al. 2010) and subsequently, GVBD. Since *Erk2* expression is not disrupted in the granulosa cells of the *Erk1/Erk2* DKO mutant females, we predicted that meiotic resumption, as measured by GVBD, would not be affected in the double mutants. As expected, resumption of meiosis in oocytes collected from large antral follicles in of *Erk1* SKO and *Erk 1/Erk2* DKO mutants was similar to that seen in wildtype controls (Fig S2A), indicating that oocyte ERK activity is not required for meiotic resumption. These observations contradict earlier studies in which pharmacological activation of the intra-oocyte MAPK pathway results in activation of MPF, in turn leading to GVBD (Fissore, He et al. 1996; Liang, Su et al. 2007).

Figure 3.3. Evaluation of early embryonic development *in vitro* using oocytes harvested from wildtype, *Erk1* SKO, and *Erk1/2* DKO females. (A) Images showing each of the four stages represented in the graph (B) from *Erk1* SKO and *Erk1/2* DKO animals. Scale bar, 100 μm. (B) Quantitation of oocyte development: Fertilized oocytes were collected from the oviducts of wildtype controls (n=8), *Erk1* SKO (n=8) and *Erk1/2* DKO (n=9) animals mated with wildtype males and cultured till blastocyst stage. Percentages indicated in each stage are with respect to total fertilized oocytes in the respective group. Values for each group were compared by One-way ANOVA, $P<0.01$.

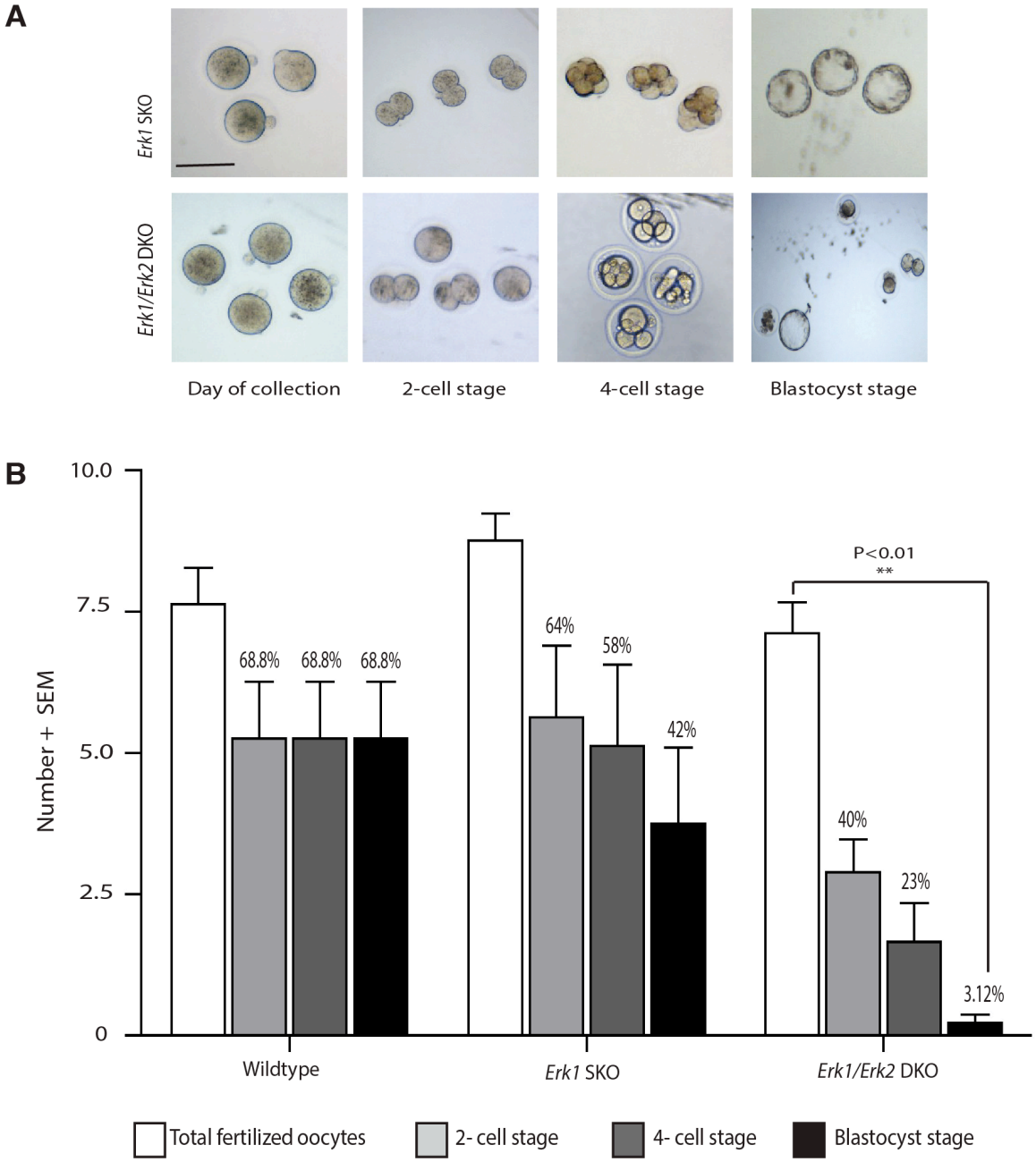
A
Erk1 SKO
Erk1/Erk2 DKO
Day of collection
2-cell stage
4-cell stage
Blastocyst stage
B
Number + SEM
10.0
7.5
5.0
2.5
0
68.8%
68.8%
68.8%
64%
58%
42%
40%
23%
3.12%
P<0.01
**
Wildtype
Erk1 SKO
Erk1/Erk2 DKO
Total fertilized oocytes
2- cell stage
4- cell stage
Blastocyst stage

4.7 *Erk1/2* DKO oocytes demonstrate severe defects in spindle assembly, chromosome segregation and polar body formation

Following GVBD, the oocyte proceeds into the first meiotic division and finally to meiosis II (metaphase stages of these being referred to as MI and MII respectively). Absence of ERKs, as seen in *Mos*$^{-/-}$ oocytes and pharmacological disruption of MEK 1 and 2, results in abnormal spindle assembly at MI (Araki, Naito et al. 1996; Choi, Fukasawa et al. 1996; Fan and Sun 2004) and MII (Yu, Xiong et al. 2007). MAPKs play an important role in the formation and maintenance of a bipolar spindle in both MI and MII (Verlhac, de Pennart et al. 1993; Liang, Su et al. 2007; Yu, Xiong et al. 2007), but this requirement has only been studied thus far by pharmacological methods. Using our mouse models for genetic loss of *Erk1* and *Erk2,* we observed that the MII spindle structure of the *Erk1/Erk2* DKO oocytes was grossly abnormal compared to that seen in oocytes from wildtype (Fig 4A, panel a) and *Erk1* SKO females (Fig 4A, panel b). Chromosome placement at the metaphase plate in the *Erk1/Erk2* DKO females showed significant rates of misalignment, while the spindle itself had a less compact appearance in the *Erk1/Erk2* DKO oocytes, characterized by a more diffuse staining pattern of anti β-tubulin antibody and a less compact appearance of microtubules on the spindles (Fig 4A, panels c(i)-c(iii)). Quantitation of spindle abnormalities showed a significant increase in the percentage of

oocytes exhibiting chromosome misalignment as compared to wildtype and *Erk1* SKO oocytes (Fig 4B).

MAPKs have also been shown to associate with the microtubule-organizing center (MTOC) at spindle poles during meiosis (Verlhac, de Pennart et al. 1993). Further analysis of the spindle structure revealed an abnormality in the spindle MTOC at the spindle poles based on gamma-tubulin immunostaining patterns. MTOCs of wildtype oocytes had the normal ring shape (Ou, Li et al. 2010), while that of the *Erk1/Erk2* DKO oocytes appeared to be severely fragmented (Fig 4C), indicating that spindle defects may be caused by abnormal nucleation of microtubules. These phenotypes, together with the association of ERKs with γ-tubulin, demonstrate that the ERKs play an important role in microtubule nucleation, organization and dynamics(Verlhac, de Pennart et al. 1993; Fan and Sun 2004).

ERKs are thought to regulate spindle migration to the cortex via their action on microfilament network in oocytes (Sun, Lai et al. 2001), thereby ensuring the asymmetric division that is essential for preserving the accumulated stores of proteins within the oocytes (Chaigne, Verlhac et al. 2012). Pharmacological inhibition at any step of the ERK pathway, therefore, leads to improper migration of the spindle, extrusion of bigger polar bodies and hence, a loss of resources for the developing embryo (Verlhac, Lefebvre et al. 2000; Chaigne, Verlhac et al. 2012). The

Figure 3.4. Morphology and quantitation of oocyte defects in *Erk1/2* DKO females. (A) MII arrested oocytes from wildtype control (n= 20), *Erk1* SKO (n= 20) and *Erk1/2* DKO (n= 18) animals were immunolabelled with antibody against b tubulin (Texas- Red conjugated in panel A, FITC conjugated in panels B and C) and with DAPI to visualize chromatin. Arrows indicate chromosomes that are misaligned on the spindle. Scale bar, 10 μm. (B) Polar body size by measurement of diameter shown as a percentage of total oocyte diameter in wildtype (n=10) and *Erk1/2* DKO (n=10) oocytes. Bars represent mean + standard error of the mean (SEM). Statistical comparisons were performed using Student's unpaired T tests, $P<0.0001$. (C) Comparison of spindle MTOC structure by gamma tubulin immunolabeling of *Erk1* SKO (n= 5) and *Erk1/2* DKO (n= 7). Arrow indicates MTOC at the spindle pole. (D) Percentages of misaligned chromosomes on MII spindles were calculated in oocytes from wildtype controls (n= 72), *Erk1* SKO (n= 67) and *Erk1/2* DKO (n= 73). Bars represent mean + SEM. Statistical comparisons were performed using one-way ANOVA, followed by Tukey's multiple comparison test, p= 0.048. (E) Pole-to-pole spindle lengths were measured in spindles from MII arrested oocytes from wildtype controls (n= 20), *Erk1* SKO (n= 20) and *Erk1/2* DKO (n= 20). Bars represent mean + SEM. Statistical comparisons were performed using one-way ANOVA, followed by Tukey's multiple comparison test, p= 0.017.

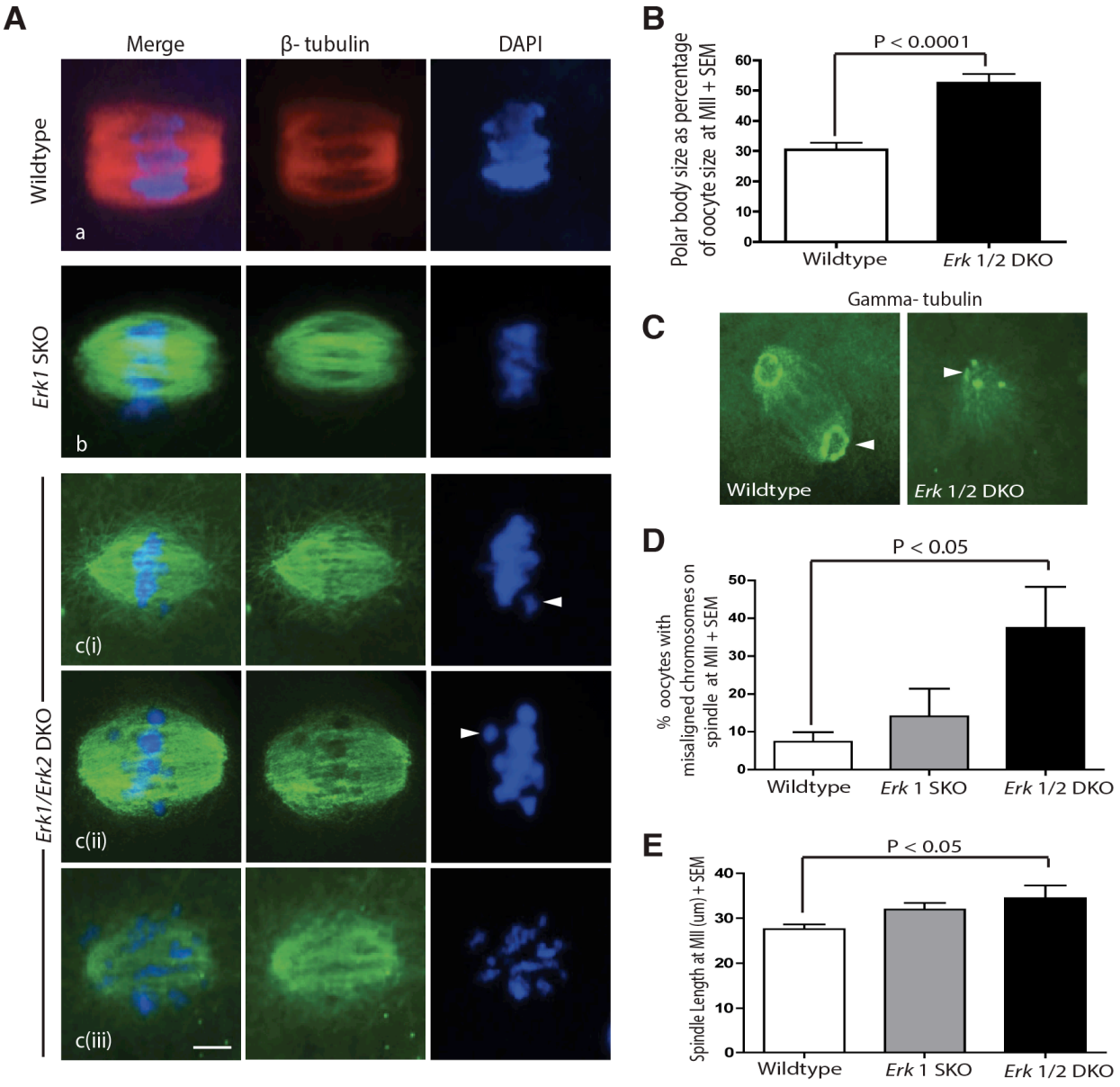
A
Merge
β- tubulin
DAPI
Wildtype
a
Erk1 SKO
b
Erk1/Erk2 DKO
c(i)
c(ii)
c(iii)
B
P < 0.0001
Polar body size as percentage of oocyte size at MII + SEM
60
50
40
30
20
10
0
Wildtype
Erk 1/2 DKO
C
Gamma- tubulin
Wildtype
Erk 1/2 DKO
D
P < 0.05
% oocytes with misaligned chromosomes on spindle at MII + SEM
50
40
30
20
10
0
Wildtype
Erk 1 SKO
Erk 1/2 DKO
E
P < 0.05
Spindle Length at MII (um) + SEM
40
30
20
10
0
Wildtype
Erk 1 SKO
Erk 1/2 DKO

polar body size with respect to the size of the oocyte was observed to be significantly higher in the *Erk1/Erk2* DKO females (Fig 4D). Pole-to-pole spindle length was significantly higher in oocytes from *Erk1/Erk2* DKO females (Fig 4E). However, the width of the MII spindle across the midplate, and the distance of the spindle from the cortex did not show any significant differences between the genotypes (Fig S3A,B).

4.8 *Erk1/2* DKO oocytes exhibit deficiency of phosphorylation of kinase downstream of ERK1 and ERK2.

To elucidate the downstream signaling events for ERK1 and ERK2 in the oocyte, we examined the phosphorylation status of classic ERK targets such as Ribosomal S6 Kinase (RSK) and Mitogen and Stress activated protein Kinase (MSK1). Of these MSK1 showed differential phosphorylation status in the *Erk1/Erk2* DKO oocytes (Fig 5A,B), while RSK1/2/3, previously thought to be the canonical downstream targets of the MAPK pathway during meiotic maturation, showed no such change (data not shown). Whereas oocytes from wildtype females show an accumulation of phospho-MSK1 (p-MSK1) on the MII spindle, *Erk1/Erk2* DKO oocytes show a complete absence of p-MSK1 (Fig 5A). Absence of p-MSK1 was further demonstrated in the *Erk1/Erk2* DKO oocytes by western blotting (Fig 5B) while total MSK1 levels were similar in both the *Erk1/Erk2* DKO oocytes and the control (Fig S4). So far one

study on mouse oocytes the possible involvement of MSK1 in oocyte division. In that, the authors shown a similar localization of pMSK1 on the metaphase II spindle and an absence of MSK1 phosphorylation in the presence of MEK inhibitor U0126, confirming the phosphorylation of MSK1 by the MAPK pathway (Miyagaki, Kanemori et al. 2011). Moreover, pharmacological inhibition of MSK1 produced absence of a bipolar MII spindle and failure to maintain sister chromatid alignment at the metaphase plate (Miyagaki, Kanemori et al. 2011). Pharmacological inhibition of MSK1 was involved in spontaneous release from MII arrest possibly due to defective phosphorylation of Emi2 (Miyagaki, Kanemori et al. 2011). However, because we did not observe a significant increase in spontaneous release from MII arrest (Fig S5), we investigated other possible pathways of MSK1 activity in oocytes.

4.9 *Erk1/2* DKO oocytes demonstrate reduction in the phosphorylation status of chromatin condensation factor Histone H3.

The actual biological pathway of MSK1 is not completely understood as *Msk1*$^{-/-}$ mice are viable and fertile (Drobic, Espino et al. 2004). In mouse fibroblasts, the ERK signaling pathway has been shown to elevate activated (phosphorylated) MSK1 levels, resulting in the elevation of steady-state levels of Serine10 phosphorylated Histone-3 (H3S10), a target of MSK1(Drobic, Espino et al. 2004). Phospho-histone H3 plays a central role in chromosome condensation and

spindle assembly during mitosis in *Drosophila* (Giet and Glover 2001) making it a strong candidate in the ERK-mediated control of oocyte division and spindle function, as demonstrated by our current data. Moreover, morpholino knockdown of histone H3.3, a variant of histone H3, results in mis-segregation of chromosomes, aneuploidy and developmental arrest of early mouse embryos (Lin, Conti et al. 2013). Analysis of histone H3 function in our *Erk* deficient oocytes shows a significant reduction in the levels of phosphorylated H3 at Serine 10 in the *Erk1/Erk2* DKO oocytes (Fig 5C). Immunohistochemical staining of oocytes demonstrated the localization of p-H3S10 on the chromosomes of MII spindles; however, this localization was significantly reduced in the *Erk1/Erk2* DKO oocytes (Fig 5D,E). This suggests that MSK1 phosphorylation by ERKs may play a key role in maintaining spindle integrity via its action on chromatin condensation factors such as histone H3.

Figure 3.5. Identification of downstream signaling targets of ERK1/2 in mouse oocytes. (A) MII arrested oocytes from wildtype control (n= 15) and *Erk1/2* DKO (n= 17) animals were immunolabelled with antibody against b tubulin (Texas- Red conjugated), phospho-MSK1 (FITC conjugated) and with DAPI to visualize chromatin. Arrows indicate co-localization of pMSK1 on the spindle. Scale bar, 10 μm. (B) Absence of phospho-MSK1 in oocyte lysates confirmed by western blot. Wildtype and *Erk1/2* DKO oocyte pools of 80 oocytes each in adjacent lanes, probed by phospho-MSK1 antibody showing band (~ 90kDa) in the wildtype lane and absence of band in the *Erk1/2* DKO lanes. Tubulin used as loading control (~50kDa). (C) Analysis of phospho-Histone H3 in oocyte lysates confirmed by western blot. Wildtype and *Erk1/2* DKO oocyte pools of 80 oocytes each in adjacent lanes, probed by phospho-H3S10 antibody showing band (~ 17kDa) in the wildtype lane and absence of band in the *Erk1/2* DKO lanes. Tubulin used as loading control (~50kDa). (D) MII arrested oocytes from wildtype control (n= 10) and *Erk1/2* DKO (n= 10) animals were immunolabelled with antibody against phospho-H3S10 (FITC conjugated) and with DAPI to visualize chromatin. Fluorescence intensity measured with ImageJ (E), and quantitated as Corrected Total Cell Fluorescence (CTCF) calculated in oocytes from wildtype controls (n= 10) and *Erk1/2* DKO (n= 10). Bars represent mean + SEM. p= 0.0009

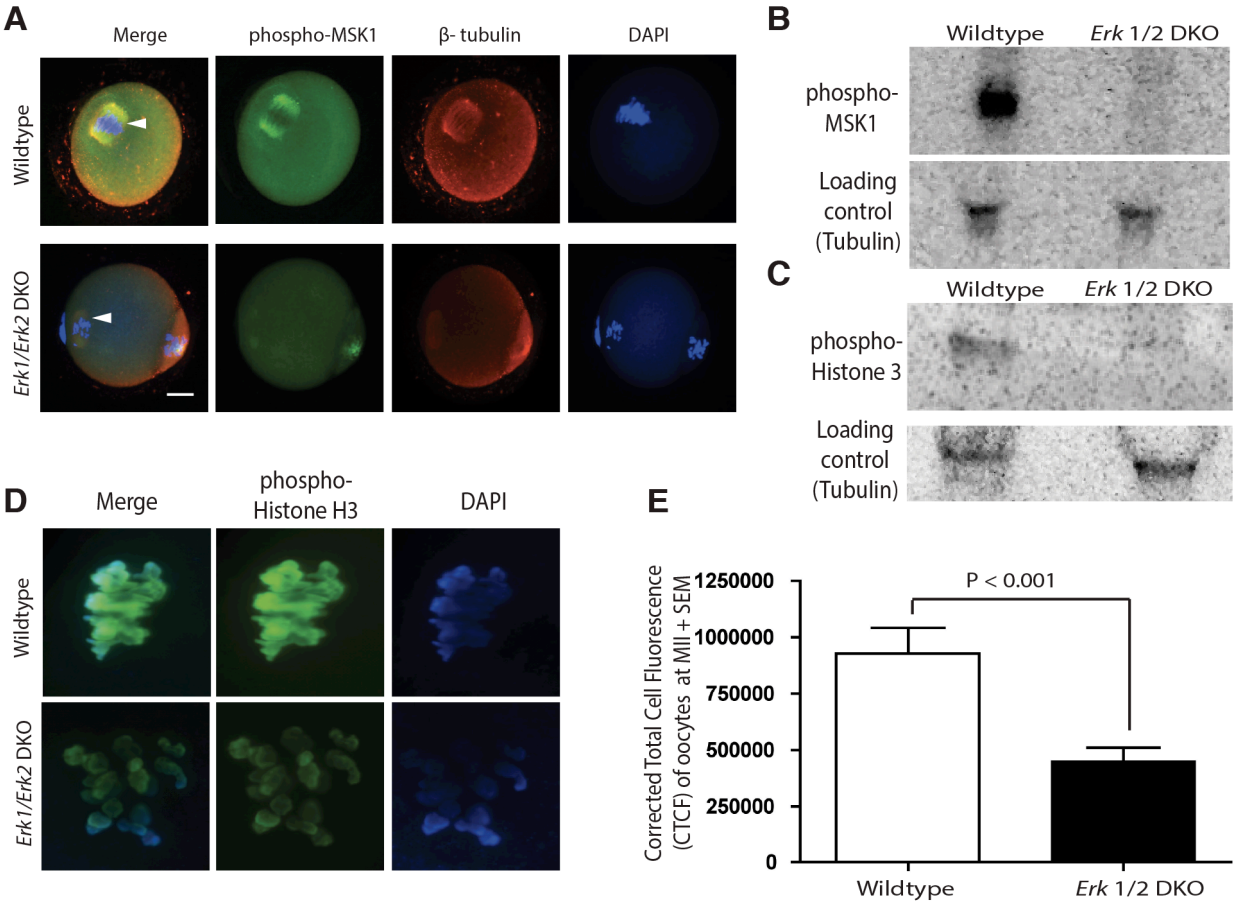
A
Merge
phospho-MSK1
β- tubulin
DAPI
Wildtype
Erk1/Erk2 DKO
B
Wildtype
Erk 1/2 DKO
phospho-MSK1
Loading control (Tubulin)
C
Wildtype
Erk 1/2 DKO
phospho-Histone 3
Loading control (Tubulin)
D
Merge
phospho-Histone H3
DAPI
Wildtype
Erk1/Erk2 DKO
E
Corrected Total Cell Fluorescence (CTCF) of oocytes at MII + SEM
1250000
1000000
750000
500000
250000
0
P < 0.001
Wildtype
Erk 1/2 DKO

5. Conclusions

Our work on the *Erk1/Erk2* DKO mice demonstrates a specific requirement for ERK1 and ERK2 for proper function of, and chromosome placement on, the MI and MII spindles. Taken together, our data demonstrate an essential role for ERK signaling in meiotic resumption and progression through fertilization in the mouse. Specifically, combined loss of ERK1 and ERK2 drastically alters spindle function and chromosome placement that, in turn, results in abnormal oocyte division and embryo loss prior to implantation. We cannot exclude, however, the possibility that the abnormal oocyte cytokinesis at MI and MII, as demonstrated by larger polar bodies, may result in loss of resources required for proper embryo development, and that this may contribute to the embryonic loss prior to implantation. Furthermore, the fact that these embryos are themselves heterozygous for *Erk1* and *Erk2* could suggest that ERK-dependent events in the oocyte are essential for survival of the post-fertilization pre-implantation embryo, and that any potential rescue by paternal *Erk* gene expression is inadequate or mis-timed.

Our studies also demonstrate for the first time that ERK signaling in the oocyte is required for phosphorylation of at least one downstream target, MSK1, whose localization on the MII spindle is, in turn required for phosphorylation of histone H3. Our data point to an essential role for phosphorylated histone H3 in maintaining spindle integrity at the second meiotic division. Loss

of this MSK1-mediated phosphorylation event leads to disrupted MTOC structure, and an inability to properly assemble chromosomes on the MII spindle, and subsequent aneuploidy leading to pre-implantation embryonic demise. Thus, our data indicate that ERK signaling, while not required for oocyte activation *per se,* is instead essential for the assembly and normal function of the MII spindle in the mammalian oocyte.

Previous studies with upstream pharmacological inhibitors (Petrunewich, Trimarchi et al. 2009) and antisense oligomers (Ou, Li et al. 2010) have shown the involvement of the ERK pathway and other MAPK modules in these events but so far, specific involvement of ERKs have not been studied. Moreover, while previous studies on ERK disruption in oocytes have demonstrated severe spindle defects, such studies involving the use of pharmacological inhibitors are limited by factors such as cell permeability, necessitating the use of much higher concentrations (100-1000 fold) than cell free assays (MacKintosh and MacKintosh 1994). This may have an effect on the severity of spindle disruption phenotype displayed in these results. Our use of oocyte-specific genetic knockout of ERKs provides an insight into the action of these kinases on spindle dynamics and also provides a method for continued assessment of the action of possible downstream targets of ERKs, including those that involve MSK1-driven alterations in histone status.

6. Supplementary Materials

Figure 3.S1. Evaluation of estrous cycle duration and resumption of meiosis in *Erk1/2* DKO females. (A) Estrous cycle length determined in each genotype by taking average of estrous duration in each animal. Values found to be non-significant by Student t-test, p= 0.98. (B) Estrous cycles were assessed by the type and abundance of cells in the vaginal smear of each genotype. *Erk1* SKO (n= 17) and *Erk1/2* DKO (n= 23). (C) Mating efficiency of *Erk1* SKO (n= 8) and *Erk1/2* DKO (n= 8) measured by the presence of vaginal plugs. (D) Percentage of oocytes showing germinal vesicle breakdown in each genotype. Wildtype (n=15), *Erk 1*$^{-/-}$ (n=16) and *Erk 1/2 DKO* (n= 13). Statistical comparisons using one-way ANOVA, p= 0.106.

Estrous cycles, mating frequency and GVBD rates normal in Erk1/2 DKO

A

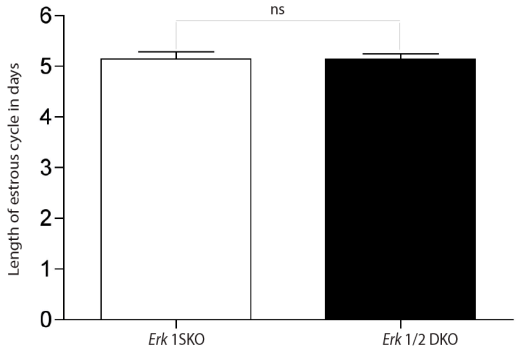

B

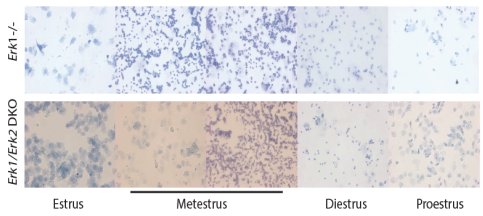

C

	*Erk1*SKO	*Erk1/Erk2* DKO
Number used for mating	8	8
Number plugged	7	6

D

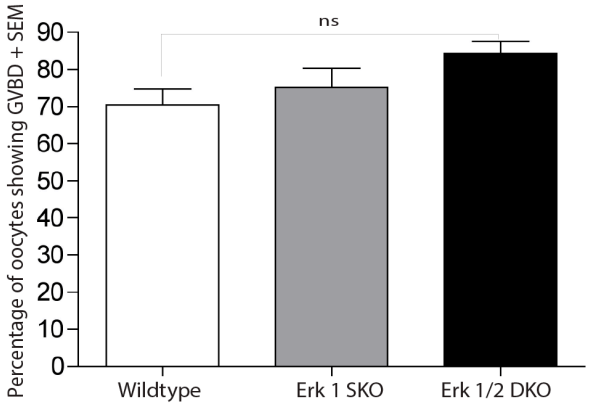

Figure 3.S2. Dimensions and position of the MII spindle in *Erk1* SKO and *Erk1/2* DKO oocytes. (A) Width of the spindle measured in the middle at the widest part from wildtype controls (n= 20), *Erk1* SKO (n= 20) and *Erk1/2* DKO (n= 18). Bars represent mean + SEM. One-way ANOVA with Tukey's multiple comparison test showed p= 0.001 with significant difference between *Erk1*$^{-/-}$ and wildtype spindle length. (B) Distance of the MII spindle from the cortex of the oocyte from wildtype controls (n= 4), *Erk1* SKO (n= 12) and *Erk1/2* DKO (n= 9). Bars represent mean + SEM. Kruskal-Wallis test used p= 0.075

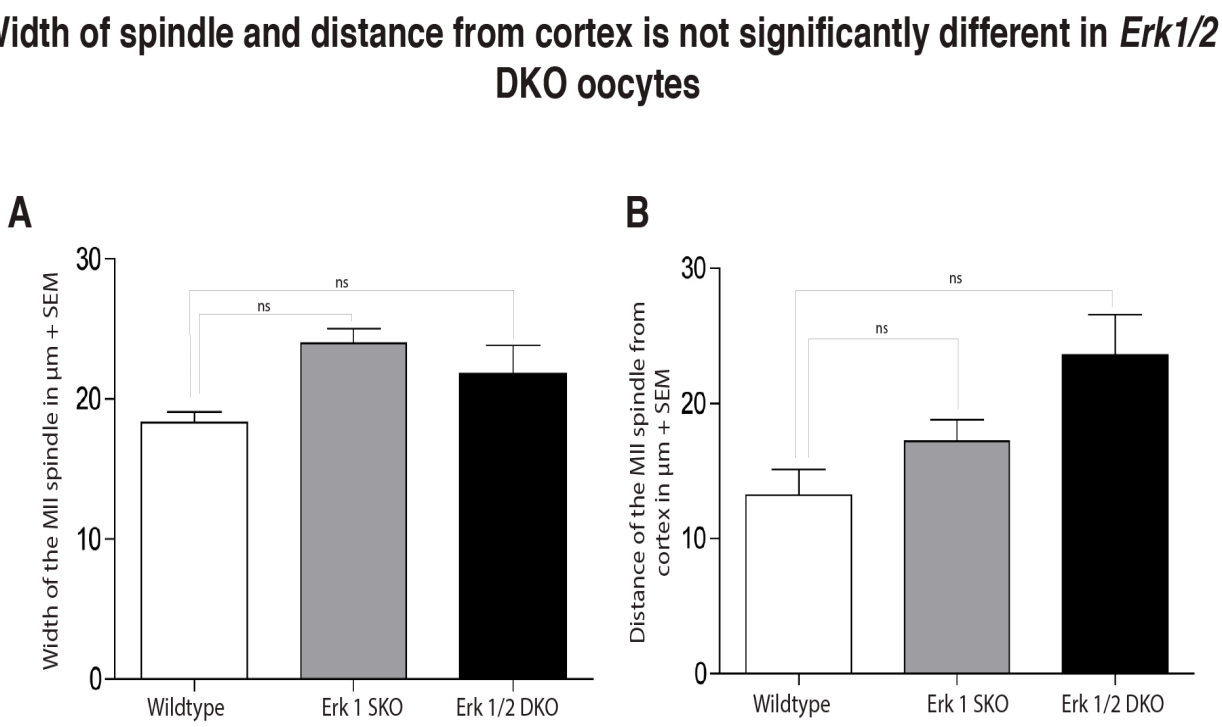

Figure 3.S3. Total MSK1 and spontaneous release from MII arrest in *Erk1/2* DKO oocytes.

(A) Presence of Total MSK1in oocyte lysates confirmed by western blot. Wildtype and *Erk1/2* DKO oocyte pools of 80 oocytes each in adjacent lanes, probed by MSK1 antibody showing band (~ 90kDa) in both the wildtype and the *Erk1/2* DKO lanes. Tubulin used as loading control (~50kDa). (B) Percentage of oocytes showing spontaneous entry into Anaphase II. Wildtype (n=72), *Erk1* SKO (n= 67) and *Erk1/2* DKO (n= 73) where n is the number of oocytes counted in each group. Kruskal-Wallis test used p= 0.104

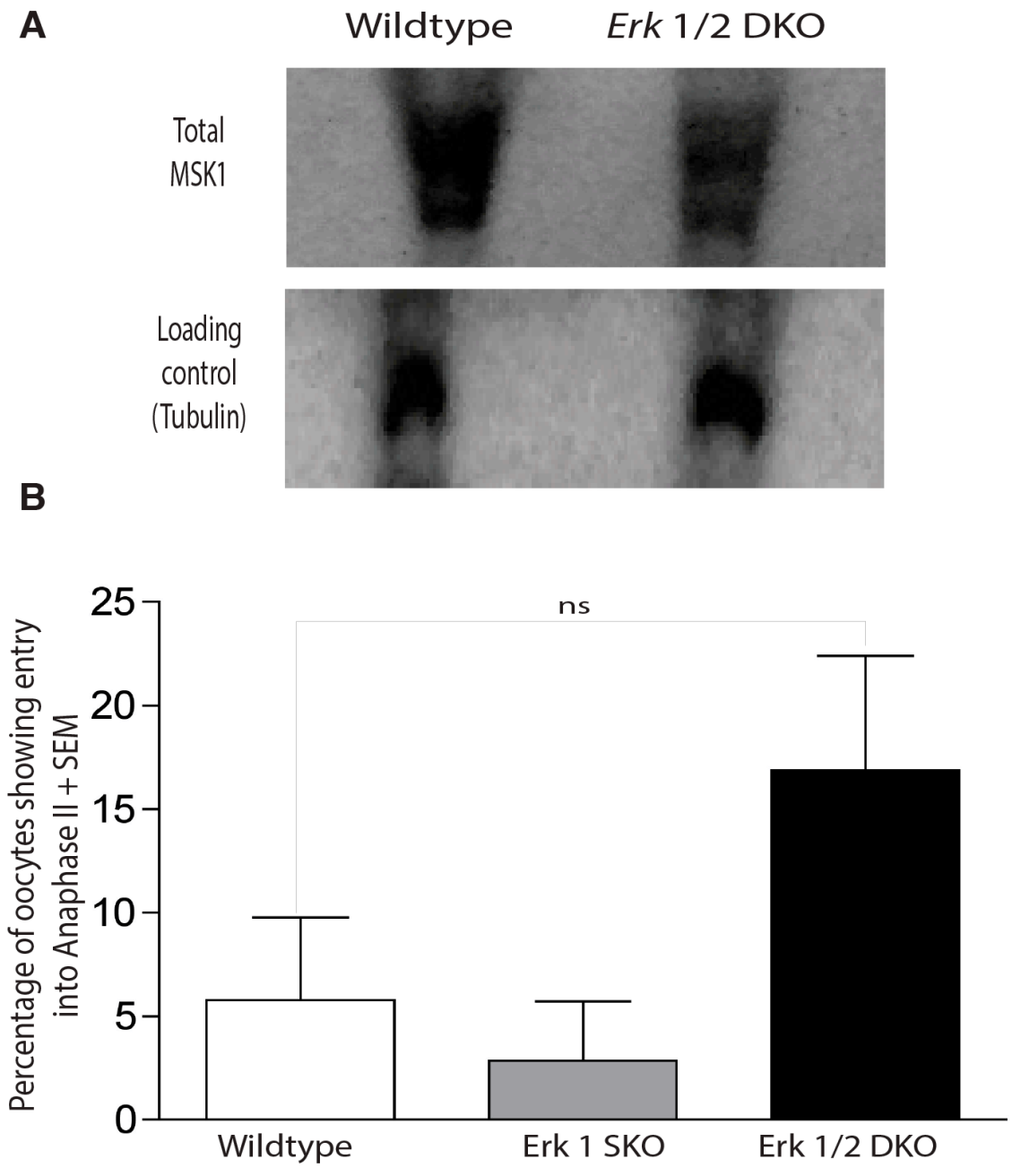
A
Wildtype
Erk 1/2 DKO
Total MSK1
Loading control (Tubulin)
B
ns
Percentage of oocytes showing entry into Anaphase II + SEM
25
20
15
10
5
0
Wildtype
Erk 1 SKO
Erk 1/2 DKO

7. References

Abrieu, A., M. Doree, et al. (2001). "The interplay between cyclin-B-Cdc2 kinase (MPF) and MAP kinase during maturation of oocytes." Journal of cell science **114**(Pt 2): 257-267.

Araki, K., K. Naito, et al. (1996). "Meiotic abnormalities of c-mos knockout mouse oocytes: activation after first meiosis or entrance into third meiotic metaphase." Biology of reproduction **55**(6): 1315-1324.

Bhatt, R. R. and J. E. Ferrell, Jr. (1999). "The protein kinase p90 rsk as an essential mediator of cytostatic factor activity." Science **286**(5443): 1362-1365.

Bliss, S. P., A. Miller, et al. (2009). "ERK signaling in the pituitary is required for female but not male fertility." Molecular endocrinology **23**(7): 1092-1101.

Boshier, D. P. (1970). "The pontamine blue reaction in pregnant sheep uteri." Journal of reproduction and fertility **22**(3): 595-596.

Cameron, M. R., J. S. Foster, et al. (1996). "Activation of mitogen-activated protein kinases by gonadotropins and cyclic adenosine 5'-monophosphates in porcine granulosa cells." Biology of reproduction **55**(1): 111-119.

Cargnello, M. and P. P. Roux (2011). "Activation and function of the MAPKs and their substrates, the MAPK-activated protein kinases." Microbiology and molecular biology reviews : MMBR **75**(1): 50-83.

Chaigne, A., M. H. Verlhac, et al. (2012). "Spindle positioning in mammalian oocytes." Experimental cell research.

Choi, T., K. Fukasawa, et al. (1996). "The Mos/mitogen-activated protein kinase (MAPK) pathway regulates the size and degradation of the first polar body in maturing mouse oocytes." Proceedings of the National Academy of Sciences of the United States of America **93**(14): 7032-7035.

Cross, D. A. and C. Smythe (1998). "PD 98059 prevents establishment of the spindle assembly checkpoint and inhibits the G2-M transition in meiotic but not mitotic cell cycles in Xenopus." Experimental cell research **241**(1): 12-22.

Drobic, B., P. S. Espino, et al. (2004). "Mitogen- and stress-activated protein kinase 1 activity and histone h3 phosphorylation in oncogene-transformed mouse fibroblasts." Cancer research **64**(24): 9076-9079.

Fan, H. Y., Z. Liu, et al. (2009). "MAPK3/1 (ERK1/2) in ovarian granulosa cells are essential for female fertility." Science **324**(5929): 938-941.

Fan, H. Y. and Q. Y. Sun (2004). "Involvement of mitogen-activated protein kinase cascade during oocyte maturation and fertilization in mammals." Biology of reproduction **70**(3): 535-547.

Fissore, R. A., C. L. He, et al. (1996). "Potential role of mitogen-activated protein kinase during meiosis resumption in bovine oocytes." Biology of reproduction **55**(6): 1261-1270.

Giet, R. and D. M. Glover (2001). "Drosophila aurora B kinase is required for histone H3 phosphorylation and condensin recruitment during chromosome condensation and to organize the central spindle during cytokinesis." The Journal of cell biology **152**(4): 669-682.

Hatano, N., Y. Mori, et al. (2003). "Essential role for ERK2 mitogen-activated protein kinase in placental development." Genes to cells : devoted to molecular & cellular mechanisms **8**(11): 847-856.

Kang, S. K., C. J. Tai, et al. (2000). "Gonadotropin-releasing hormone activates mitogen-activated protein kinase in human ovarian and placental cells." Molecular and cellular endocrinology **170**(1-2): 143-151.

Lewandoski, M., K. M. Wassarman, et al. (1997). "Zp3-cre, a transgenic mouse line for the activation or inactivation of loxP-flanked target genes specifically in the female germ line." Curr Biol **7**(2): 148-151.

Li, J. J., H. Y. Lian, et al. (2011). "Regulation of fusion of the nucleolar precursor bodies following activation of mouse oocytes: roles of the maturation-promoting factors and mitogen-activated protein kinases." Zygote: 1-13.

Liang, C. G., Y. Q. Su, et al. (2007). "Mechanisms regulating oocyte meiotic resumption: roles of mitogen-activated protein kinase." Molecular endocrinology **21**(9): 2037-2055.

Lin, C. J., M. Conti, et al. (2013). "Histone variant H3.3 maintains a decondensed chromatin state essential for mouse preimplantation development." Development **140**(17): 3624-3634.

MacKintosh, C. and R. W. MacKintosh (1994). "Inhibitors of protein kinases and phosphatases." Trends in biochemical sciences **19**(11): 444-448.

Madgwick, S., D. V. Hansen, et al. (2006). "Mouse Emi2 is required to enter meiosis II by reestablishing cyclin B1 during interkinesis." The Journal of cell biology **174**(6): 791-801.

Miyagaki, Y., Y. Kanemori, et al. (2011). "Possible involvement of mitogen- and stress-activated protein kinase 1, MSK1, in metaphase-II arrest through phosphorylation of EMI2 in mouse oocytes." Developmental biology **359**(1): 73-81.

Mullen, S. F. and J. K. Critser (2004). "Immunocytochemical staining of the metaphase II spindle in mammalian oocytes." Methods in molecular biology **253**: 201-213.

Norris, R. P., M. Freudzon, et al. (2008). "Luteinizing hormone causes MAP kinase-dependent phosphorylation and closure of connexin 43 gap junctions in mouse ovarian follicles: one of two paths to meiotic resumption." Development **135**(19): 3229-3238.

Norris, R. P., W. J. Ratzan, et al. (2009). "Cyclic GMP from the surrounding somatic cells regulates cyclic AMP and meiosis in the mouse oocyte." Development **136**(11): 1869-1878.

Oh, J. S., S. J. Han, et al. (2010). "Wee1B, Myt1, and Cdc25 function in distinct compartments of the mouse oocyte to control meiotic resumption." The Journal of cell biology **188**(2): 199-207.

Ou, X. H., S. Li, et al. (2010). "p38alpha MAPK is a MTOC-associated protein regulating spindle assembly, spindle length and accurate chromosome segregation during mouse oocyte meiotic maturation." Cell cycle **9**(20): 4130-4143.

Pages, G., S. Guerin, et al. (1999). "Defective thymocyte maturation in p44 MAP kinase (Erk 1) knockout mice." Science **286**(5443): 1374-1377.

Petrunewich, M. A., J. R. Trimarchi, et al. (2009). "Second meiotic spindle integrity requires MEK/MAP kinase activity in mouse eggs." The Journal of reproduction and development **55**(1): 30-38.

Phillips, K. P., M. A. Petrunewich, et al. (2002). "Inhibition of MEK or cdc2 kinase parthenogenetically activates mouse eggs and yields the same phenotypes as Mos(-/-) parthenogenotes." Developmental biology **247**(1): 210-223.

Raman, M., W. Chen, et al. (2007). "Differential regulation and properties of MAPKs." Oncogene **26**(22): 3100-3112.

Richards, J. S. and S. A. Pangas (2010). "The ovary: basic biology and clinical implications." The Journal of clinical investigation **120**(4): 963-972.

Saba-El-Leil, M. K., F. D. Vella, et al. (2003). "An essential function of the mitogen-activated protein kinase Erk2 in mouse trophoblast development." EMBO reports **4**(10): 964-968.

Schwab, M. S., B. T. Roberts, et al. (2001). "Bub1 is activated by the protein kinase p90(Rsk) during Xenopus oocyte maturation." Current biology : CB **11**(3): 141-150.

Su, Y. Q., K. Wigglesworth, et al. (2002). "Mitogen-activated protein kinase activity in cumulus cells is essential for gonadotropin-induced oocyte meiotic resumption and cumulus expansion in the mouse." Endocrinology **143**(6): 2221-2232.

Sun, Q. Y., L. Lai, et al. (2001). "Dynamic events are differently mediated by microfilaments, microtubules, and mitogen-activated protein kinase during porcine oocyte maturation and fertilization in vitro." Biology of reproduction **64**(3): 879-889.

Sun, Q. Y., Y. L. Miao, et al. (2009). "Towards a new understanding on the regulation of mammalian oocyte meiosis resumption." Cell cycle **8**(17): 2741-2747.

Tripathi, A., K. V. Kumar, et al. (2010). "Meiotic cell cycle arrest in mammalian oocytes." Journal of cellular physiology **223**(3): 592-600.

Verlhac, M. H., H. de Pennart, et al. (1993). "MAP kinase becomes stably activated at metaphase and is associated with microtubule-organizing centers during meiotic maturation of mouse oocytes." Developmental biology **158**(2): 330-340.

Verlhac, M. H., C. Lefebvre, et al. (2000). "Asymmetric division in mouse oocytes: with or without Mos." Current biology : CB **10**(20): 1303-1306.

Yu, L. Z., B. Xiong, et al. (2007). "MEK1/2 regulates microtubule organization, spindle pole tethering and asymmetric division during mouse oocyte meiotic maturation." Cell cycle **6**(3): 330-338.

8. Addendum*

8.1 Analysis of karyotype to detect possible aneuploidy in embryos from *Erk1/2* DKO oocytes

I hypothesized that any abnormality in the spindle morphology is likely to produce chromosome segregation defects and consequently, aneuploidy. Mis-segregation/misalignment in the oocyte is likely to produce embryos that get progressively more aneuploid with each mitotic division, ultimately resulting in embryo death. Since embryo death at each stage of cell division was the hallmark of our *Erk1/2* DKO oocytes, I analyzed the chromosome number of these oocytes and the embryos formed from them after fertilization. In addition to having less compact chromosomes at the metaphase mid-plate (Chpater2, Fig 1), some of the *Erk1/2* DKO oocytes exhibited a much higher number of chromosome univalents at metaphase II (Fig 6a). In order to detect aneuploidy in embryos, chromosome spreads from the blastomeres of wildtype blastocysts (Wt X Wt) and *Erk* 1/2 DKO blastocysts (*Erk1/2* DKO X Wt) were compared. Blastomeres were arrested at mitotic metaphase by colcemid treatment. However, due to inadequate number of blastocysts from the *Erk1/2* DKO oocytes, a comparison was not possible (Fig 6b). These results point to aneuploidy in the embryos derived from the *Erk1/2* DKO oocytes, however, more analysis is required to conclusively demonstrate aneuploidy as a cause of embryo death.

Fig 3.6. Detection of aneuploidy in *Erk1/2* DKO oocytes

MII arrested oocytes from wildtype control (n= 10) and *Erk1/2* DKO (n= 10) animals were immunolabelled with antibody against phospho-H3S10 (FITC conjugated) and with DAPI to visualize chromatin.

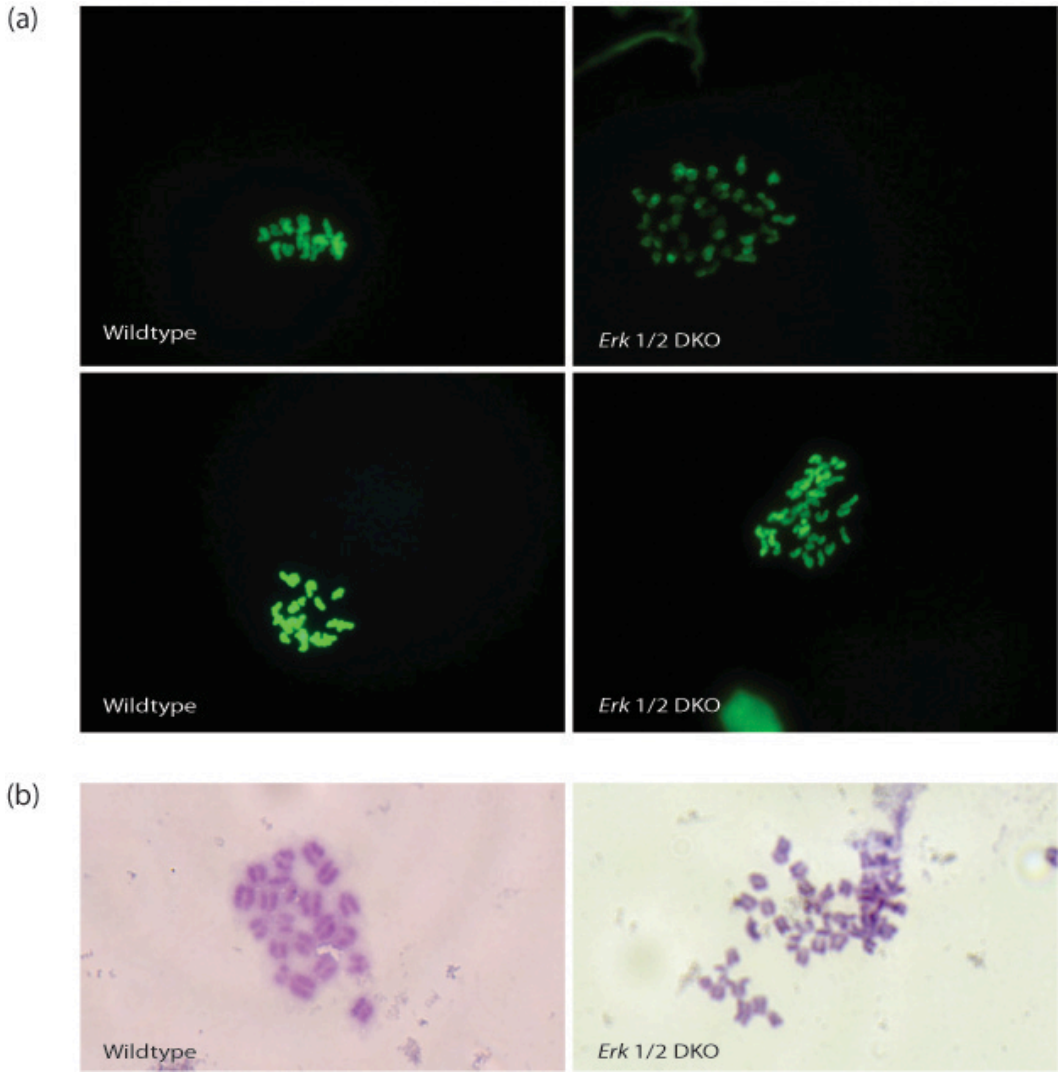

8.2 Analysis of the effect of ERK deletion on metaphase II arrest in oocytes

Mammalian oocytes stay arrested in metaphase II till fertilization with the help of an anaphase inhibitor known as EMI2 (Early mitotic inhibitior2) (Madgwick, Hansen et al. 2006). For maintaining MII arrest till fertilization, EMI2 is stabilized by a series of phosphorylations. In *Xenopus* oocytes these phosphorylations are brought about by p90Rsk (Bhatt and Ferrell 1999). It is possible that in the mammalian oocyte this stabilization is mediated by MSK1 instead. EMI2 phosphorylation by MSK1 has been demonstrated in vitro and the use of pharmacological inhibitors of MSK1 produces disruption of the metaphase II spindle (Miyagaki, Kanemori et al. 2011).

In our *Erk1/2* DKO oocytes, although we demonstrate an ERK-MSK1 phosphorylation cascade and abnormal spindle assembly at MII, arrest at MII did not seem to be affected. A number of *Erk1/2* DKO oocytes show spontaneous entry into anaphase II; however, their numbers were not significantly different from wildtype controls (Fig 7). However, this might change when more replicates make the data statistically sound. If that is the case, then mis-segregation of chromosomes that is seen in the *Erk* 1/2 DKO oocytes could likely be the result of premature entry into anaphase in addition to the other effects observed.

Fig 3.7. Spontaneous release from MII arrest in the *Erk1/2* DKO oocytes

Percentage of spontaneous release from MII arrest was calculated in oocytes from wildtype controls (n= 72), *Erk1* SKO (n= 67) and *Erk1/2* DKO (n= 73). Bars represent mean + SEM. Statistical comparisons were performed using t-test.

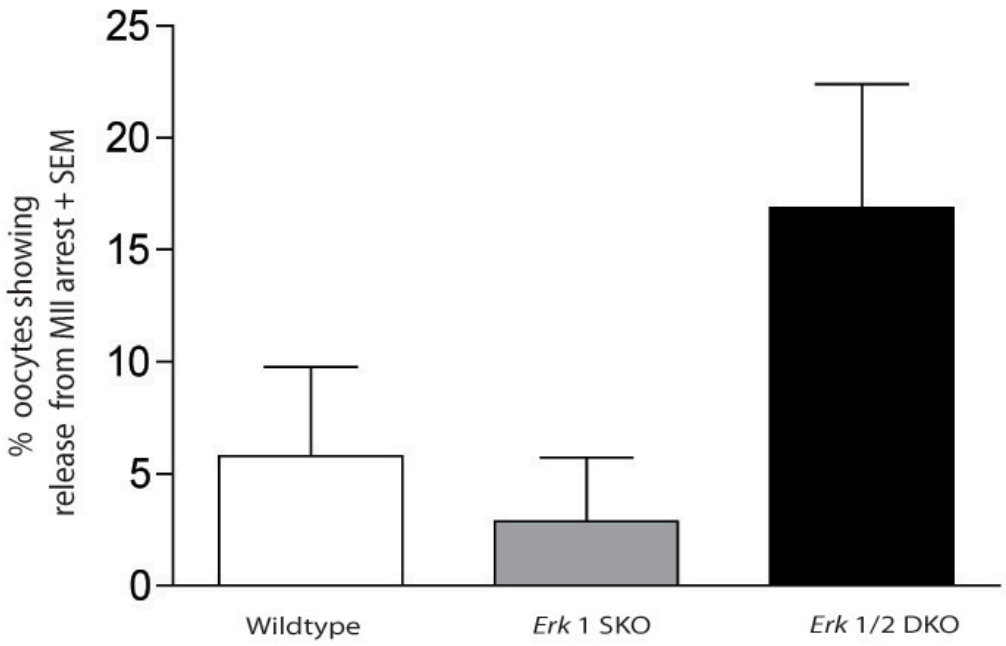

CHAPTER 4

Erk1/2 deletion disrupts downstream effector elements required for oocyte meiotic progression and cytokinesis

1. Abstract

ERKs are known to be critical upstream regulators of spindle assembly formation and function during meiosis. Disruption of ERK activity in the oocyte can bring about significant structural anomalies in the spindle and chromosome segregation defects. ERKs are known to localize on the spindle microtubules and on the spindle poles. While not much is known about the nature of action of ERKs on the spindle, in recent years several proteins have been detected on the spindle proteome. It is possible that phosphorylation events play a role in keeping these proteins functioning in an efficient, timely way. We have utilized a conditional genetic approach to create on an *Erk1* null background, an Erk2 deletion specifically in mouse oocytes prior to meiotic resumption. Using an antibody that detects ERK mediated phosphorylation we have demonstrated a reduction in phosphorylation in the *Erk1/2* double knockout oocyte. Analysis of the reduced phosphorylation revealed a series of different proteins with possible interaction with the MAPK pathway. Based on number of protein hits, molecular weight and presence of serine/threonine phosphorylation sites, the list was narrowed down to a few possible candidates.

These proteins, namely BUBR1, TACC3, NLRP5, KIF23, DNMT1 all have been shown to have action on the spindle in mitotic cells. This study is aimed at elucidating several possible targets of ERK1 and ERK2 in the oocyte spindle assembly using an immunohistochemical and a mass proteomics approach.

2. Introduction

Post prophase I meiotic divisions in mammalian oocytes are characterized by a strictly coordinated set of key events leading to the formation of a spindle –chromosome complex (SCC). A spindle-chromosome complex is an assembly of microtubules attached to the kinetochores of chromosomes anchored by spindle poles. Oocyte meiosis requires the coordinated formation of a bipolar spindle, maintenance of proper microtubule chromosome attachment, tension on the bipolar spindle, migration of the spindle to the cortex and functioning spindle assembly checkpoint (Vogt, Kirsch-Volders et al. 2008). Formation of a bipolar spindle with correct microtubule kinetochore attachment ensures faithful chromosome segregation thereby ensuring genomic integrity of daughter cells (Ai, Wang et al. 2008). Regulated spindle movements and migration ensures asymmetric division in the female germ cell, which helps in the retention of the cytoplasmic reserves for the embryo. Checkpoint controls are in place to

ensure error-free progression of the above-mentioned events. The spindle assembly checkpoint (SAC) monitors the tension exerted by the pulling forces of the microtubules on the chromosomes and interrupts cell cycle progression in cases of abnormal assembly to prevent aneuploidy in the developing embryos (Cross and Smythe 1998).

A spindle apparatus is formed from the Microtubule Organizing Centers (MTOC), ring shaped structures that eventually form what are known as the spindle poles (Verlhac, de Pennart et al. 1993; Ou, Li et al. 2010). One of the components of MTOCs is ɣ tubulin, which functions as the positive end of microtubules. α and β tubulin molecules form dimers, which then polymerize into long microtubules. The negative ends of these microtubules grow away from MTOCs or poles towards chromosomes where they bind to the kinetochore in the centromeric region (Figure 1) (Walczak and Heald 2008). Once attached to the kinetochore, the microtubules exert tension on the condensed chromosomes, keeping them aligned at the metaphase plate (Walczak and Heald 2008). At the onset of anaphase, cohesive forces keeping chromosomes together are severed and the chromosomes are pulled apart to each pole. The positioning of the spindle within the oocyte is also very important for the asymmetric cytokinesis that takes place during oocyte meiosis (Sun, Lai et al. 2001).

Figure 4.1. Formation of spindle assembly at metaphase

α and β tubulin dimers polymerize from the MTOCs which function as anchoring points for the positive ends of microtubules. The growth of the microtubules is towards the metaphase plate where chromosomes assemble after condensation. The microtubules then attach to the kinetochores of the chromosomes to bring about bipolar orientation of the spindle. Several proteins are involved in the formation, maintenance and function of the bipolar spindle, which are activated or deactivated at specific time points in order to regulate their timed functions. Most of these activations/ deactivations are brought about by phosphorylations by various kinases. MAPKs are thought to play a major role in this regulation.

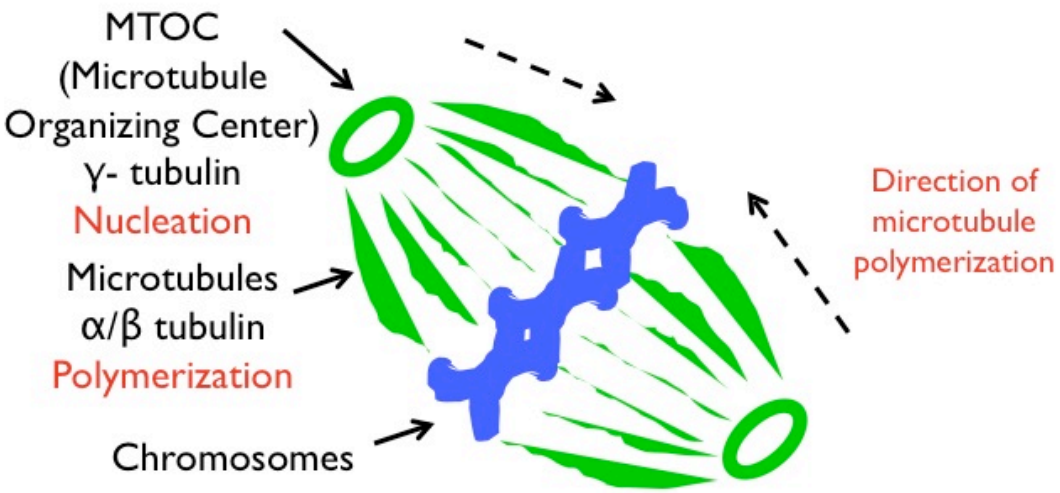

Numerous proteins associate with the spindle to regulate its formation, function and maintenance. Many of them are motor proteins such as kinesins and dyneins that function to transport other molecules along microtubules, and help in microtubule and chromosome movement. Other proteins are microtubule associated proteins that function in stabilizing and destabilizing microtubules, cross-linking parallel strands of microtubules and guiding their direction of polymerization. Still others, such as members of the SAC (Spindle Assembly Checkpoint), ensure error-free progression of spindle function. Finally, there are several signaling proteins such as kinases and phosphatases that regulate and coordinate the temporal and spatial organization of the spindle. A proteomic analysis of the mammalian oocyte spindle using LC-MS/MS (Liquid chromatography Mass Spectrometry) recovered about 600 proteins with the spindle assembly of which about 200 were associated with the spindle-chromosome complex (Han, Liang et al. 2010). Similarly, a large-scale phosphoproteome analysis of the human mitotic spindle using mass spectrometry in combination with phosphopeptide enrichment has revealed approximately 600 proteins and 2000 unique phosphorylation sites associated with the spindle (Nousiainen, Sillje et al. 2006). Several of these phosphorylation sites have been identified as corresponding to consensus motifs of kinases such as CDK1, PLK1, AURK A/B etc

(Nousiainen, Sillje et al. 2006). However, not much is known about the role of MAPK on the spindle phosphoproteome.

Previous work has shown that disruption of ERK/MAPK pathway produces drastic spindle defects and chromosome segregation defects in the oocyte. These results also point to a possible defect in spindle cytokinesis owing to the improper migration of spindle assembly in the oocyte. So, in order to delineate the exact mechanism of action of ERKs in regulating spindle assembly, we used an oocyte specific *Erk* deletion model to study the downstream pathways affected in the absence of ERKs leading to previously defined spindle defects. For this, we employed a very specific LoxP-Cre recombinase mediated conditional deletion of *Erk2* in the oocyte on an *Erk1* null background.

Analysis of the phosphorylation status of certain proteins of the SAC in both the wildtype and the *Erk1/2* DKO oocytes indicated their possible interaction with the ERK/MAPK pathway to bring about spindle assembly. Components of the SAC are believed to interact with the MAPK pathway (and other signaling cascades) to prevent activation of the anaphase-promoting complex during metaphase. Function of the SAC to prevent anaphase might require the action of a MAPK cascade in order to co-ordinate and choreograph various simultaneous events involved in the proper functioning of the SAC. These events include possible activation of the SAC proteins and

transportation to and from various sites on the spindle. And because ERKs might play an important role in the function of SAC proteins, absence of ERKs can cause possible inhibition (or lack of activation) of the SAC in the oocyte, leading to abnormal chromosome segregation.

In addition to the proteins of the SAC, delineation of other possible downstream ERK targets is also described in this study. These possible ERK targets provide a basis for defining factors involved in the spindle function.

3. Materials and Methods

3.1 Generation of the *Erk2* $^{fl/fl}$ *Erk1*$^{-/-}$ mouse

Wildtype control mice and *Zp3-Cre* mice were obtained from Jackson Laboratories. The *Erk1* knockout strain (*Erk2* fl/fl *Erk1*$^{-/-}$) have been reported in previous study (Bliss, Miller et al. 2009). Mice with *Erk 1/2* double deletion in oocytes were generated by crossing *Zp3-cre* line with the *Erk2*$^{fl/fl}$ *Erk1*$^{-/-}$ line. All experiments were performed with wildtype, *Erk1* SKO (*Erk1* $^{-/-}$) and *Erk1/2* DKO (*Erk2* $^{fl/fl}$ *Zp3Cre*$^{+/-}$ *Erk1* $^{-/-}$) animals. All the mice used in this study are on a C57BL/6 background. Animals were housed according to the Cornell University Institutional Animal Care and Use Committee regulations.

3.2 Genotyping

Tail snips were used as a source of genomic DNA. PCR genotyping strategies for *Erk1* and *Erk2* were performed as described previously (Bliss, Miller et al. 2009). Cre PCR for confirming the recombination at $Erk2^{fl/fl}$ employed the following primers-

Forward:GTCGATGCAACGAGTGATGAGGTTCG and

Reverse:CCAGGCTAAGTGCCTTCTCTACACCTGC.

3.3 Oocyte retrieval and culture

For assessment of MI and MII spindle structures, oocytes were collected from ovaries of 21-day-old mice by follicle puncture with a 26.5 gauge needle in M2 medium containing hyaluronidase (MR 051F, EMD Millipore, Billerica, MA). For superovulation, 4 week old females were injected with PMSG (5 IU, i/p) followed by hCG (5IU, i/p), and oocytes were collected from oviducts the following morning. The oocytes were then transferred to M2 medium without hyaluronidase (MR 015D, EMD Millipore, Billerica, MA) and finally to KSOM medium (MR 020P, EMD Millipore, Billerica, MA) under oil in a 35 mm culture dish. The oocytes were then incubated in conditions of 5% O2 and 5% CO2 at 37C for specific time periods: MI (~8hrs) and MII (16hrs). MII stage was confirmed by the presence of a polar body.

3.4 Immunofluorescent labeling

Oocytes were fixed in buffer containing 2% PFA, blocked for 1 hour at room temperature and incubated in primary antibody overnight at 4C. Oocytes were then washed, incubated in secondary antibody at room temperature for 1 hour and mounted in Antifade containing DAPI. The cover glass was fixed over the slide using a 1:1 mixture of paraffin and petroleum jelly. Antibodies used were mouse anti-beta tubulin (T8328, Sigma-Aldrich, St Louis, MO), Rabbit anti-ERK 1/2 (4695, Cell Signaling Technology, Boston, MA), mouse anti-Gamma tubulin (ab27074, Abcam, Cambridge, MA), Rabbit anti-RSK1/RSK2/RSK3 (32D7) (9355P, Cell Signaling Technology, Boston, MA), Rabbit anti- Phospho-p90RSK (Thr359/Ser363), (9344P Cell Signaling Technology, Boston, MA), Rabbit anti- Phospho-p90RSK (Thr573) (9346P Cell Signaling Technology, Boston, MA), Rabbit anti-TACC3 (D9E4) XP mAb (8069, Cell Signaling Technology, Boston, MA), Rabbit anti-Phospho-TACC3 (Ser558) (5645, Cell Signaling Technology, Boston, MA), Rabbit anti-BubR1 antibody-N-terminal (ab135682, Abcam, Cambridge, MA), Rabbit anti-Mad2L1 antibody (ab24588, Abcam, Cambridge, MA) and Mouse anti-MPM-2 (05368, EMD Millipore, Billerica, MA).

3.5 Western Blotting

For protein detection with western blot, oocytes were pooled from 4-6 week old superovulated female mice and lysed in 2X Laemelli buffer. Samples were immediately boiled at 95C and cooled on ice. Proteins were separated in an SDS-PAGE electrophoretic system and transferred onto Immuno-Blot PVDF membrane (162-0177, BioRad, Hercules, CA). Membranes were probed with mouse anti-beta tubulin (T8328, Sigma-Aldrich, St Louis, MO), Rabbit anti-ERK 1/2 (4695, Cell Signaling Technology, Boston, MA), mouse anti-Gamma tubulin (ab27074, Abcam, Cambridge, MA), Rabbit anti-RSK1/RSK2/RSK3 (32D7) (9355P, Cell Signaling Technology, Boston, MA), Rabbit anti- Phospho-p90RSK (Thr359/Ser363), (9344P Cell Signaling Technology, Boston, MA), Rabbit anti- Phospho-p90RSK (Thr573) (9346P Cell Signaling Technology, Boston, MA), Rabbit anti-TACC3 (D9E4) XP mAb (8069, Cell Signaling Technology, Boston, MA), Rabbit anti-Phospho-TACC3 (Ser558) (5645, Cell Signaling Technology, Boston, MA) and Mouse anti-MPM-2 (05368, EMD Millipore, Billerica, MA) according to manufacturer instructions.

3.6 Immunoprecipitation

Oocyte lysates were prepared by sonicating ~500 superovulated oocytes in cold RIPA plus buffer 3 times at 20% amplitude for 10 sec each. Lysate was pre-cleared by incubation with Protein A/G PLUS-Agarose beads (sc-2003, Santa Cruz Biotechnology, Dallas, Texas). Pre-cleared lysates were then incubated with 1:200 Mouse anti-MPM-2 (05368, EMD Millipore, Billerica, MA) and subsequently with Protein A/G PLUS-Agarose beads. Proteins were extracted from the Protein A/G PLUS-Agarose beads by boiling at 95C for 10 minutes. Proteins were separated in an SDS-PAGE electrophoretic system and transferred onto a Immuno-Blot PVDF membrane (162-0177, BioRad, Hercules, CA). Membranes were then probed with mouse anti-MPM-2 (05368, EMD Millipore, Billerica, MA).

3.7 Sample preparation for Liquid chromatography- Mass spectrometry (LC-MS)

Lysates were prepared from~1500 oocytes and immunoprecipitated with anti-MPM-2 antibody as described above. The sample was subjected to electrophoresis on a 12% SDS-PAGE gel. Gel was fixed for 30 minutes in 45% methanol, 45% water, and 10% glacial acetic acid (Fixing solution) and then moved to 7% methanol, 83% water, and 10% glacial acetic acid (Storage solution). The gel in storage solution was delivered to the Cornell Proteomics facility where it was stained with Sypro Ruby. Bands at ~130 kDa and ~80 kDa were excised and used for LC-

MS. Results were searched using Mascot® against the Mouse Reference Sequence with a confidence threshold of 99% and an ion cutoff score of 20.

3.8 Statistical analysis

Statistical analysis of experiments was done by student t-test and analysis of variance as applicable. All statistical tests were performed using Prism 4.0 software (Graphpad).

3.9 Microscope image acquisition

Acquisition and processing of images was performed by microscope (Imager Z1; Carl Zeiss, Inc.) under a 10x eye-piece and 40× 0.5 NA ECPlan Neofluar air immersion (Carl Zeiss, Inc.) or 63× 1.4 NA Plan Apochromat oil immersion (Carl Zeiss, Inc.) magnifying objective at room temperature, cooled charged-coupled device camera (AxioCam MRm; Carl Zeiss, Inc.) and AxioVision software (version 4.7.2; Carl Zeiss, Inc.). Images were analyzed using ImageJ program (ImageJ64.app, NIH).

4. Results and Discussion

4.1 Analysis of the Spindle Assembly checkpoint (SAC) proteins in the *Erk* 1/2 DKO oocytes

Components of the SAC are believed to interact with the MAPK pathway (and other signaling cascades) to prevent activation of the anaphase-promoting complex during metaphase. In *Xenopus* oocytes, for instance, Bub1 is activated by p90Rsk mediated phosphorylation (Schwab MS 2001), while BUBR1 in the mouse SAC is inhibited by p38 mediated phosphorylation (Wei L 2010). In addition to this, several indirect interactions with MAPK components are also believed to take place for SAC function. For example, localization of BUB3 on kinetochores is dependent on PARP1, which in turn, requires possible MAPK regulation (Yang F 2009). Similarly, Dynein, a motor protein required for transportation of the SAC proteins along the microtubules, is phosphorylated on a highly conserved serine residue by ERKs (Bader JR 2010; Pullikuth AK 2013).

Inhibition (or lack of activation) of the SAC in the absence of ERKs, may lead to imperfect attachment of the kinetochores to the spindle microtubules causing improper assembly of the

spindle. Lack of SAC activation in the absence of ERKs may also cause abnormal exit from metaphase before all chromosomes are aligned properly on the metaphase plate, leading to abnormal chromosome segregation.

Immunostaining of BUBR1, a major component of the mammalian SAC, on wildtype oocytes and *Erk* 1/2 DKO oocytes showed absence of this protein on the spindle of either genotype (Fig 2). There is no discernible pattern of localization of BUBR1 protein on either wildtype (Fig 2 Left panel) or *Erk* 1/2 DKO (Fig 2 Right panel) oocytes. This might indicate a lack of SAC activation in both the wildtype oocyte (due to error-free completion of meiosis) and in the *Erk* 1/2 DKO oocytes (due to absence of ERKs that may be required for SAC activation). However, it should be noted that this data is very preliminary and further analysis is essential to understand this phenomenon of inhibition (or lack of activation) of the SAC in the absence of ERKs, leading to abnormal chromosome segregation.

Fig 4.2. Immunostaining of BUBR1

Localization of BUBR1 protein in MII arrested oocytes from wildtype control and *Erk1/2* DKO animals with antibodies against BUBR1 (FITC conjugated) and β-tubulin (Texas-red conjugated). No discernible pattern of localization of BUBR1 protein on either wildtype (Left panel) or *Erk* 1/2 DKO (Right panel) oocytes observed.

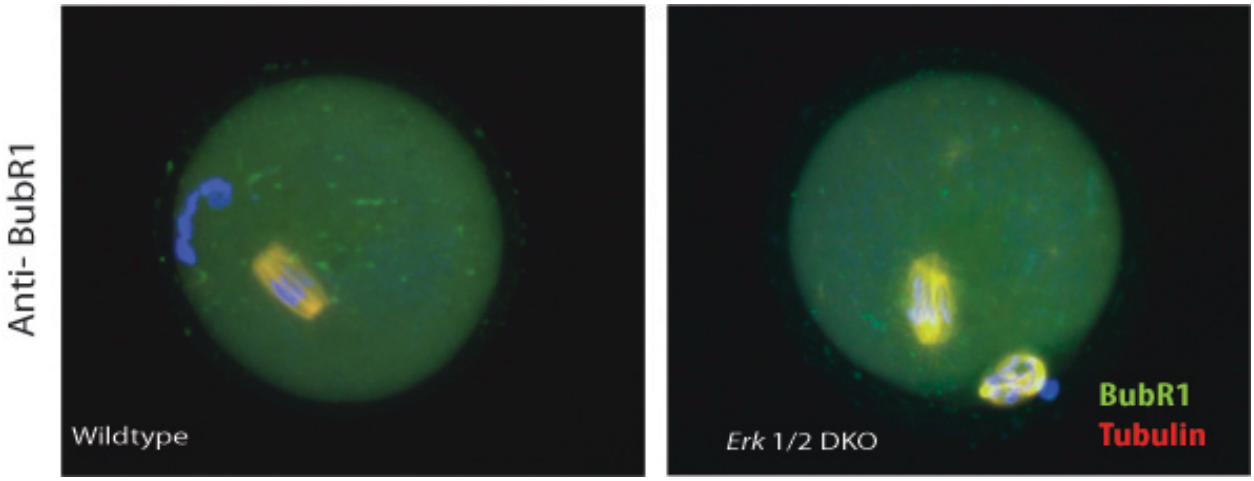

4.2 Identification of other potential ERK phosphorylation targets in mammalian oocytes

In order to ascertain and assess localization of possible downstream targets, an ERK specific phosphorylation detection antibody was used to immunostain oocytes. MPM2 (Mitotic Protein 2) is an antibody that detects proline directed serine threonine phosphorylation in mitotic cells. A proline directed serine/threonine type of phosphorylation is characteristic of the kinases ERK1 ERK2, CDK1 and certain other kinases. Some of the major known substrates of MPM2 in mitotic cells are Topoisomerase IIα, MAP (Microtubule associated proteins) and NIMA (Renzi, Gersch et al. 1997). Since *Erk1/2* DKO oocytes are expected to show normal expression of CDK1 and other kinases, any difference in MPM2 staining is likely due to the deficiency in ERK activity.

Immunostaining of *Erk1/2* DKO oocytes revealed prominent absence of MPM2 substrates from the MII spindle assembly. (Fig3a). This indicates that potential targets for ERK phosphorylation are present in the oocyte at Meiosis II and that these targets are possibly involved in spindle assembly and function. In order to further determine the nature of target molecules, I compared the expression of phosphorylated proteins in oocyte lysates from wildtype, *Erk1* SKO and *Erk1/2* DKO animals. Lysates were subjected to gel electrophoresis and probed with MPM2 antibody. Of the multiple protein bands detected by this antibody, one band that migrated at approximately

120-130 kDa showed a significant reduction in the *Erk1/2* DKO lysates as compared with the wildtype and *Erk1* SKO lysates. The *Erk1* SKO lane itself showed a slightly lower band intensity when compared to the wildtype at 120-130 kDa, indicating that any phosphorylation deficiency caused by *Erk1* deletion cannot be fully compensated by *Erk2* (Fig 3b).

To identify proteins within the 120-130 kDa range of molecular weight that in mouse oocytes, Liquid Chromatography - Mass Spectrometry assay (LC-MS) was employed. For this, immunoprecipitation of wildtype oocyte lysates was performed with the MPM2 antibody. Western blot of immunopreciptated material showed the presence of a strong band at the 120-130 kDa range. Next, the MPM2 immunoprecipitate from 1500 wild type oocytes was run on a 5% SDS-PAGE gel. The gel was then stained with Sypro Ruby and a region of gel corresponding to 130 kDa and 80 kDa (for comparison) and analyzed by LC-MS. The two bands were searched using Mascot Distiller (Version 2.2) against Mouse reference sequence. A second replicate was also performed with 1500 oocytes. Fifty-one (51) and forty-seven (47) proteins were identified from each band, respectively; in the first replicate and seventy-one (71) and thirty-three (33) respectively in the second replicate (Appendix 1).

Fig 4.3. Erk1/2 DKO oocytes show absence of MPM-2 substrates

(a) Localization of total MPM2 protein substrates on meiotic spindles of MII arrested oocytes from wildtype control and *Erk1/2* DKO animals with antibodies against MPM2 (Cy5 conjugated). MPM2 signal absent from *Erk1/2* DKO oocyte spindle (Yellow arrowhead). Scale bar 10 μm. (b) MPM2 substrates in oocyte lysates confirmed by western blot. Wildtype and *Erk1/2* DKO oocyte pools of 100 oocytes each in adjacent lanes, probed by MPM2 antibody (~ 130kDa) in the wildtype lane and absence of bands in the *Erk1/2* DKO lanes (Red arrowhead).

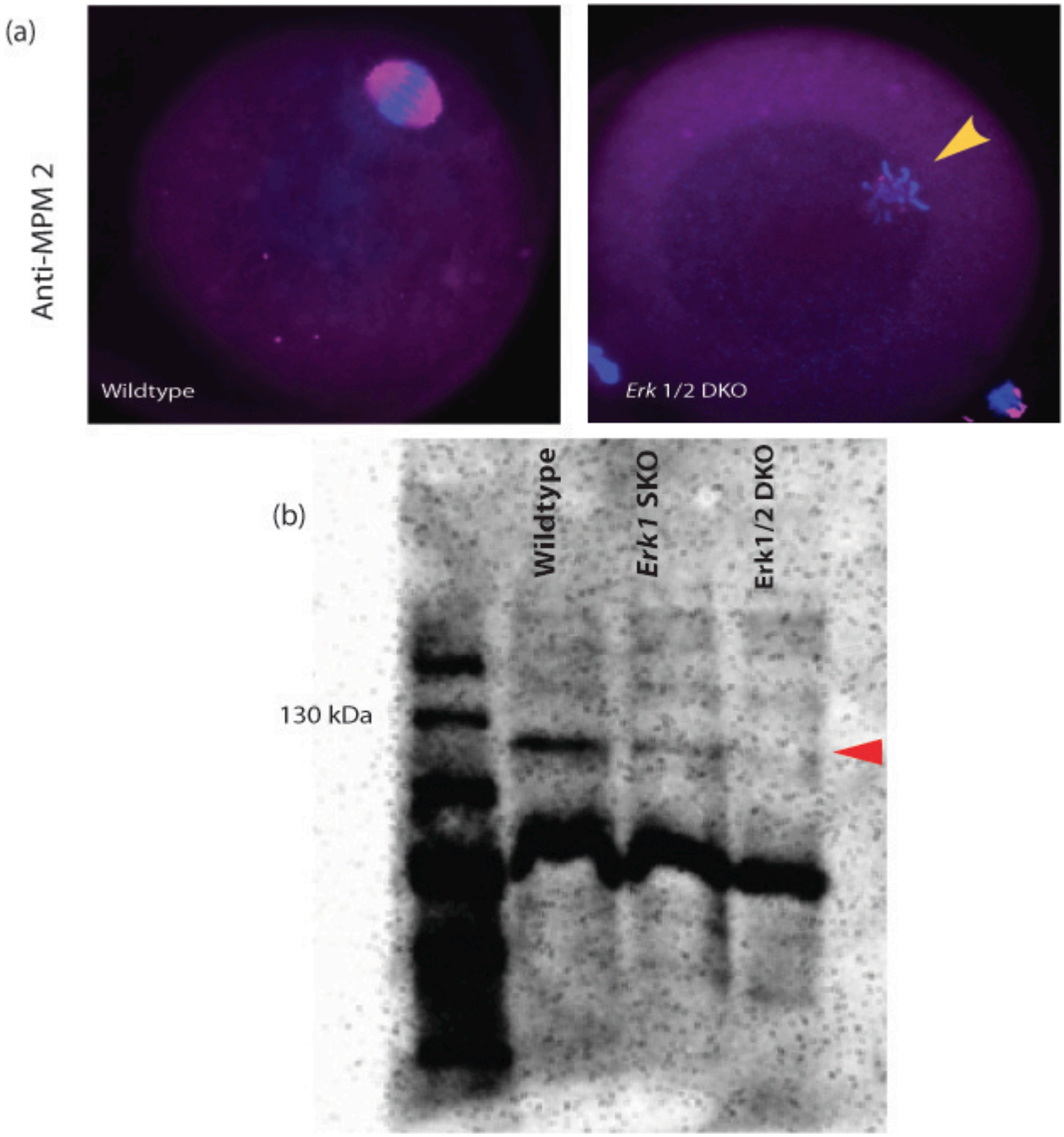
(a)
Anti-MPM 2
Wildtype
Erk 1/2 DKO
(b)
Wildtype
Erk1 SKO
Erk1/2 DKO
130 kDa

From these LC-MS results, potential protein targets were identified based on a) Number of protein hits b) Approximate molecular weight or MW at which the protein travels during electrophoresis and c) Presence of proline directed phosphorylation sites.

4.3 Possible downstream effectors involved in spindle assembly and function

Several interesting proteins were identified from the LC-MS results, which are discussed here. The discussion below describes the candidate protein, known functions of the protein in spindle assembly, possible interaction with MAPKs, whether present in the mammalian oocyte and a mutant phenotype, if any.

4.3.1 TACC3 (Transforming Acidic Coiled Coil 3) is a centrosomal protein involved in mitotic cell function. Phosphorylated TACC3 has been shown to increase microtubule stability and regulate chromosome alignment in mitotic cells (Schneider, Essmann et al. 2007). TACC3 has several Serine/Threonine phosphorylation sites and many kinases have been implicated in their activation such as TPX2 (Serine 558), Aurora kinase A (also Serine 558) etc (Schneider, Essmann et al. 2007). RNAi directed TACC3 depletion in mitotic cells showed aberrant spindle morphology, misaligned chromosomes and aneuploidy (Schneider, Essmann et al. 2007; Yurttas P 2010). Two-dimensional gel electrophoresis showed the presence of TACC3 in GV stage

oocytes in the mouse, indicating its importance in oocyte function (Hao, Stoler et al. 2002; Yurttas P 2010).

4.3.2 KIF23- Kinesin-like protein 23 is a member of the Kinesin-like family of the Kinesin super-family of proteins. They are microtubule associated motor proteins that are central to the formation of the spindle mid-zone for proper assembly of chromosomes during cell division (White and Glotzer 2012). KIF23 is known to form the spindle mid-body by interconnecting parallel microtubules to stabilize them (Zhu, Bossy-Wetzel et al. 2005). Many kinases such as Aurora B and CDC2 have been implicated in the phosphorylation of KIF23. However none of these have been shown to be essential for KIF23 function. KIF23 may also have multiple phosphorylation sites (Zhu, Bossy-Wetzel et al. 2005). siRNA knockdown of KIF23 and its recruiting protein INCENP in human mitotic cells produced abnormal cytokinesis and chromosome segregation indicating that it is essential for these processes (Vernos, Heasman et al. 1993; Minestrini, Mathe et al. 2002). Though not much is known about the exact functions of KIF23 in the oocyte, it has been found in the transcriptome of oocytes in *Xenopus* and *Drosophila* and during oogonial division in mouse (Greenbaum, Iwamori et al. 2009).

4.3.3 Junction plakoglobin is also known as ϒ-catenin and is closely related to β-catenin. It is found in association with β catenins and cadherin proteins in cell membranes and is involved in

cell-to-cell adhesion (Kofron, Heasman et al. 2002). In Xenopus, plakoglobin has been shown to be required for maintenance of the cortical actin cytoskeleton. Depletion of plakoglobin in *Xenopus* embryos leads to loss of embryo shape and architecture (Kofron, Spagnuolo et al. 1997). Plakoglobin has also been found in Zebrafish oocytes where it likely plays a role in follicle development and interaction with granulosa cells. While the kinase regulators of plakoglobin are not known, it has been shown to have multiple serine/threonine phosphorylation sites *in vivo* which affect the stability of the protein (Pasdar, Li et al. 1995; Cerda, Berrios et al. 1999).

4.3.4 DNMT1 (DNA (cytosine-5) methyl transferase 1 isoform 2) - DNA methyl transferases are proteins required for DNA methylation. DNMT1 disruption in human cancer cells showed an accumulation of tetraploid cells in G2 arrest possibly due to the failure of cytokinesis (Chen, Hevi et al. 2007). DNMT1 depletion by RNAi produced aneuploidy and chromosome instability (Barra, Schillaci et al. 2012). Over expression of DNMT1 in human and mouse fibroblasts have shown defective spindle morphology and tumorogenicity (McCabe, Low et al. 2006). The enzymatic activity of DNMT1 is dependent upon the phosphorylation status of its various Serine/Threonine residues. While some cyclin dependent kinases have been implicated in this, the exact pathway of DNMT1 activation is poorly understood (McCabe, Low et al. 2006).

DNMT1 is present in the mammalian oocyte in all stages of development and has been shown to be crucial for early embryonic development (Lodde, Modina et al. 2009).

4.3.5 PARG - Poly (ADP-ribose) glycohydrolase is an enzyme responsible for the degradation of Poly (ADP-ribose) or PAR, a large polymeric macromolecule required for spindle assembly and function (Finch, Knezevic et al. 2012). PARG have been shown to localize on the mitotic spindle and is required for the timely degradation of PARs after spindle formation (Chang P 2004). PARG null mice show embryonic lethality and PARG null cells show high rates of apoptosis (Finch, Knezevic et al. 2012). In drosophila disruption of PAR degradation by PARGs can cause defects in oocyte development and infertility (Ji and Tulin 2012).

4.3.6 NLRP5 or MATER (NACHT, LRR and PYD domains containing protein 5) is a maternal affector protein that function in cytoplasmic lattice formation (Kim, Kan et al. 2010). $Nlrp5^{-/-}$ oocytes display 2-cell stage arrest after fertilization (Tong, Gold et al. 2000). Deletion of a downstream effector of NLRP5, PtdIns (3,4,5)P3 disrupts asymmetric division of oocytes due to impaired regulation of F-actin organization and spindle translocation (Zheng, Baibakov et al. 2013).

4.4 Detection of TACC3 in Erk1/2 double Knockout oocytes

Of the above-mentioned putative downstream targets of ERKs, TACC3 showed a high number of protein hits and very high number of S/T phosphorylation sites. And hence, TACC3 was chosen as the first putative target for analysis in the *Erk1/2* DKO oocytes. To determine the presence of total TACC3 and its phosphorylation activity in the oocyte, I performed immunocytochemistry using TACC3 antibodies on MII stage oocytes. Total TACC3 localization was observed to be on the spindle in MII oocytes (Fig4a). *Erk1/2* DKO oocytes showed similar localization of TACC3 on the MII spindle. Commercially available antibodies for the detection of phosphoTACC3 use p-serine 558 as the epitope for detection. While Ser 558 is known to be one of the target sites for Aurora A Kinase-mediated phosphorylation in mitotic cells, it has been implicated in other phosphorylation pathways in mammalian meiotic oocytes. Phosphorylated TACC3 plays a role in chromosome alignment, segregation and cytokinesis (Schneider, Essmann et al, 2007).

Antibody directed against phosphoTACC3 serine 558 did not show any localization on the spindle of MII oocytes. However, there was a disseminated signal indicating a generalized distribution of the protein in the whole oocyte cytosol of wild type oocytes, which was absent in the *Erk1/2* DKO oocytes (Fig 4a).

Protein detection by western blot and comparison between wildtype and *Erk1/2* DKO oocyte protein lysates when probed with phospho-TACC3 however was inconclusive (Fig 4b). However, this could be because TACC3 is a heavily phosphorylated protein with multiple serine and threonine phosphorylation sites. While there is some information regarding Serine 558, the extent of ERK activity on Ser 558 is poorly understood. Moreover, other phosphorylation sites on TACC3 such as S25, S317, T30 etc, and their upstream phosphorylating kinases remain unknown. Therefore, a more thorough quantitation of the TACC3 phosphorylation profile of oocytes is essential both through *in vitro* and *in vivo* methods. Importantly, the changes in phosphorylation states of TACC3 in absence of ERK will help understand the role of these kinases in TACC3 mediated spindle stability.

Fig 4.4. TACC3 immunochemistry

(a) Localization of total TACC3 protein and phosphorylated TACC3 (Ser 558) on meiotic spindles of MII arrested oocytes from wildtype control and *Erk1/2* DKO animals with antibodies against TACC3, phospho- TACC3 (FITC conjugated) and β-tubulin (Texas-red conjugated). (b) Analysis of phospho-TACC3 by western blot. Wildtype and *Erk1/2* DKO oocyte pools of 100 oocytes each in adjacent lanes, probed by pTACC3 antibody in the wildtype lane and in the *Erk1/2* DKO lanes. Bands at 140 KDa marked by yellow arrowheads. Tubulin used as loading control.

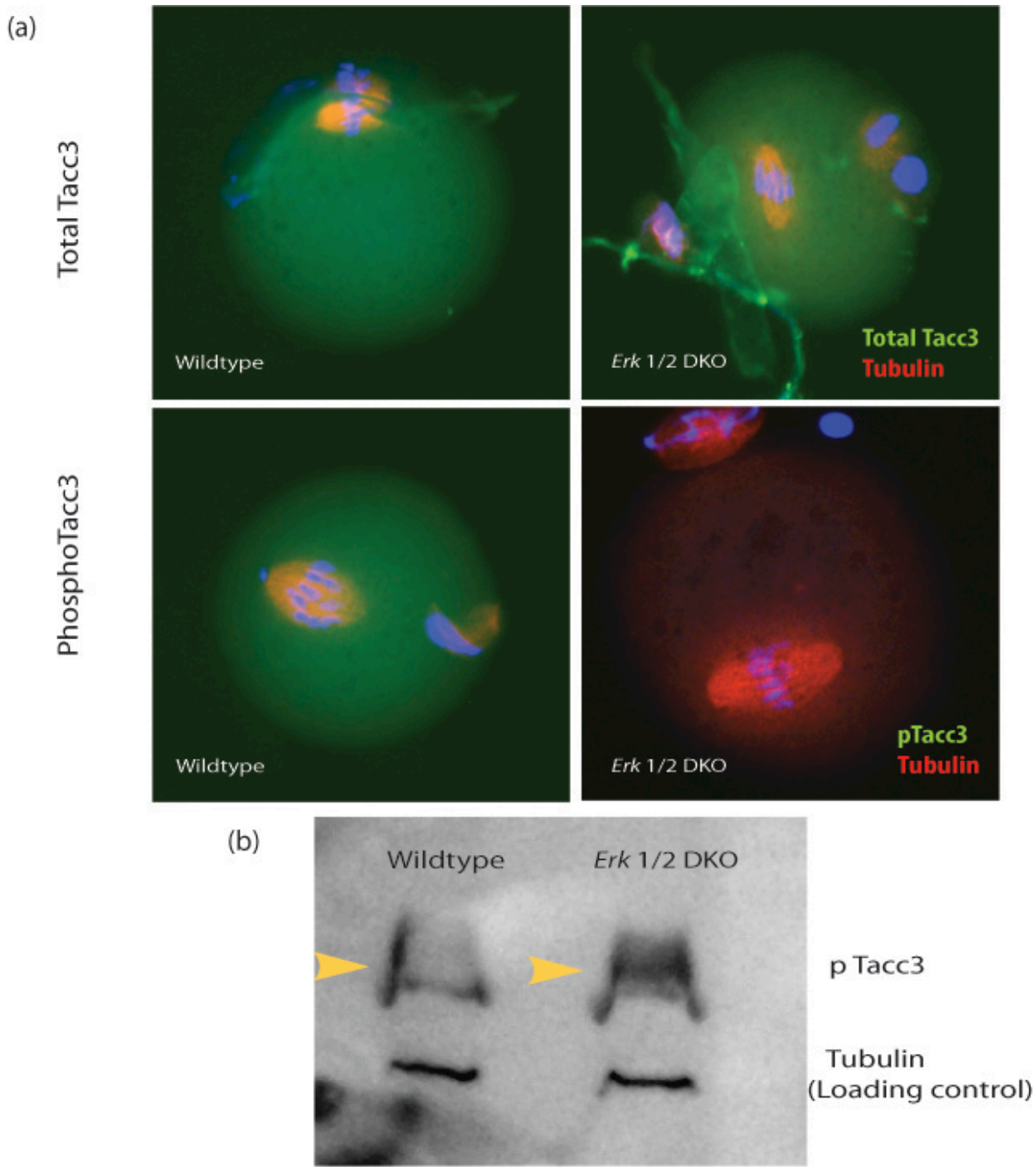
(a)
Total Tacc3
PhosphoTacc3
Wildtype
Erk 1/2 DKO
Total Tacc3
Tubulin
Wildtype
Erk 1/2 DKO
pTacc3
Tubulin
(b)
Wildtype
Erk 1/2 DKO
p Tacc3
Tubulin
(Loading control)

4.5 Analysis of Ribosomal s6 Kinases in Erk1/2 double knockout oocytes

Studies delineating the MAPK pathway in *Xenopus* oocytes have always pointed to RSK (also known as p90RSK or ribosomal s6 kinase) as the most crucial downstream effector of MAP Kinases (Bhatt and Ferrell 1999). However, *Rsk1,2,3* triple knockout studies in the mouse have demonstrated no defects in the spindle morphology or meiotic function of oocytes, indicating that RSKs are not essential in the mouse (Dumont J 2005). Since we have already demonstrated an ERK-MSK1 mediated phosphorylation in the oocyte (See Chapter 2), I decided to look at these closely related kinases RSK1/2/3 in the *Erk1/2* DKO oocyte. Total RSK, phospho-RSK localization and levels within the oocyte were assessed by immunostaining and western blots respectively. Neither total RSK nor phospho-RSK showed any specific localization patterns in the oocytes (Fig 5). There was no significant difference in these patterns between the wildtype and *Erk* 1/2 DKO oocytes either (Fig 5A-D). These results suggest that deletion of *Erk1/2* does not affect RSKs, indicating that they may not be direct ERK targets in the murine oocyte.

Fig 4.5. RSK, pRSK immunostaining

Localization of RSK protein in MII arrested oocytes from wildtype control and *Erk1/2* DKO animals with antibodies against RSK and pRSK (FITC conjugated) and β-tubulin (Texas-red conjugated). Panels show, from left to right, merged images from both flurochromes (i), β-tubulin (ii) and RSK/pRSK (iii). Panels (A) Wildtype oocytes immunostained with total RSK. Merged images from both flurochromes (i), β-tubulin (ii) and RSK (iii). Panels (B) *Erk1/2* DKO oocytes immunostained with total RSK. Merged images from both flurochromes (i), β-tubulin (ii) and RSK (iii). Panels (C) Wildtype oocytes immunostained with phospho RSK. Merged images from both flurochromes (i), β-tubulin (ii) and phospho-RSK (iii). Panels (D) *Erk1/2* DKO oocytes immunostained with phospho RSK. Merged images from both flurochromes (i), β-tubulin (ii) and phospho RSK (iii).

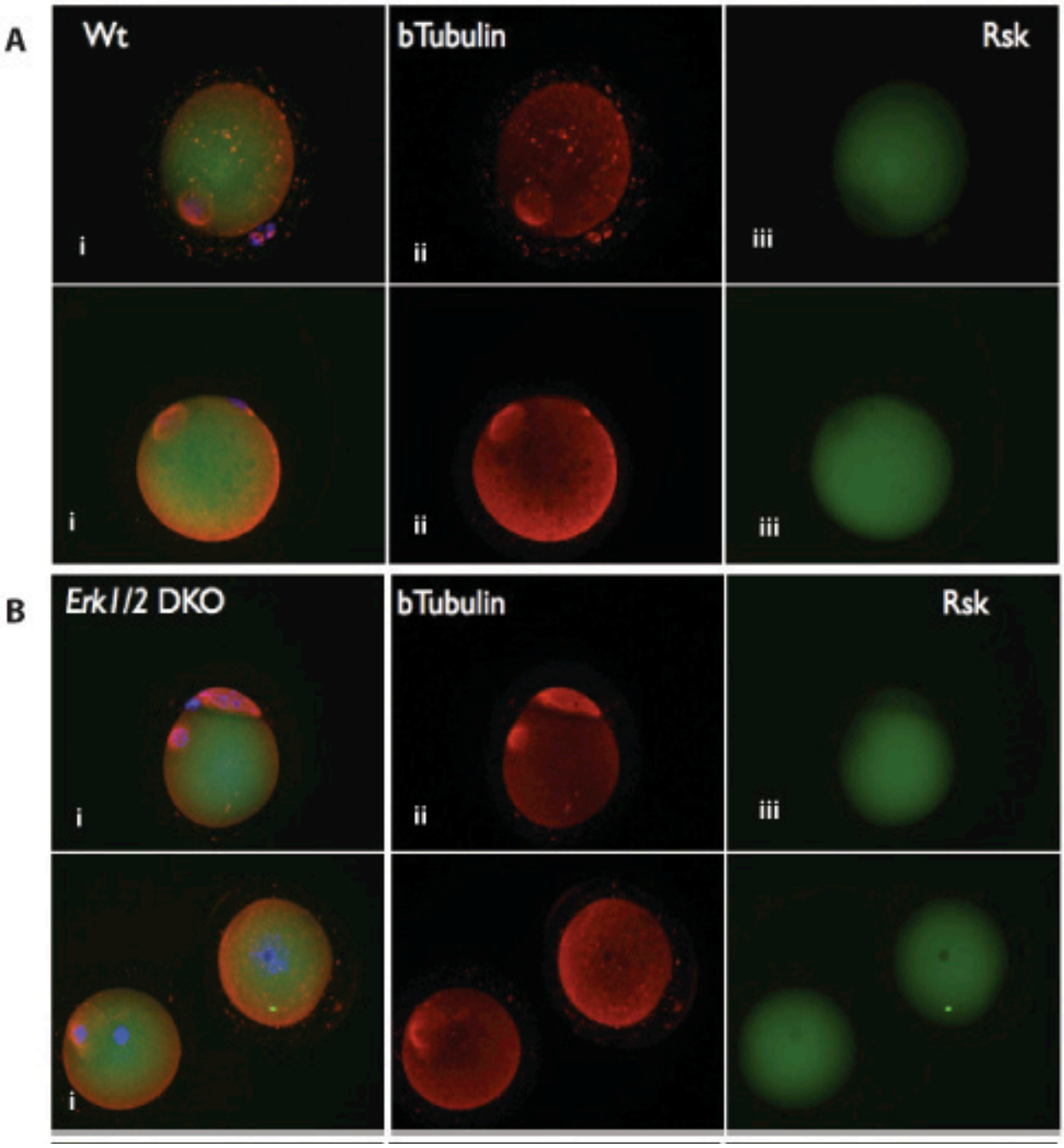
A
Wt
bTubulin
Rsk
i
ii
iii
i
ii
iii
B
Erk1/2 DKO
bTubulin
Rsk
i
ii
iii
i

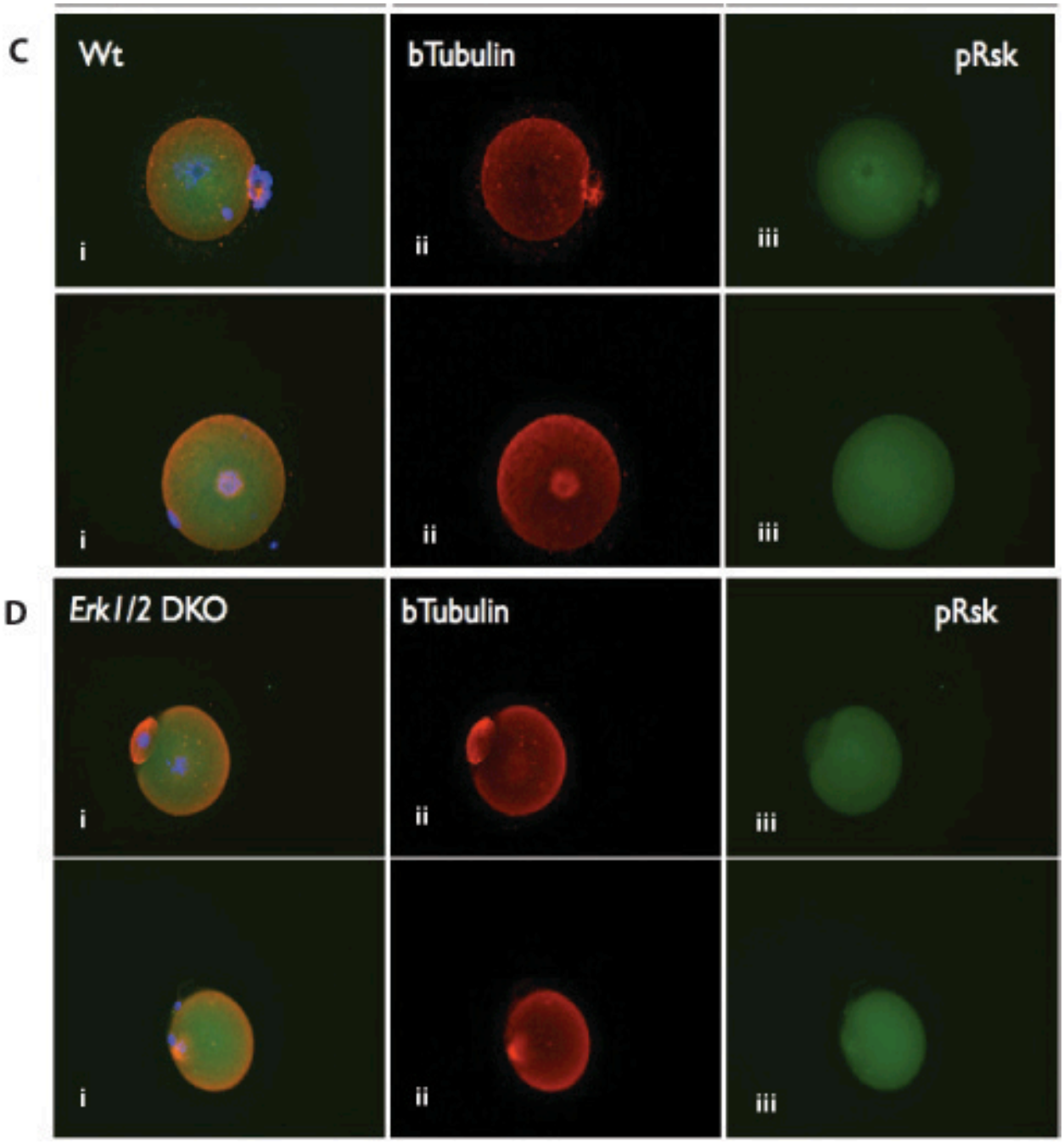
C
Wt
bTubulin
pRsk
i
ii
iii
i
ii
iii
D
Erk1/2 DKO
bTubulin
pRsk
i
ii
iii
i
ii
iii

5. Conclusions

An important possible action of ERKs is on the SAC function. While there are several different proteins comprising the SAC, some of the major ones such as BUB and MAD family of proteins can be assessed on the oocyte. However, localization of the SAC proteins is transient and so the exact temporal localization needs to be pinpointed first, in order to determine if they are absent from the *Erk1/2* DKO oocyte. Absence of SAC proteins from *Erk1/2* DKO oocytes could also point to an inability to activate the SAC in the absence of ERKs. Hence a very thorough, time specific analysis of the expression profile of oocyte proteome is necessary to assess SAC function in relation to the ERK status.

In order to elucidate possible downstream targets of ERKs a mass proteomic screening was employed using an antibody that detects phosphorylations characteristic of ERKs. Of the several proteins that showed upon the screen, many are known to be involved in spindle assembly and function in mitotic cells. Several of those proteins are reported to show spindle structural anomalies in RNAi mediated knockdown studies. A much more detailed examination of each of those possible targets is required to assess the extent of their involvement of the oocyte Metaphase I and II spindles. Expression of one such protein from the screen, TACC3, was further analyzed. However the commercially available antibody for phosphoTACC3 uses only

Serine558 as an epitope. Since TACC3 is known to have about 40 Serine/Threonine phosphorylation sites, a more thorough *in vitro* analysis of ERK-TACC3 interaction is essential.

It has been demonstrated in our work that *Erk* deletion produces a disruption in the ERK-MSK1-Histone H3 pathway leading to defects in chromosome condensation and in spindle formation. However, ERKs have a multitude of targets within the cell for regulating each step of the cell cycle. Therefore, other effectors are likely disrupted in the absence of ERKs. Based on the phenotype observed, it is possible that many of these effectors are involved in other aspects of cytokinesis such as spindle movement, cytoskeletal rearrangement, SAC function, metaphase II arrest etc. a much more detailed and expansive study of ERK targets are required in order to shed light on these various downstream pathways.

6. References

Ai, J. S., Q. Wang, et al. (2008). "Roles of microtubules and microfilaments in spindle movements during rat oocyte meiosis." The Journal of reproduction and development **54**(5): 391-396.

Bader JR, V. K. (2010). "Dynein at the kinetochore: Timing, Interactions and Functions." Semin Cell Dev Biol. **21(3):269-75.**

Barra, V., T. Schillaci, et al. (2012). "Bypass of cell cycle arrest induced by transient DNMT1 post-transcriptional silencing triggers aneuploidy in human cells." Cell division **7**(1): 2.

Bhatt, R. R. and J. E. Ferrell, Jr. (1999). "The protein kinase p90 rsk as an essential mediator of cytostatic factor activity." Science **286**(5443): 1362-1365.

Bliss, S. P., A. Miller, et al. (2009). "ERK signaling in the pituitary is required for female but not male fertility." Molecular endocrinology **23**(7): 1092-1101.

Cerda, M. C., S. Berrios, et al. (1999). "Organisation of complex nuclear domains in somatic mouse cells." Biology of the cell / under the auspices of the European Cell Biology Organization **91**(1): 55-65.

Chang P, J. M., Mitchison TJ. (2004). "Poly(ADP-ribose) is required for spindle assembly and structure." Nature. **2;432(7017):645-9.**

Chen, T., S. Hevi, et al. (2007). "Complete inactivation of DNMT1 leads to mitotic catastrophe in human cancer cells." Nature genetics **39**(3): 391-396.

Cross, D. A. and C. Smythe (1998). "PD 98059 prevents establishment of the spindle assembly checkpoint and inhibits the G2-M transition in meiotic but not mitotic cell cycles in Xenopus." Experimental cell research **241**(1): 12-22.

Dumont J, U. M., Rassinier P, Hanauer A, Verlhac MH. (2005). "p90Rsk is not involved in cytostatic factor arrest in mouse oocytes." J Cell Biol. **25;169(2):227-31.**

Finch, K. E., C. E. Knezevic, et al. (2012). "Selective small molecule inhibition of poly(ADP-ribose) glycohydrolase (PARG)." ACS chemical biology **7**(3): 563-570.

Greenbaum, M. P., N. Iwamori, et al. (2009). "Mouse TEX14 is required for embryonic germ cell intercellular bridges but not female fertility." Biology of reproduction **80**(3): 449-457.

Han, Z., C. G. Liang, et al. (2010). "Oocyte spindle proteomics analysis leading to rescue of chromosome congression defects in cloned embryos." Journal of proteome research **9**(11): 6025-6032.

Hao, Z., M. H. Stoler, et al. (2002). "TACC3 expression and localization in the murine egg and ovary." Molecular reproduction and development **63**(3): 291-299.

Ji, Y. and A. V. Tulin (2012). "Poly(ADP-ribose) controls DE-cadherin-dependent stem cell maintenance and oocyte localization." Nature communications **3**: 760.

Kim, B., R. Kan, et al. (2010). "Potential role for MATER in cytoplasmic lattice formation in murine oocytes." PloS one **5**(9): e12587.

Kofron, M., J. Heasman, et al. (2002). "Plakoglobin is required for maintenance of the cortical actin skeleton in early Xenopus embryos and for cdc42-mediated wound healing." The Journal of cell biology **158**(4): 695-708.

Kofron, M., A. Spagnuolo, et al. (1997). "The roles of maternal alpha-catenin and plakoglobin in the early Xenopus embryo." Development **124**(8): 1553-1560.

Lodde, V., S. C. Modina, et al. (2009). "Localization of DNA methyltransferase-1 during oocyte differentiation, in vitro maturation and early embryonic development in cow." European journal of histochemistry : EJH **53**(4): e24.

McCabe, M. T., J. A. Low, et al. (2006). "Inhibition of DNA methyltransferase activity prevents tumorigenesis in a mouse model of prostate cancer." Cancer research **66**(1): 385-392.

Minestrini, G., E. Mathe, et al. (2002). "Domains of the Pavarotti kinesin-like protein that direct its subcellular distribution: effects of mislocalisation on the tubulin and actin cytoskeleton during Drosophila oogenesis." Journal of cell science **115**(Pt 4): 725-736.

Nousiainen, M., H. H. Sillje, et al. (2006). "Phosphoproteome analysis of the human mitotic spindle." Proceedings of the National Academy of Sciences of the United States of America **103**(14): 5391-5396.

Ou, X. H., S. Li, et al. (2010). "p38alpha MAPK is a MTOC-associated protein regulating spindle assembly, spindle length and accurate chromosome segregation during mouse oocyte meiotic maturation." Cell cycle **9**(20): 4130-4143.

Pasdar, M., Z. Li, et al. (1995). "Plakoglobin: kinetics of synthesis, phosphorylation, stability, and interactions with desmoglein and E-cadherin." Cell motility and the cytoskeleton **32**(4): 258-272.

Pullikuth AK, O. A., Cardenas D, Bailey E, Sherman NE, Pfister KK, Catling AD. (2013). "Epidermal growth factor stimulates extracellular-signal regulated kinase phosphorylation of a novel site on cytoplasmic Dynein intermediate chain 2." Int J Mol Sci. **;14(2):3595-620.** .

Renzi, L., M. S. Gersch, et al. (1997). "MPM-2 antibody-reactive phosphorylations can be created in detergent-extracted cells by kinetochore-bound and soluble kinases." Journal of cell science **110 (Pt 17)**: 2013-2025.

Schneider, L., F. Essmann, et al. (2007). "The transforming acidic coiled coil 3 protein is essential for spindle-dependent chromosome alignment and mitotic survival." The Journal of biological chemistry **282**(40): 29273-29283.

Schwab MS, R. B., Gross SD, Tunquist BJ, Taieb FE, Lewellyn AL, Maller JL. (2001). "Bub1 is activated by the protein kinase p90(Rsk) during Xenopus oocyte maturation." Curr Biol. **6;11(3):141-50.**

Sun, Q. Y., L. Lai, et al. (2001). "Dynamic events are differently mediated by microfilaments, microtubules, and mitogen-activated protein kinase during porcine oocyte maturation and fertilization in vitro." Biology of reproduction **64**(3): 879-889.

Tong, Z. B., L. Gold, et al. (2000). "Mater, a maternal effect gene required for early embryonic development in mice." Nature genetics **26**(3): 267-268.

Verlhac, M. H., H. de Pennart, et al. (1993). "MAP kinase becomes stably activated at metaphase and is associated with microtubule-organizing centers during meiotic maturation of mouse oocytes." Developmental biology **158**(2): 330-340.

Vernos, I., J. Heasman, et al. (1993). "Multiple kinesin-like transcripts in Xenopus oocytes." Developmental biology **157**(1): 232-239.

Vogt, E., M. Kirsch-Volders, et al. (2008). "Spindle formation, chromosome segregation and the spindle checkpoint in mammalian oocytes and susceptibility to meiotic error." Mutation research **651**(1-2): 14-29.

Wei L, L. X., Zhang QH, Li M, Yuan J, Li S, Sun SC, Ouyang YC, Schatten H, Sun QY. (2010). "BubR1 is a spindle assembly checkpoint protein regulating meiotic cell cycle progression of mouse oocyte." Cell Cycle. **15;9(6):1112-21.** .

White, E. A. and M. Glotzer (2012). "Centralspindlin: at the heart of cytokinesis." Cytoskeleton **69**(11): 882-892.

Yang F, B. C., De La Fuente R. (2009). "Persistence of histone H2AX phosphorylation after meiotic chromosome synapsis and abnormal centromere cohesion in poly (ADP-ribose) polymerase (Parp-1) null oocytes." Dev Biol. **15;331(2):326-38.**

Yurttas P, M. E., Coonrod SA. (2010). "Use of proteomics to identify highly abundant maternal factors that drive the egg-to-embryo transition." Reproduction. **May;139(5):809-23**.

Zheng, P., B. Baibakov, et al. (2013). "PtdIns(3,4,5)P3 is constitutively synthesized and required for spindle translocation during meiosis in mouse oocytes." Journal of cell science **126**(Pt 3): 715-721.

Zhu, C., E. Bossy-Wetzel, et al. (2005). "Recruitment of MKLP1 to the spindle midzone/midbody by INCENP is essential for midbody formation and completion of cytokinesis in human cells." The Biochemical journal **389**(Pt 2): 373-381.

CHAPTER 5

Discussion and Future Directions

Mitogen-activated protein kinases or MAPKs translate diverse extracellular signals into various cellular responses that are both critical and specific for the physiological function of each cell type. MAPK pathways are present in all eukaryotic cells and participate in almost all physiological responses of the cell, including division, growth, metabolism, apoptosis, gene regulation and differentiation. In order to bring about these diverse biological functions, the MAPK system employs several kinases at each step of its phosphorylation cascade, each of which have a distinct regulatory function. Together these components act on a variety of substrates to bring about a wide range of responses (Cargnello and Roux 2011).

The goals of my studies were to tease apart the distinct functions of ERK1 and ERK2 within the mammalian oocyte, and to differentiate these functions from those of the supporting somatic cell lineages. Furthermore, by using a defined array of Cre-expressing transgenic mouse lines, the aim was to delineate these oocyte-specific functions both spatially and temporally, through the course of oogenesis. The use of the *Zp3-Cre* line described in this thesis was the "proof of principle" to show that this exquisite genetic approach would work. Over the course of this work I have demonstrated that ERK1 and ERK2, specifically within the oocyte, play significant roles

in the completion of oocyte meiosis, spindle formation, chromosome segregation and asymmetric division of the oocytes. In somatic cells ERK1 and ERK2 are known to be global signaling molecules exerting transcriptional control over a variety of genes (Saba-El-Leil, Vella et al. 2003). Since ERK1/2 have such a wide network of influence over cellular processes, *Erk* deletion in the oocyte at a time as crucial as meiotic resumption, completion and fertilization was bound to produce significant changes. In addition to preparation of meiotic resumption after dictyate arrest (when *Erk* deletion occur in our *Erk1/2* double knockouts) the oocytes are also growing and accumulating proteins and RNA transcripts for later use (Fan and Sun 2004). Hence, we postulated early on that *Erk* deletion at this stage would bring about abrogation of multiple protein functions. My studies offer a starting point for this analysis by first pinpointing the timeline of events that are dependent on functional ERK signaling following meiotic resumption. A better picture of the entire impact of *Erk1/2* deletion will emerge with the use of large-scale screening such as whole proteome profiling, whole transcriptome profiling and global phosphoproteome analysis of the oocyte.

In chapter1, I provided an in-depth analysis on the complete genetic network that is active within an oocyte during its development from a germ to cell to a fully functional haploid gamete. Because of the accelerated pace of technology, it is now possible to delineate several distinct but

interconnected gene networks that co-ordinate the various steps in gametogenesis. Each network can help shed light on the function of individual components within these set of events. Furthermore, it can be seen that most of the events in oogenesis, as well as the genetic networks precipitating them, are interconnected with each other. And signaling cascades such as the MAPK are what connect them, both with each other as well as with external mitogenic signals. This is of particular importance as this tells us that extrinsic factors and the environment may influence oogenesis and oocyte function, thereby affecting the reproductive health of an individual.

Next in chapter 2, I summarized the specific connections between MAPK signaling cascades within the oocyte and oocyte-specific gene networks. The picture that begins to emerge here is that MAPK, specifically ERK1 and 2, are an intrinsic part of most regulatory mechanisms of oogenesis and oocyte maturation. From previous literature, it becomes clear that ERKs participate in a variety of oocyte specific functions such as germinal vesicle breakdown, interaction with the granulosa cell compartment etc. Inhibition of the MAPK cascade upstream of ERKs can provide insight into their roles in each oocyte specific event. Such studies have shown the involvement of ERKs in asymmetric division of oocytes, spindle formation etc. However, all of these studies aimed at the inhibition of the MAPK pathway have utilized

pharmacological inhibitors, which produce global inhibition of MAPKs in both somatic and germinal compartments of the ovary. While these methods are effective they are not a true reflection of *in vivo* conditions. Moreover, in order to overcome factors such as cell permeability etc, very high concentrations of the pharmacological agents need to be used, which would bring about a more severe phenotype than that of a knockout due to cytotoxicity (MacKintosh and MacKintosh 1994). Knockdown studies using oligos are also not very effective because of residual protein within the cell.

Therefore, in order to investigate the role of ERK1 and ERK2 in the oocyte I generated a mouse line with oocyte specific conditional deletion of *Erk2* on an *Erk1* null background. Previous work on ERK1 and ERK2 has shown that these kinases may have non-redundant functions in certain tissues. While deletion of *Erk1* seems to have no effect on the viability of the mice, *Erk2* deletion causes embryonic lethality (Hatano, Mori et al. 2003). Therefore by using a ZP3 promoter driving *Cre* expression, on a background of constitutive *Erk1* loss, I produced a model for *Erk1/Erk2* double knockout (*Erk1/2* DKO) oocytes that induces a complete, consistent absence of ERK specifically within the oocyte while keeping the rest of the physiological parameters of the oocyte intact.

In chapter 3, I provide a detailed phenotypic characterization of the *Erk1/2* DKO mouse line. *Erk1/2* DKO oocytes showed a complete absence of total ERKs in the oocyte at all stages of development in the postnatal ovary. Due to normal ERK expression in the somatic cells of the ovary, the follicle development, ovarian morphology, ovulation and estrous cycles are normal in these animals. However, the *Erk1/2* DKO females were infertile and exhibited failure of implantation. *In vitro* culture of *Erk1/2* DKO oocytes revealed normal meiotic resumption -as expressed by normal GVBD rates-and meiotic progression through MI and MII. A normal GVBD rate was expected in these oocytes owing to normal MAPK signaling within the granulosa cell compartment. However, *in vitro* culture of fertilized oocytes showed progressively higher rate of embryonic death with each cleavage. Analysis of MI and MII stage oocytes demonstrated severe spindle defects with large, spread out spindles, misaligned chromosomes, disrupted MTOCs at spindle poles and abnormally large polar bodies.

The extrusion of large polar bodies from oocytes with *Erk* deletion proved to be an interesting phenomenon as it showed us that early embryonic death in the absence of ERKs might be due to multiple factors. In addition to disrupted spindle assembly leading to improper segregation of chromosomes, it can also be inferred that ERKs play a role in migration of the spindle within the oocyte. This event is essential in oocyte division as it ensures the asymmetric division

characteristic of the anisogenic gametogeneis seen in mammals. Absence of asymmetry during oocgenesis means that large polar bodies, when extruded take away with them much of the cytoplasmic content kept as reserve for future embryo development. Since oocytes are believed to transcriptionally silent at this stage, it is not possible to restore the cytoplasmic milieu by protein synthesis.

The next step was to analyze the cause of severe spindle defects in the *Erk* deleted oocytes. Perhaps the most surprising finding came when I examined downstream targets of ERK1/2 in our wildtype and DKO oocytes. Unexpectedly, RSK, the canonical target of ERKs, was shown to be unaffected the DKO oocytes. Instead, upon examination of the phosphorylation profiles of the other various MAPK activated kinases, phosphorylation of MSK1 (Mitogen and Stress activated Kinase 1) was found to be absent. Not much is known about the function of MSK1 in the mammalian oocyte. It is believed to be involved in EMI2 phosphorylation during MII arrest, an event that is critical for maintenance of MII arrest. However, since we did not observe spontaneous release of MII arrest in the *Erk1/2* DKO oocytes, EMI2 did not seem to be a likely target. it is also possible that MSK1, owing to its localization on the spindle microtubules, has more than target on the spindle assembly itself.

In ES cells MSK1 phosphorylates Histone H3 in an ERK mediated pathway to bring about differentiation (Lee, McCool et al. 2006). Analysis of histone H3 in oocytes revealed an overall reduction in phosphorylation levels of Histone H3 at specifically Serine 10 (H3S10). This result is particularly interesting as H3S10 phosphorylation in somatic cells is more commonly associated with Aurora Kinase activity, and brings about chromatin condensation during mitosis (Sawicka and Seiser 2012). Disruption of H3 phosphorylation at S10 reduces access of condensation factors to chromatin leading to uncondensed chromosomes at metaphase. Improper condensation disrupts bipolar spindle formation by affecting the tension exerted at the kinetochores by microtubules and can result in spindle defects. Since an abnormal spindle is the primary phenotype of the *Erk1/2* DKO oocyte, it can be inferred that reduction in Histone H3 phosphorylation is responsible for uncondensed chromatin and hence, the spindle defects. However, this is the first time that histone mediated spindle defects are being demonstrated to occur via the ERK-MSK1 cascade in mammalian oocytes (Figure 1).

Figure 5.1. Model for downstream events of the ERK/MAPK cascade in spindle assembly.

Downstream signaling events of the ERK pathway produces modification of histones via the action of the ERK activated kinase, MSK1. Histone H3 modification by phosphorylation brings about chromatin condensation. Proper condensation of chromatin ensures bipolar attachment of the spindle microtubules onto the kinetochores of chromosomes (K-MT). Correct placement of the microtubules is required to maintain the spindle tension that then signals accurate formation of the metaphase spindle which, in turn precipitates timely entry into anaphase.

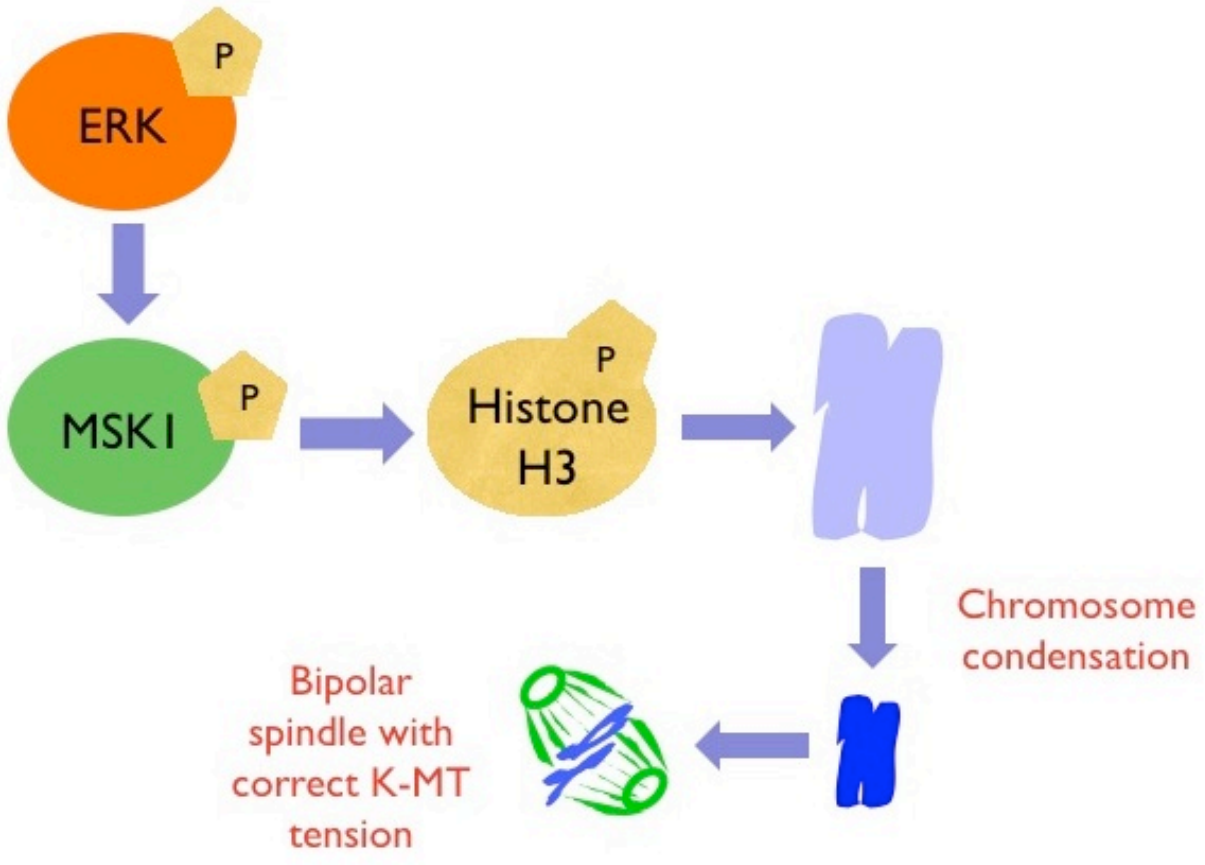

Nonetheless the effects of MSK1 mediated H3S10 phosphorylation on transcriptional control have yet to be studied in the oocyte. MII stage oocytes are believed to be transcriptionally silent, so it will be interesting to see if the ERK-MSK1-H3S10 cascade induces any transcriptional changes within the oocyte before or after fertilization. In addition to transcriptional activity, the translational activity is also likely to be affected in the absence of ERKs owing to the likelihood of ERKs being involved in translation and post-translational modifications. In order to study all these changes, analysis of the phosphoproteome and transcriptome of the whole oocyte is essential.

Assessment of the whole proteome of the oocyte is important because of two factors- (a) As established before, formation of large less compact spindles and improper migration of the spindle can cause extrusion of large polar bodies and *Erk* deletion in oocytes produce this phenotype. Assessment of the total protein content will help understand how protein loss with large polar bodies can affect embryonic development and the embryo protein reserve. It can also help in establishing a threshold value for total protein content required for embryo development. For the specific purpose of our research it would tell us how *Erk* deletion might bring about embryonic death. (b) It would shed light on the very important question of how involved MAPK pathway is in transcription and protein production within the oocyte.

Oocytes are cells with a highly complex store of proteins, RNAs, lipids and other small molecules required for the development and early embryonic survival. The most in-depth analysis to date on the oocyte proteome show the presence of approximately 4000 distinct proteins in the Metaphase II oocyte cytosol (Pfeiffer, Siatkowski et al. 2011). Comparison of oocyte at different stages of meiotic progression (GV, MI and MII) have revealed that the total peptide content of oocyte become progressively higher with each stage (Wang, Kou et al. 2010). This indicates that oocyte is transcriptionally and translationally active prior to MII and that the proteome of oocytes is dynamic.

Compared with early embryos and ES cells, oocytes produce more proteins that are required for post-translational modification of other proteins (ARF family), maternal affector proteins (NLRP family), and ubiquitin degradation pathway (F-box family) (Wang, Kou et al. 2010). Specifically in the MII stage, proteins that are highly represented include transcription factors, translation proteins, DNA repair proteins, and proteins required for epigenetic modifications such as histone demethylases, methyl transferases etc. Among highly represented proteins are several MAP Kinases including ERK1 and ERK2, and several downstream transcription factors such as FAK1 (Wang, Kou et al. 2010). Comparison of the protein content of the ERK depleted oocyte could give us a good idea on how important the ERKs are in the synthesis of proteins.

Another essential analysis to be performed on the *Erk1/2* double knockout oocytes would be the whole transcriptome comparison with the intact oocytes. The most in-depth analysis of MII oocyte transcriptome has revealed an approximate total of 9000 transcripts (Bettegowda and Smith 2007). Many mRNA transcripts in the oocyte are believed to be translationally quiescent and mRNAs transcripts are stored in the oocyte cytoplasm as reserve to be translated during early embryonic cleavage and reprogramming in the embryo. However, the presence of mRNA transcripts of other proteins required for metabolic processes, transport and cellular component organization indicate that a constant turnover these proteins is occurring in the oocyte.

Whether fated for immediate translation of embryo reserve or for immediate use, these mRNAs are transcribed in the oocyte during the follicular growth phase (Fair, Carter et al. 2007). Since ERK1 and ERK2 are absent at this stage in our *Erk1/2* double knockout mutants, comparison of global transcriptome would help in delineating the role of ERK in transcriptional activity within the oocyte.

Beyond the MII stage till the activation of the zygote genome there is believed to be no transcription within the oocyte. There is however, much post-translational modification of preexisting maternal mRNAs and proteins. Many of these modifications are brought about by alteration of the phosphorylation status of proteins. Several kinases and phosphatases are active

during this time. So far only a small set of phosphorylation events has been identified in the mammalian oocyte, most of which are in the context of meiotic resumption only. There is the need to define phosphoproteome at a more comprehensive level, identifying not only the status of phosphoproteins but also key sites of phosphorylation as well.

Advances in mass screening methods such as metal ion chromatography have provided us with techniques to perform mass spectrometry analysis with enrichment of phosphorylated peptides. Studies performed using these techniques have proven to be veritable mines of information regarding phosphoproteome profiles of cells. For instance, the phosphoproteome analysis of *Xenopus* eggs just prior to embryo transcription revealed multiple simultaneous phosphorylations on closely spaced residues on proteins that were previously unknown (Vernos, Heasman, et al. 1993). Another study using a mass spectrometry based analysis of the human mitotic spindle identified an approximate 300 previously unknown phosphorylations on established spindle proteins and an approximate 400 phosphorylation sites on other proteins providing further insights into the temporal regulation of a mitotic spindle.

In chapter 4, I examined other possible downstream targets of ERK by performing a mass spectrometry analysis of proteins separated with a phosphorylation specific antibody MPM2. MPM2 detects the specific type of serine/ threonine phosphorylations that are characteristic of

ERK activity. The protein signatures that got resolved were screened based on number of protein hits, presence and number of S/T sites and molecular weight. Of the selected proteins, several interesting ones showed involvement in spindle formation, assembly and function (Table 1).

Table 5.1. Selected proteins with ERK-specific phosphorylations from MS analysis of oocytes.

Protein	Action on spindle
TACC3 (Transforming Acidic Coiled Coil 3)	Increases microtubule stability and regulate chromosome alignment in mitotic cells
KIF23 (Kinesin-like protein 23)	Forms the spindle mid-body by interconnecting parallel microtubules to stabilize them
Junction plakoglobin	Maintenance of the cortical actin cytoskeleton
DNMT1 (DNA (cytosine-5) methyl transferase 1)	DNA methylation. Knockdown affects cytokinesis
PARG - Poly (ADP-ribose) glycohydrolase	Degradation of Poly (ADP-ribose) or PAR, required for spindle assembly
NLRP5/ MATER	Cytoplasmic lattice formation

One such protein with the highest number of hits and a very high number of S/T sites, TACC3, was selected for further analysis. However, experiments to detect its presence in the oocyte did not show conclusive results possibly because of unspecific antibodies. Nevertheless it would be interesting to look at the interaction between TACC3 and ERK1/2 *in vitro* to assess the phosphorylation activity of latter. It would also be exciting to look at the function of other interesting proteins of which I mentioned in chapter 3. Comparison of the phosphorylation status of these proteins during MII in the *Erk1/2DKO* oocytes with its wild type counterpart would reveal more information on the function of ERK1 and 2.

One other interesting aspect of this project is the spindle assembly checkpoint that I have discussed in Chapter 4. I had hypothesized that since spindle defects are numerous in the *Erk1/2* DKO oocyte, the SAC proteins would be activated and localized in the spindle. However SAC protein localization showed very inconclusive results indicating that either the antibodies were not specific or that SAC fails to be activated in the absence of ERKs and hence there is no regulation of spindle assembly in these oocytes leading to chromosome segregation defects and aneuploidy in the embryo. A much more thorough investigation is required to better understand how the SAC function is affected by the absence of MAPKs.

Conclusions

ERKs are some of the most significant signaling molecules with involvement in almost all major cell cycle events. There is a growing body of evidence to support the importance of ERK signaling pathways in gametogenesis. This is especially true of the oocyte where, there is much information showing that MAPK signaling and meiotic resumption are strongly coupled. However, not much is known about the roles of ERKs beyond meiotic resumption in the oocyte. While disruption of ERK signaling has certainly been reported to produce spindle and cytoskeletal defects, the actual mechanism by which these effects are produced are not known. Exact downstream mechanism(s) have yet to be delineated. The work described in this thesis attempts to increase our understanding of specific effector pathways of ERKs on cell cycle progression and cytokinesis in the oocyte. This study provides a global hypothesis of the action of ERK signaling in the oocyte, namely, the temporal and spatial organization of cellular machinery to convert a diploid germ cell to a haploid oocyte. Here I have demonstrated that ERKs play a pivotal role in ensuring chromosome segregation and asymmetric division of the oocyte.

However, the results of this study uncover only a small part of the global picture of ERK involvement in gametogenesis. The exact mechanism of ERK action on important events in

gametogenesis such as primordial germ cell development, somatic cell interactions, sex differentiation, meiosis, early embryo development etc are poorly understood. The studies in this thesis will serve as a framework for exploration of these events described above as well as further downstream effects of ERKs on the whole proteome and transcriptome of the oocyte. This work will contribute towards a better understanding of the concerted mechanisms that bring about the change of a germ cell into a highly specialized oocyte capable of supporting new life as an embryo.

References

Abrieu, A., M. Doree, et al. (2001). "The interplay between cyclin-B-Cdc2 kinase (MPF) and MAP kinase during maturation of oocytes." Journal of cell science **114**(Pt 2): 257-267.

Acevedo, N. and G. D. Smith (2005). "Oocyte-specific gene signaling and its regulation of mammalian reproductive potential." Frontiers in bioscience : a journal and virtual library **10**: 2335-2345.

Ai, J. S., Q. Wang, et al. (2008). "Roles of microtubules and microfilaments in spindle movements during rat oocyte meiosis." The Journal of reproduction and development **54**(5): 391-396.

Amleh, A. and J. Dean (2002). "Mouse genetics provides insight into folliculogenesis, fertilization and early embryonic development." Human reproduction update **8**(5): 395-403.

Anderson, E. L., A. E. Baltus, et al. (2008). "Stra8 and its inducer, retinoic acid, regulate meiotic initiation in both spermatogenesis and oogenesis in mice." Proceedings of the National Academy of Sciences of the United States of America **105**(39): 14976-14980.

Araki, K., K. Naito, et al. (1996). "Meiotic abnormalities of c-mos knockout mouse oocytes: activation after first meiosis or entrance into third meiotic metaphase." Biology of reproduction **55**(6): 1315-1324.

Assou, S., T. Anahory, et al. (2006). "The human cumulus--oocyte complex gene-expression profile." Human reproduction **21**(7): 1705-1719.

Bader JR, V. K. (2010). "Dynein at the kinetochore: Timing, Interactions and Functions." Semin Cell Dev Biol. **21(3):269-75.**

Barra, V., T. Schillaci, et al. (2012). "Bypass of cell cycle arrest induced by transient DNMT1 post-transcriptional silencing triggers aneuploidy in human cells." Cell division **7**(1): 2.

Bettegowda, A. and G. W. Smith (2007). "Mechanisms of maternal mRNA regulation: implications for mammalian early embryonic development." Frontiers in bioscience : a journal and virtual library **12**: 3713-3726.

Bhatt, R. R. and J. E. Ferrell, Jr. (1999). "The protein kinase p90 rsk as an essential mediator of cytostatic factor activity." Science **286**(5443): 1362-1365.

Bliss, S. P., A. Miller, et al. (2009). "ERK signaling in the pituitary is required for female but not male fertility." Molecular endocrinology **23**(7): 1092-1101.

Boshier, D. P. (1970). "The pontamine blue reaction in pregnant sheep uteri." Journal of reproduction and fertility **22**(3): 595-596.

Cameron, M. R., J. S. Foster, et al. (1996). "Activation of mitogen-activated protein kinases by gonadotropins and cyclic adenosine 5'-monophosphates in porcine granulosa cells." Biology of reproduction **55**(1): 111-119.

Cargnello, M. and P. P. Roux (2011). "Activation and function of the MAPKs and their substrates, the MAPK-activated protein kinases." Microbiology and molecular biology reviews : MMBR **75**(1): 50-83.

Cerda, M. C., S. Berrios, et al. (1999). "Organisation of complex nuclear domains in somatic mouse cells." Biology of the cell / under the auspices of the European Cell Biology Organization **91**(1): 55-65.

Chaigne, A., M. H. Verlhac, et al. (2012). "Spindle positioning in mammalian oocytes." Experimental cell research.

Chang P, J. M., Mitchison TJ. (2004). "Poly(ADP-ribose) is required for spindle assembly and structure." Nature. **2;432(7017):645-9.**

Chen, T., S. Hevi, et al. (2007). "Complete inactivation of DNMT1 leads to mitotic catastrophe in human cancer cells." Nature genetics **39**(3): 391-396.

Choi, T., K. Fukasawa, et al. (1996). "The Mos/mitogen-activated protein kinase (MAPK) pathway regulates the size and degradation of the first polar body in maturing mouse oocytes." Proceedings of the National Academy of Sciences of the United States of America **93**(14): 7032-7035.

Cohen, P. E. and J. K. Holloway (2010). "Predicting gene networks in human oocyte meiosis." Biology of reproduction **82**(3): 469-472.

Combes A, S. C., Koopman P (2010). Sex determination and gonadal development. Oogenesis: The universal process. V. A. Verlhac MH, John Wiley and Sons**:** 27-78.

Cross, D. A. and C. Smythe (1998). "PD 98059 prevents establishment of the spindle assembly checkpoint and inhibits the G2-M transition in meiotic but not mitotic cell cycles in Xenopus." Experimental cell research **241**(1): 12-22.

Cui, X. S., X. Y. Li, et al. (2007). "Maternal gene transcription in mouse oocytes: genes implicated in oocyte maturation and fertilization." The Journal of reproduction and development **53**(2): 405-418.

D'Haeseleer, P. (2005). "How does gene expression clustering work?" Nature biotechnology **23**(12): 1499-1501.

Di Agostino, S., P. Rossi, et al. (2002). "The MAPK pathway triggers activation of Nek2 during chromosome condensation in mouse spermatocytes." Development **129**(7): 1715-1727.

Drobic, B., P. S. Espino, et al. (2004). "Mitogen- and stress-activated protein kinase 1 activity and histone h3 phosphorylation in oncogene-transformed mouse fibroblasts." Cancer research **64**(24): 9076-9079.

Dumont J, U. M., Rassinier P, Hanauer A, Verlhac MH. (2005). "p90Rsk is not involved in cytostatic factor arrest in mouse oocytes." J Cell Biol. **25;169(2):227-31.**

Ehmsen, K. and W.-D. Heyer (2008). Biochemistry of Meiotic Recombination: Formation, Processing, and Resolution of Recombination Intermediates. Recombination and Meiosis. R. Egel and D.-H. Lankenau, Springer Berlin Heidelberg. **3:** 91-164.

Ewen, K., A. Jackson, et al. (2010). "A male-specific role for p38 mitogen-activated protein kinase in germ cell sex differentiation in mice." Biology of reproduction **83**(6): 1005-1014.

Ewen, K. A. and P. Koopman (2010). "Mouse germ cell development: from specification to sex determination." Molecular and cellular endocrinology **323**(1): 76-93.

Fair, T., F. Carter, et al. (2007). "Global gene expression analysis during bovine oocyte in vitro maturation." Theriogenology **68 Suppl 1**: S91-97.

Fan, H. Y., Z. Liu, et al. (2009). "MAPK3/1 (ERK1/2) in ovarian granulosa cells are essential for female fertility." Science **324**(5929): 938-941.

Fan, H. Y. and Q. Y. Sun (2004). "Involvement of mitogen-activated protein kinase cascade during oocyte maturation and fertilization in mammals." Biology of reproduction **70**(3): 535-547.

Finch, K. E., C. E. Knezevic, et al. (2012). "Selective small molecule inhibition of poly(ADP-ribose) glycohydrolase (PARG)." ACS chemical biology **7**(3): 563-570.

Fissore, R. A., C. L. He, et al. (1996). "Potential role of mitogen-activated protein kinase during meiosis resumption in bovine oocytes." Biology of reproduction **55**(6): 1261-1270.

Garcia-Cruz, R., I. Roig, et al. (2009). "Maternal origin of the human aneuploidies. Are homolog synapsis and recombination to blame? Notes (learned) from the underbelly." Genome dynamics **5**: 128-136.

Gasca, S., F. Pellestor, et al. (2007). "Identifying new human oocyte marker genes: a microarray approach." Reproductive biomedicine online **14**(2): 175-183.

Giet, R. and D. M. Glover (2001). "Drosophila aurora B kinase is required for histone H3 phosphorylation and condensin recruitment during chromosome condensation and to organize the central spindle during cytokinesis." The Journal of cell biology **152**(4): 669-682.

Gill, M. E., Y. C. Hu, et al. (2011). "Licensing of gametogenesis, dependent on RNA binding protein DAZL, as a gateway to sexual differentiation of fetal germ cells." Proceedings of the National Academy of Sciences of the United States of America **108**(18): 7443-7448.

Greenbaum, M. P., N. Iwamori, et al. (2009). "Mouse TEX14 is required for embryonic germ cell intercellular bridges but not female fertility." Biology of reproduction **80**(3): 449-457.

Griswold, M. D., C. A. Hogarth, et al. (2012). "Initiating meiosis: the case for retinoic acid." Biology of reproduction **86**(2): 35.

Hallinan, J. S., K. James, et al. (2011). "Network approaches to the functional analysis of microbial proteins." Advances in microbial physiology **59**: 101-133.

Han, Z., C. G. Liang, et al. (2010). "Oocyte spindle proteomics analysis leading to rescue of chromosome congression defects in cloned embryos." Journal of proteome research **9**(11): 6025-6032.

Handel, M. A. and J. C. Schimenti (2010). "Genetics of mammalian meiosis: regulation, dynamics and impact on fertility." Nature reviews. Genetics **11**(2): 124-136.

Hao, Z., M. H. Stoler, et al. (2002). "TACC3 expression and localization in the murine egg and ovary." Molecular reproduction and development **63**(3): 291-299.

Hatano, N., Y. Mori, et al. (2003). "Essential role for ERK2 mitogen-activated protein kinase in placental development." Genes to cells : devoted to molecular & cellular mechanisms **8**(11): 847-856.

Hayashi, K., S. M. de Sousa Lopes, et al. (2007). "Germ cell specification in mice." Science **316**(5823): 394-396.

Hiraoka, Y. and A. F. Dernburg (2009). "The SUN rises on meiotic chromosome dynamics." Developmental cell **17**(5): 598-605.

Hogarth, C. A., D. Mitchell, et al. (2011). "Identification and expression of potential regulators of the mammalian mitotic-to-meiotic transition." Biology of reproduction **84**(1): 34-42.

Holloway, J. K., J. Booth, et al. (2008). "MUS81 generates a subset of MLH1-MLH3-independent crossovers in mammalian meiosis." PLoS genetics **4**(9): e1000186.

Hunt, P. A., K. E. Koehler, et al. (2003). "Bisphenol a exposure causes meiotic aneuploidy in the female mouse." Current biology : CB **13**(7): 546-553.

Ji, Y. and A. V. Tulin (2012). "Poly(ADP-ribose) controls DE-cadherin-dependent stem cell maintenance and oocyte localization." Nature communications **3**: 760.

Jincho, Y. K., T. (2008). "Dynamism in the Gene Expression Profile after Oocyte Activation in Mice." Journal of Mammalian Ova Research **25**(3): 150-162.

Kang, S. K., C. J. Tai, et al. (2000). "Gonadotropin-releasing hormone activates mitogen-activated protein kinase in human ovarian and placental cells." Molecular and cellular endocrinology **170**(1-2): 143-151.

Keeney, S. (2001). "Mechanism and control of meiotic recombination initiation." Current topics in developmental biology **52**: 1-53.

Keeney, S. (2008). "Spo11 and the Formation of DNA Double-Strand Breaks in Meiosis." Genome dynamics and stability **2**: 81-123.

Kim, B., R. Kan, et al. (2010). "Potential role for MATER in cytoplasmic lattice formation in murine oocytes." PloS one **5**(9): e12587.

Kim, J., I. C. Bagchi, et al. (2009). "Control of ovulation in mice by progesterone receptor-regulated gene networks." Molecular human reproduction **15**(12): 821-828.

Kofron, M., J. Heasman, et al. (2002). "Plakoglobin is required for maintenance of the cortical actin skeleton in early Xenopus embryos and for cdc42-mediated wound healing." The Journal of cell biology **158**(4): 695-708.

Kofron, M., A. Spagnuolo, et al. (1997). "The roles of maternal alpha-catenin and plakoglobin in the early Xenopus embryo." Development **124**(8): 1553-1560.

Kolas, N. K., A. Svetlanov, et al. (2005). "Localization of MMR proteins on meiotic chromosomes in mice indicates distinct functions during prophase I." The Journal of cell biology **171**(3): 447-458.

Koubova, J., D. B. Menke, et al. (2006). "Retinoic acid regulates sex-specific timing of meiotic initiation in mice." Proceedings of the National Academy of Sciences of the United States of America **103**(8): 2474-2479.

Krentz, A. D., M. W. Murphy, et al. (2011). "DMRT1 promotes oogenesis by transcriptional activation of Stra8 in the mammalian fetal ovary." Developmental biology **356**(1): 63-70.

Kumar, R., H. M. Bourbon, et al. (2010). "Functional conservation of Mei4 for meiotic DNA double-strand break formation from yeasts to mice." Genes & development **24**(12): 1266-1280.

Le Bouffant, R., B. Souquet, et al. (2011). "Msx1 and Msx2 promote meiosis initiation." Development **138**(24): 5393-5402.

Le Masson, F., Z. Razak, et al. (2011). "Identification of heat shock factor 1 molecular and cellular targets during embryonic and adult female meiosis." Molecular and cellular biology **31**(16): 3410-3423.

Lee, E. R., K. W. McCool, et al. (2006). "Dynamic changes in histone H3 phosphoacetylation during early embryonic stem cell differentiation are directly mediated by mitogen- and stress-activated protein kinase 1 via activation of MAPK pathways." The Journal of biological chemistry **281**(30): 21162-21172.

Lee, H. S., E. Y. Kim, et al. (2010). "Obox4 critically regulates cAMP-dependent meiotic arrest and MI-MII transition in oocytes." FASEB journal : official publication of the Federation of American Societies for Experimental Biology **24**(7): 2314-2324.

Lee, H. S., E. Y. Kim, et al. (2011). "Changes in gene expression associated with oocyte meiosis after Obox4 RNAi." Clinical and experimental reproductive medicine **38**(2): 68-74.

Lenzi, M. L., J. Smith, et al. (2005). "Extreme heterogeneity in the molecular events leading to the establishment of chiasmata during meiosis i in human oocytes." American journal of human genetics **76**(1): 112-127.

Lewandoski, M., K. M. Wassarman, et al. (1997). "Zp3-cre, a transgenic mouse line for the activation or inactivation of loxP-flanked target genes specifically in the female germ line." Curr Biol **7**(2): 148-151.

Li, J. J., H. Y. Lian, et al. (2011). "Regulation of fusion of the nucleolar precursor bodies following activation of mouse oocytes: roles of the maturation-promoting factors and mitogen-activated protein kinases." Zygote: 1-13.

Li, W. and H. Ma (2006). "Double-stranded DNA breaks and gene functions in recombination and meiosis." Cell research **16**(5): 402-412.

Li, Y., K. S. Lam, et al. (2010). "A yeast's eye view of mammalian reproduction: cross-species gene co-expression in meiotic prophase." BMC systems biology **4**: 125.

Liang, C. G., Y. Q. Su, et al. (2007). "Mechanisms regulating oocyte meiotic resumption: roles of mitogen-activated protein kinase." Molecular endocrinology **21**(9): 2037-2055.

Lin, C. J., M. Conti, et al. (2013). "Histone variant H3.3 maintains a decondensed chromatin state essential for mouse preimplantation development." Development **140**(17): 3624-3634.

Lodde, V., S. C. Modina, et al. (2009). "Localization of DNA methyltransferase-1 during oocyte differentiation, in vitro maturation and early embryonic development in cow." European journal of histochemistry : EJH **53**(4): e24.

MacKintosh, C. and R. W. MacKintosh (1994). "Inhibitors of protein kinases and phosphatases." Trends in biochemical sciences **19**(11): 444-448.

Madgwick, S., D. V. Hansen, et al. (2006). "Mouse Emi2 is required to enter meiosis II by reestablishing cyclin B1 during interkinesis." The Journal of cell biology **174**(6): 791-801.

Martin, A. C. and D. G. Drubin (2003). "Impact of genome-wide functional analyses on cell biology research." Current opinion in cell biology **15**(1): 6-13.

Masson, J. Y., M. C. Tarsounas, et al. (2001). "Identification and purification of two distinct complexes containing the five RAD51 paralogs." Genes & development **15**(24): 3296-3307.

McCabe, M. T., J. A. Low, et al. (2006). "Inhibition of DNA methyltransferase activity prevents tumorigenesis in a mouse model of prostate cancer." Cancer research **66**(1): 385-392.

Minestrini, G., E. Mathe, et al. (2002). "Domains of the Pavarotti kinesin-like protein that direct its subcellular distribution: effects of mislocalisation on the tubulin and actin cytoskeleton during Drosophila oogenesis." Journal of cell science **115**(Pt 4): 725-736.

Miyagaki, Y., Y. Kanemori, et al. (2011). "Possible involvement of mitogen- and stress-activated protein kinase 1, MSK1, in metaphase-II arrest through phosphorylation of EMI2 in mouse oocytes." Developmental biology **359**(1): 73-81.

Morelli, M. A. and P. E. Cohen (2005). "Not all germ cells are created equal: aspects of sexual dimorphism in mammalian meiosis." Reproduction **130**(6): 761-781.

Mullen, S. F. and J. K. Critser (2004). "Immunocytochemical staining of the metaphase II spindle in mammalian oocytes." Methods in molecular biology **253**: 201-213.

Munroe, R. J., R. A. Bergstrom, et al. (2000). "Mouse mutants from chemically mutagenized embryonic stem cells." Nature genetics **24**(3): 318-321.

Nagamatsu, G., T. Kosaka, et al. (2012). "Tracing the conversion process from primordial germ cells to pluripotent stem cells in mice." Biology of reproduction **86**(6): 182.

Nagaoka, S. I., C. A. Hodges, et al. (2011). "Oocyte-specific differences in cell-cycle control create an innate susceptibility to meiotic errors." Current biology : CB **21**(8): 651-657.

Neale, M. J., J. Pan, et al. (2005). "Endonucleolytic processing of covalent protein-linked DNA double-strand breaks." Nature **436**(7053): 1053-1057.

Norris, R. P., M. Freudzon, et al. (2008). "Luteinizing hormone causes MAP kinase-dependent phosphorylation and closure of connexin 43 gap junctions in mouse ovarian follicles: one of two paths to meiotic resumption." Development **135**(19): 3229-3238.

Norris, R. P., W. J. Ratzan, et al. (2009). "Cyclic GMP from the surrounding somatic cells regulates cyclic AMP and meiosis in the mouse oocyte." Development **136**(11): 1869-1878.

Nousiainen, M., H. H. Sillje, et al. (2006). "Phosphoproteome analysis of the human mitotic spindle." Proceedings of the National Academy of Sciences of the United States of America **103**(14): 5391-5396.

Oh, J. S., S. J. Han, et al. (2010). "Wee1B, Myt1, and Cdc25 function in distinct compartments of the mouse oocyte to control meiotic resumption." The Journal of cell biology **188**(2): 199-207.

Oktem, O. and B. Urman (2010). "Understanding follicle growth in vivo." Human reproduction **25**(12): 2944-2954.

Ou, X. H., S. Li, et al. (2010). "p38alpha MAPK is a MTOC-associated protein regulating spindle assembly, spindle length and accurate chromosome segregation during mouse oocyte meiotic maturation." Cell cycle **9**(20): 4130-4143.

Pages, G., S. Guerin, et al. (1999). "Defective thymocyte maturation in p44 MAP kinase (Erk 1) knockout mice." Science **286**(5443): 1374-1377.

Pasdar, M., Z. Li, et al. (1995). "Plakoglobin: kinetics of synthesis, phosphorylation, stability, and interactions with desmoglein and E-cadherin." Cell motility and the cytoskeleton **32**(4): 258-272.

Petrunewich, M. A., J. R. Trimarchi, et al. (2009). "Second meiotic spindle integrity requires MEK/MAP kinase activity in mouse eggs." The Journal of reproduction and development **55**(1): 30-38.

Pfeiffer, M. J., M. Siatkowski, et al. (2011). "Proteomic analysis of mouse oocytes reveals 28 candidate factors of the "reprogrammome"." Journal of proteome research **10**(5): 2140-2153.

Pfeuty, B., J. F. Bodart, et al. (2012). "A dynamical model of oocyte maturation unveils precisely orchestrated meiotic decisions." PLoS computational biology **8**(1): e1002329.

Phillips, K. P., M. A. Petrunewich, et al. (2002). "Inhibition of MEK or cdc2 kinase parthenogenetically activates mouse eggs and yields the same phenotypes as Mos(-/-) parthenogenotes." Developmental biology **247**(1): 210-223.

Pullikuth AK, O. A., Cardenas D, Bailey E, Sherman NE, Pfister KK, Catling AD. (2013). "Epidermal growth factor stimulates extracellular-signal regulated kinase phosphorylation of a novel site on cytoplasmic Dynein intermediate chain 2." Int J Mol Sci. **;14(2):3595-620.** .

Rajkovic, A., C. Yan, et al. (2002). "Obox, a family of homeobox genes preferentially expressed in germ cells." Genomics **79**(5): 711-717.

Raman, M., W. Chen, et al. (2007). "Differential regulation and properties of MAPKs." Oncogene **26**(22): 3100-3112.

Rapaport, F., A. Zinovyev, et al. (2007). "Classification of microarray data using gene networks." BMC bioinformatics **8**: 35.

Renzi, L., M. S. Gersch, et al. (1997). "MPM-2 antibody-reactive phosphorylations can be created in detergent-extracted cells by kinetochore-bound and soluble kinases." Journal of cell science **110 (Pt 17)**: 2013-2025.

Richards, J. S. and S. A. Pangas (2010). "The ovary: basic biology and clinical implications." The Journal of clinical investigation **120**(4): 963-972.

Rolland, A. D., K. P. Lehmann, et al. (2011). "Uncovering gene regulatory networks during mouse fetal germ cell development." Biology of reproduction **84**(4): 790-800.

Roy Choudhury, D., C. Small, et al. (2010). "Microarray-based analysis of cell-cycle gene expression during spermatogenesis in the mouse." Biology of reproduction **83**(4): 663-675.

Saba-El-Leil, M. K., F. D. Vella, et al. (2003). "An essential function of the mitogen-activated protein kinase Erk2 in mouse trophoblast development." EMBO reports **4**(10): 964-968.

Santucci-Darmanin, S. a. B., F. (2010). Meiotic recombination in mammals. Oogenesis: The universal process. V. A. Verlhac MH, Wiley & Sons**:** 141-177.

Sawicka, A. and C. Seiser (2012). "Histone H3 phosphorylation - a versatile chromatin modification for different occasions." Biochimie **94**(11): 2193-2201.

Schneider, L., F. Essmann, et al. (2007). "The transforming acidic coiled coil 3 protein is essential for spindle-dependent chromosome alignment and mitotic survival." The Journal of biological chemistry **282**(40): 29273-29283.

Schwab MS, R. B., Gross SD, Tunquist BJ, Taieb FE, Lewellyn AL, Maller JL. (2001). "Bub1 is activated by the protein kinase p90(Rsk) during Xenopus oocyte maturation." Curr Biol. **6;11(3):141-50.**

Schwab, M. S., B. T. Roberts, et al. (2001). "Bub1 is activated by the protein kinase p90(Rsk) during Xenopus oocyte maturation." Current biology : CB **11**(3): 141-150.

Sonn, S., G. T. Oh, et al. (2011). "Nek2 and its substrate, centrobin/Nip2, are required for proper meiotic spindle formation of the mouse oocytes." Zygote **19**(1): 15-20.

Steuerwald, N., J. Cohen, et al. (2001). "Association between spindle assembly checkpoint expression and maternal age in human oocytes." Molecular human reproduction **7**(1): 49-55.

Su, Y., Y. Li, et al. (2011). "Mammalian meiosis is more conserved by sex than by species: conserved co-expression networks of meiotic prophase." Reproduction **142**(5): 675-687.

Su, Y. Q., K. Wigglesworth, et al. (2002). "Mitogen-activated protein kinase activity in cumulus cells is essential for gonadotropin-induced oocyte meiotic resumption and cumulus expansion in the mouse." Endocrinology **143**(6): 2221-2232.

Sun, Q. Y., L. Lai, et al. (2001). "Dynamic events are differently mediated by microfilaments, microtubules, and mitogen-activated protein kinase during porcine oocyte maturation and fertilization in vitro." Biology of reproduction **64**(3): 879-889.

Sun, Q. Y., Y. L. Miao, et al. (2009). "Towards a new understanding on the regulation of mammalian oocyte meiosis resumption." Cell cycle **8**(17): 2741-2747.

Tong, Z. B., L. Gold, et al. (2000). "Mater, a maternal effect gene required for early embryonic development in mice." Nature genetics **26**(3): 267-268.

Tripathi, A., K. V. Kumar, et al. (2010). "Meiotic cell cycle arrest in mammalian oocytes." Journal of cellular physiology **223**(3): 592-600.

Verlhac, M. H., H. de Pennart, et al. (1993). "MAP kinase becomes stably activated at metaphase and is associated with microtubule-organizing centers during meiotic maturation of mouse oocytes." Developmental biology **158**(2): 330-340.

Verlhac, M. H., C. Lefebvre, et al. (2000). "Asymmetric division in mouse oocytes: with or without Mos." Current biology : CB **10**(20): 1303-1306.

Vernos, I., J. Heasman, et al. (1993). "Multiple kinesin-like transcripts in Xenopus oocytes." Developmental biology **157**(1): 232-239.

Vogt, E., M. Kirsch-Volders, et al. (2008). "Spindle formation, chromosome segregation and the spindle checkpoint in mammalian oocytes and susceptibility to meiotic error." Mutation research **651**(1-2): 14-29.

Wang, S., Z. Kou, et al. (2010). "Proteome of mouse oocytes at different developmental stages." Proceedings of the National Academy of Sciences of the United States of America **107**(41): 17639-17644.

Wei L, L. X., Zhang QH, Li M, Yuan J, Li S, Sun SC, Ouyang YC, Schatten H, Sun QY. (2010). "BubR1 is a spindle assembly checkpoint protein regulating meiotic cell cycle progression of mouse oocyte." Cell Cycle. **15;9(6):1112-21.** .

White, E. A. and M. Glotzer (2012). "Centralspindlin: at the heart of cytokinesis." Cytoskeleton **69**(11): 882-892.

Yang F, B. C., De La Fuente R. (2009). "Persistence of histone H2AX phosphorylation after meiotic chromosome synapsis and abnormal centromere cohesion in poly (ADP-ribose) polymerase (Parp-1) null oocytes." Dev Biol. **15;331(2):326-38.**

Yao, H. H., M. M. Matzuk, et al. (2004). "Follistatin operates downstream of Wnt4 in mammalian ovary organogenesis." Developmental dynamics : an official publication of the American Association of Anatomists **230**(2): 210-215.

Yu, L. Z., B. Xiong, et al. (2007). "MEK1/2 regulates microtubule organization, spindle pole tethering and asymmetric division during mouse oocyte meiotic maturation." Cell cycle **6**(3): 330-338.

Yurttas P, M. E., Coonrod SA. (2010). "Use of proteomics to identify highly abundant maternal factors that drive the egg-to-embryo transition." Reproduction. **May;139(5):809-23**.

Yurttas, P., A. M. Vitale, et al. (2008). "Role for PADI6 and the cytoplasmic lattices in ribosomal storage in oocytes and translational control in the early mouse embryo." Development **135**(15): 2627-2636.

Zhang, P., M. Zucchelli, et al. (2009). "Transcriptome profiling of human pre-implantation development." PloS one **4**(11): e7844.

Zheng, P., B. Baibakov, et al. (2013). "PtdIns(3,4,5)P3 is constitutively synthesized and required for spindle translocation during meiosis in mouse oocytes." Journal of cell science **126**(Pt 3): 715-721.

Zheng, P. and J. Dean (2007). "Oocyte-specific genes affect folliculogenesis, fertilization, and early development." Seminars in reproductive medicine **25**(4): 243-251.

Zheng, P., M. D. Griswold, et al. (2010). "Predicting meiotic pathways in human fetal oogenesis." Biology of reproduction **82**(3): 543-551.

Zhu, C., E. Bossy-Wetzel, et al. (2005). "Recruitment of MKLP1 to the spindle midzone/midbody by INCENP is essential for midbody formation and completion of cytokinesis in human cells." The Biochemical journal **389**(Pt 2): 373-381.

APPENDIX 1

MS analysis from MPM2 IP from 130 and 80 KDa bands

Wildtype oocytes (~1500 per replicate) were lysed, immunoprecipitated with MPM2 antibody and run on a 7% SDS-PAGE gel. Regions of the gel corresponding to 130 and 80 KDa were excised and used for Mass Spectrometry analysis. Results from MS assay presented as p130 or p80 (proteins from the 130 or 80 KDa bands respectively) from the first and second replicates. Column Titles explained below.

column title	explanation
prot_hit_num	number of protein hits
prot_acc	protein accession number
prot_desc	protein description
prot_score	protein score, which are derived from peptides score
prot_mass	mass of the protein
prot_matches	Peptide numbers matching to the protein
prot_matches_sig	Significant peptide # matching to the protein
prot_sequences	Unique peptide # to the protein
prot_sequences_sig	Unique peptide # to the protein with significance
prot_cover	protein sequence coverage
prot_pi	pI value of the protien
pep_query	Original MS/MS spectra query number
pep_rank	Peptide ranking number, 1 is the best.
pep_isbold	1 means peptide shown in first time will be bolded
pep_isunique	unique peptide=1, non unique peptide=0
pep_exp_mz	Detected peptide m/z by MS instrument
pep_exp_mr	Detected peptide mass
pep_exp_z	Detected peptide charges
pep_calc_mr	Theoretically calculated peptide mass
pep_delta	difference between experimental mass and the theoretical mass
emPAI*	The Exponentially Modified Protein Abundance Index (emPAI) offers approximate, label-free, relative quantitation of the proteins in a mixture based on protein coverage by the peptide matches in a database search result.

P130 1st replicate MS analysis Wildtype oocytes								
prot_hit_num	**prot_acc**	**prot_desc**	**prot_score**	**prot_mass**	**prot_cover**	**prot_pi**	**emPAI**	**molar %**
1	gil16716569	protease, serine, 1 [Mus musculus]	797	26802	12.2	4.75	1.56	10.07101356
2	gil112983636	keratin complex 1, acidic, gene 10 [Mus musculus]	582	57178	13.7	5	0.65	4.196255649
3	gil6756081	zona pellucida glycoprotein 2 [Mus musculus]	557	81413	23.7	6.12	1.04	6.714009038
4	gil21489935	keratin 14 [Mus musculus]	513	53176	17.4	5.1	0.72	4.648160103

5	gil126116585	keratin complex 2, basic, gene 1 [Mus musculus]	483	66079	5.2	8.39	0.55	3.550677857
6	gil31981596	ubiquitin-like, containing PHD and RING finger domains, 1 [Mus musculus]	470	89689	30.9	8.63	1.2	7.746933505
7	gil6680602	keratin 15 [Mus musculus]	421	49243	10	4.78	0.68	4.389928986
8	gil6680604	keratin 16 [Mus musculus]	382	51973	8.1	5.13	0.36	2.324080052
9	gil6756083	zona pellucida glycoprotein 3 [Mus musculus]	347	47187	25.2	6.09	0.97	6.262104584

10	gil47059013	keratin 73 [Mus musculus]	292	59502	5.9	8.36	0.38	2.45319561
11	gil94681040	transforming, acidic coiled-coil containing protein 3 [Mus musculus]	288	70767	18.4	4.56	0.8	5.164622337
12	gil9910294	keratin 71 [Mus musculus]	276	57860	5.9	6.6	0.39	2.517753389
13	gil51092293	keratin 77 [Mus musculus]	269	61379	5.2	7.74	0.3	1.936733376
14	gil47679095	keratin 42 [Mus musculus]	266	50488	15.5	5.05	0.37	2.388637831
15	gil124249092	zona pellucida glycoprotein 1 [Mus musculus]	231	69934	8.5	6.07	0.38	2.45319561

16	gil20911031	keratin 5 [Mus musculus]	211	61957	12.6	7.59	0.36	2.324080052
17	gil84781771	trypsin 10 [Mus musculus]	199	26888	14.6	5.5	0.6	3.873466753
18	gil124487419	keratin complex 2, basic, gene 17 [Mus musculus]	171	71336	4.5	8.26	0.2	1.291155584
19	gil149255637	PREDICTED: similar to Chain L, Structural Basis Of Antigen Mimicry In A Clinically Relevant Melanoma Antigen System isoform 1 [Mus musculus]	169	26430	11.8	5.13	0.61	3.938024532

20	gil50872155	NLR family, pyrin domain containing 14 [Mus musculus]	135	115738	6.8	6.06	0.18	1.162040026
21	gil54607171	keratin 6A [Mus musculus]	109	59641	7.4	8.04	0.31	2.001291156
22	gil149263752	PREDICTED: similar to immunoglobulin gamma 2A chain [Mus musculus]	100	46995	8.1	6.08	0.15	0.968366688
23	gil51921343	hypothetical protein LOC433987 [Mus musculus]	100	35315	9.6	5.09	0.43	2.775984506
24	gil221647776	keratin 6L [Mus musculus]	98	57802	5.6	7.55	0.18	1.162040026

25	gil85701680	keratin 76 [Mus musculus]	85	63319	4.7	8.68	0.22	1.420271143
26	gil37574121	D10Ertd802e protein [Mus musculus]	82	103935	1.6	8.23	0.03	0.193673338
27	gil145580629	keratin Kb40 [Mus musculus]	79	114018	1.1	8.36	0.03	0.193673338
28	gil33859506	albumin [Mus musculus]	76	70730	4.4	5.75	0.1	0.645577792
29	gil71043961	trypsinogen 7 [Mus musculus]	68	27089	4.9	8.22	0.12	0.774693351
30	gil149255578	PREDICTED: similar to immunoglobulin kappa chain [Mus musculus]	63	14630	9.9	8.53	0.23	1.484828922

31	gil88758582	pyridoxal-dependent decarboxylase domain containing 1 isoform 1 [Mus musculus]	63	88136	1.4	5.31	0.04	0.258231117
32	gil23956096	vesicle docking protein [Mus musculus]	61	108000	3	4.85	0.06	0.387346675
33	gil39930413	nucleoporin 98 [Mus musculus]	61	125014	6.9	5.98	0.14	0.903808909
34	gil14097201 1	NALP, kappa [Mus musculus]	58	110195	2.3	6.43	0.06	0.387346675
35	gil29568094	kinesin family member 23 [Mus musculus]	52	109862	3.9	8.89	0.03	0.193673338

36	gil9845265	ubiquitin A-52 residue ribosomal protein fusion product 1 [Mus musculus]	47	15004	22.7	9.87	0.23	1.484828922
37	gil120444912	poly (ADP-ribose) glycohydrolase [Mus musculus]	44	109853	1.5	6.39	0.03	0.193673338
38	gil57222276	a disintegrin and metalloproteinase domain 6-like [Mus musculus]	39	87804	1.5	7.96	0.04	0.258231117
39	gil85701724	hypothetical protein LOC102991 [Mus musculus]	38	49578	3.8	9.59	0.07	0.451904454

40	gil149274956	PREDICTED: similar to hCG2038926 [Mus musculus]	38	19110	8.9	4.9	0.18	1.162040026
41	gil27369646	TBC1 domain family, member 25 [Mus musculus]	38	82949	1.2	6.31	0.04	0.258231117
42	gil56785430	disabled homolog 2 isoform b [Mus musculus]	37	58800	3.8	5.66	0.11	0.710135571
43	gil50363232	nestin [Mus musculus]	34	207627	0.5	4.3	0.02	0.129115558
44	gil19527100	oxysterol binding protein-like 9 isoform a [Mus musculus]	34	63062	2	5.89	0.05	0.322788896

45	gil149253187	PREDICTED: retinoblastoma-associated factor 600 isoform 1 [Mus musculus]	34	578883	0.2	5.72	0.01	0.064557779
46	gil27151744	SH3-domain kinase binding protein 1 [Mus musculus]	34	68949	1.6	7.05	0.05	0.322788896
47	gil58037397	zinc finger protein 509 [Mus musculus]	32	84862	0.7	7.99	0.04	0.258231117
48	gil21450287	cold shock domain containing E1, RNA binding [Mus musculus]	30	89590	0.8	5.97	0.04	0.258231117

49	gil125987599	CD2-associated protein [Mus musculus]	30	70578	1.6	6.07	0.05	0.322788896
50	gil84370361	nidogen 2 [Mus musculus]	27	156610	0.6	5.16	0.02	0.129115558
51	gil6671682	caspase 11 [Mus musculus]	24	43356	2.7	6.61	0.08	0.516462234
							15.49	100

P80 1st replicate MS analysis Wildtype oocytes									
prot_hit_num	**prot_acc**	**prot_desc**	**prot_score**	**prot_mass**	**prot_cover**	**prot_pi**	**emPAI**	**molar %**	
1	gil16716569	protease, serine, 1 [Mus musculus]	782	26802	12.2	4.75	1.56	11.0	
2	gil119372294	peptidyl arginine deiminase, egg and embryo abundant [Mus musculus]	620	77755	41.6	5.36	1.38	9.7	
3	gil6756083	zona pellucida glycoprotein 3 [Mus musculus]	474	47187	27.6	6.09	1.58	11.1	

4	gil33859506	albumin [Mus musculus]	436	70730	14.5	5.75	0.44	3.1	
5	gil31981690	heat shock protein 8 [Mus musculus]	360	71055	30.3	5.37	0.88	6.2	
6	gil112983636	keratin complex 1, acidic, gene 10 [Mus musculus]	329	57178	13.7	5	0.85	6.0	
7	gil126116585	keratin complex 2, basic, gene 1 [Mus musculus]	313	66079	5.2	8.39	0.47	3.3	
8	gil47059013	keratin 73 [Mus musculus]	221	59502	5.9	8.36	0.38	2.7	

9	gil20911031	keratin 5 [Mus musculus]	217	61957	10.5	7.59	0.36	2.5	
10	gil124487419	keratin complex 2, basic, gene 17 [Mus musculus]	183	71336	4.5	8.26	0.25	1.8	
11	gil21489935	keratin 14 [Mus musculus]	174	53176	9.1	5.1	0.43	3.0	
12	gil84781771	trypsin 10 [Mus musculus]	160	26888	14.6	5.5	0.6	4.2	
13	gil6680602	keratin 15 [Mus musculus]	152	49243	7.5	4.78	0.57	4.0	
14	gil54607171	keratin 6A [Mus musculus]	141	59641	5.8	8.04	0.31	2.2	

15	gil51921343	hypothetical protein LOC432987 [Mus musculus]	136	35315	9.6	5.09	0.57	4.0	
16	gil16716583	transducin-like enhancer protein 6 [Mus musculus]	123	65930	14.6	5.67	0.28	2.0	
17	gil13386238	keratin 34 [Mus musculus]	114	46185	9.2	4.76	0.23	1.6	
18	gil47679095	keratin 42 [Mus musculus]	105	50488	6.2	5.05	0.21	1.5	

19	gil6756081	zona pellucida glycoprotein 2 [Mus musculus]	95	81413	5.8	6.12	0.17	1.2	
20	gil94367594	PREDICTED: similar to orthologue of H. sapiens chromosome 20 open reading frame 119 (C20orf119) [Mus musculus]	95	64975	8.5	8.32	0.28	2.0	
21	gil145580629	keratin Kb40 [Mus musculus]	87	114018	1.3	8.36	0.06	0.4	

22	gil8393684	keratin 35 [Mus musculus]	87	48984	8.2	4.76	0.3	2.1	
23	gil71043961	trypsinogen 7 [Mus musculus]	79	27089	4.9	8.22	0.12	0.8	
24	gil39930427	myotubularin related protein 14 [Mus musculus]	77	59799	7.4	6.18	0.17	1.2	
25	gil85701680	keratin 76 [Mus musculus]	65	63319	3	8.68	0.16	1.1	
26	gil31980832	keratin complex 2, basic gene 18 [Mus musculus]	64	57377	5.5	6.19	0.12	0.8	

27	gil82933144	PREDICTED: coiled-coil domain containing 6 isoform 1 [Mus musculus]	63	53077	7.5	6.87	0.13	0.9	
28	gil6754482	keratin 18 [Mus musculus]	57	47475	5.9	5.22	0.14	1.0	
29	gil6754256	heat shock protein 9 [Mus musculus]	50	73768	1.6	5.91	0.04	0.3	
30	gil27369782	gem (nuclear organelle) associated protein 5 [Mus musculus]	47	169080	0.5	6.25	0.02	0.1	

31	gil74315985	keratin complex 2, basic, gene 10 [Mus musculus]	46	55098	3.7	5.63	0.12	0.8	
32	gil149255637	PREDICTED: similar to Chain L, Structural Basis Of Antigen Mimicry In A Clinically Relevant Melanoma Antigen System isoform 1 [Mus musculus]	41	26430	5.9	5.13	0.13	0.9	

33	gil17998694	fragile X mental retardation gene 1, autosomal homolog [Mus musculus]	38	61178	1.5	6.02	0.05	0.4	
34	gil21624617	RIKEN cDNA 1110007M04 [Mus musculus]	37	20070	4	9.4	0.17	1.2	
35	gil57222276	a disintegrin and metalloproteinase domain 6-like [Mus musculus]	36	87804	1.5	7.96	0.04	0.3	

36	gil9845265	ubiquitin A-52 residue ribosomal protein fusion product 1 [Mus musculus]	35	15004	12.5	9.87	0.23	1.6	
37	gil50363232	nestin [Mus musculus]	34	207627	0.5	4.3	0.02	0.1	
38	gil149253187	PREDICTED: retinoblastoma-associated factor 600 isoform 1 [Mus musculus]	33	578883	0.2	5.72	0.01	0.1	

39	gil58037397	zinc finger protein 509 [Mus musculus]	32	84862	0.7	7.99	0.04	0.3	
40	gil21746157	arylformamidase [Mus musculus]	32	34322	3.6	5.72	0.1	0.7	
41	gil21450287	cold shock domain containing E1, RNA binding [Mus musculus]	31	89590	0.8	5.97	0.04	0.3	

42	gil149234349	PREDICTED: centrosome-associated protein 350 isoform 1 [Mus musculus]	31	348035	0.3	6	0.01	0.1	
43	gil28395018	junction plakoglobin [Mus musculus]	31	82490	2.6	5.75	0.04	0.3	
44	gil134948762	protein tyrosine phosphatase, non-receptor type 13 [Mus musculus]	29	271947	0.5	5.93	0.01	0.1	

45	gil30520043	hypothetical protein LOC210757 [Mus musculus]	29	73362	1.6	5.77	0.04	0.3	
46	gil13626040	A kinase (PRKA) anchor protein (gravin) 12 [Mus musculus]	26	181156	1	4.39	0.02	0.1	
47	gil6671682	caspase 11 [Mus musculus]	26	43356	2.7	6.61	0.08	0.6	
							14.21	100	

P130 2nd replicate MS analysis Wildtype oocytes								
prot_hit_num	**prot_acc**	**prot_desc**	**prot_score**	**prot_mass**	**prot_cover**	**prot_pi**	**emPAI**	**molar %**
1	gil112983636	keratin complex 1, acidic, gene 10 [Mus musculus]	334	57178	9.8	5	0.4	2.57
2	gil16716569	protease, serine, 1 [Mus musculus]	333	26802	8.1	4.75	0.6	3.85
3	gil28395018	junction plakoglobin [Mus musculus]	289	82490	12.8	5.75	0.37	2.38
4	gil94681040	transforming, acidic coiled-coil containing protein 3 [Mus musculus]	273	70767	12.5	4.56	0.44	2.83

5	gil126116585	keratin complex 2, basic, gene 1 [Mus musculus]	244	66079	4.9	8.39	0.34	2.18
6	gil21489935	keratin 14 [Mus musculus]	230	53176	14.3	5.1	0.35	2.25
7	gil33859506	albumin [Mus musculus]	203	70730	4.4	5.75	0.2	1.28
8	gil47059013	keratin 73 [Mus musculus]	195	59502	5.6	8.36	0.24	1.54
9	gil47679095	keratin 42 [Mus musculus]	177	50488	11.7	5.05	0.29	1.86
10	gil29244176	hypothetical protein 4732456N10 [Mus musculus]	155	58629	7.6	8.47	0.24	1.54
11	gil20911031	keratin 5 [Mus musculus]	150	61957	9.1	7.59	0.3	1.93

12	gil84781771	trypsin 10 [Mus musculus]	146	26888	10.6	5.5	0.6	3.85
13	gil31621307	desmoglein 4 [Mus musculus]	139	115915	3.9	4.58	0.12	0.77
14	gil31980832	keratin complex 2, basic gene 18 [Mus musculus]	131	57377	9.5	6.19	0.25	1.61
15	gil124487419	keratin complex 2, basic, gene 17 [Mus musculus]	131	71336	4.2	8.26	0.09	0.58
16	gil9790161	plakophilin 1 [Mus musculus]	130	82270	5.6	9.15	0.12	0.77
17	gil21357425	keratin 82 [Mus musculus]	128	58673	5.4	5.99	0.24	1.54

18	gil110347402	DNA methyltransferase (cytosine-5) 1 [Mus musculus]	124	185372	2.8	7.92	0.07	0.45
19	gil13386238	keratin 34 [Mus musculus]	116	46185	9.2	4.76	0.23	1.48
20	gil149262435	PREDICTED: keratin complex 1, acidic, gene 3 [Mus musculus]	113	55405	10.7	5.21	0.19	1.22
21	gil8393684	keratin 35 [Mus musculus]	109	48984	8.5	4.76	0.22	1.41
22	gil21361209	histone cluster 2, H4 [Mus musculus]	109	11360	29.1	11.36	1.89	12.14
23	gil134023662	stratifin [Mus musculus]	108	27803	16.5	4.72	0.41	2.63

24	gil82950149	PREDICTED: desmoplakin isoform 2 [Mus musculus]	97	263538	2.9	6.53	0.04	0.26
25	gil6680604	keratin 16 [Mus musculus]	92	51973	6.6	5.13	0.2	1.28
26	gil71043961	trypsinogen 7 [Mus musculus]	88	27089	4.9	8.22	0.12	0.77
27	gil20799907	histone 2, H2aa1 [Mus musculus]	82	14087	34.6	10.9	0.91	5.84
28	gil9845257	histone 1, H1c [Mus musculus]	82	21254	15.6	11	0.55	3.53
29	gil51921343	hypothetical protein LOC432987 [Mus musculus]	81	35315	9.3	5.09	0.31	1.99

30	gil31981722	heat shock 70kD protein 5 (glucose-regulated protein) [Mus musculus]	80	72492	3.8	5.01	0.09	0.58
31	gil145580629	keratin Kb40 [Mus musculus]	79	114018	1.1	8.36	0.03	0.19
32	gil9845265	ubiquitin A-52 residue ribosomal protein fusion product 1 [Mus musculus]	78	15004	24.2	9.87	0.51	3.28
33	gil22164776	keratin 6L [Mus musculus]	78	57802	3.6	7.55	0.12	0.77
34	gil31560686	heat shock protein 2 [Mus musculus]	74	69884	3.8	5.51	0.1	0.64

35	gil149255637	PREDICTED: similar to Chain L, Structural Basis Of Antigen Mimicry In A Clinically Relevant Melanoma Antigen System isoform 1 [Mus musculus]	73	26430	8	5.13	0.27	1.73
36	gil126032329	eukaryotic translation elongation factor 1 alpha 1 [Mus musculus]	69	50424	6.1	9.1	0.21	1.35
37	gil6756081	zona pellucida glycoprotein 2 [Mus musculus]	67	81413	4.5	6.12	0.13	0.83

38	gil6755358	ribosomal protein L8 [Mus musculus]	65	28235	4.3	11.03	0.12	0.77
39	gil50355692	lamin A isoform A [Mus musculus]	58	74540	1.5	6.54	0.04	0.26
40	gil31981147	leucine aminopeptidase 3 [Mus musculus]	58	56549	2.3	7.14	0.06	0.39
41	gil6679439	peptidylprolyl isomerase A [Mus musculus]	57	18131	5.5	7.74	0.19	1.22
42	gil14926691	PREDICTED: hypothetical protein isoform 1 [Mus musculus]	52	38550	8.5	5.02	0.18	1.16

43	gil124001582	melanoma inhibitory activity 3 [Mus musculus]	51	214171	1.5	4.68	0.02	0.13
44	gil94536870	WNK lysine deficient protein kinase 2 [Mus musculus]	50	220018	1.1	5.45	0.01	0.06
45	gil31560560	ribosomal protein SA [Mus musculus]	49	33008	4.4	4.8	0.1	0.64
46	gil6680027	glutamate dehydrogenase 1 [Mus musculus]	47	61640	3.6	8.05	0.11	0.71
47	gil28316760	histone 1, H2bb [Mus musculus]	46	13944	14.3	10.31	0.55	3.53

48	gil9507079	selenium binding protein 2 [Mus musculus]	44	53165	2.1	5.78	0.06	0.39
49	gil6678465	tubulin, alpha 1a [Mus musculus]	43	50612	5.3	4.97	0.07	0.45
50	gil125987599	CD2-associated protein [Mus musculus]	42	70578	2	6.07	0.05	0.32
51	gil7106379	NACHT, leucine rich repeat and PYD containing 5 isoform a [Mus musculus]	42	127759	1.7	5.57	0.03	0.19

52	gil149259085	PREDICTED: similar to ribosomal protein isoform 1 [Mus musculus]	40	16723	7.7	10.96	0.2	1.28
53	gil9790163	plakophilin 3 [Mus musculus]	39	87758	1.4	9.43	0.04	0.26
54	gil119372294	peptidyl arginine deiminase, egg and embryo abundant [Mus musculus]	39	77755	1.8	5.36	0.04	0.26
55	gil88014720	karyopherin (importin) beta 1 [Mus musculus]	38	98377	1.4	4.68	0.03	0.19

56	gil6671509	actin, beta, cytoplasmic [Mus musculus]	38	42052	12.5	5.29	0.25	1.61
57	gil20846986	PREDICTED: similar to ribosomal protein S25 [Mus musculus]	37	13814	8	10.06	0.25	1.61
58	gil83745120	ribosomal protein, large P2 [Mus musculus]	36	11644	13.9	4.42	0.3	1.93
59	gil58037377	leucine rich repeat containing 15 [Mus musculus]	35	65048	2.8	5.96	0.05	0.32
60	gil6680159	H3 histone, family 3A [Mus musculus]	35	15376	11.8	11.27	0.22	1.41

61	gil31981100	ribosomal protein S14 [Mus musculus]	35	16434	7.3	10.07	0.21	1.35
62	gil149264187	PREDICTED: hypothetical protein [Mus musculus]	35	100771	0.8	5.55	0.03	0.19
63	gil6756083	zona pellucida glycoprotein 3 [Mus musculus]	34	47187	2.1	6.09	0.07	0.45
64	gil30520043	hypothetical protein LOC210757 [Mus musculus]	33	73362	1.6	5.77	0.04	0.26
65	gil21426893	histone 1, H1b [Mus musculus]	33	22562	4.9	10.91	0.15	0.96

66	gil149261940	PREDICTED: alpha-2-plasmin inhibitor [Mus musculus]	32	224236	0.6	5.69	0.01	0.06
67	gil148277039	alpha-2-macroglobulin precursor [Mus musculus]	30	165674	0.9	6.18	0.02	0.13
68	gil31981596	ubiquitin-like, containing PHD and RING finger domains, 1 [Mus musculus]	29	89689	1.9	8.63	0.04	0.26
69	gil7305119	G two S phase expressed protein 1 [Mus musculus]	28	79160	1.2	9.45	0.04	0.26

70	gil6755891	protease, serine, 3 [Mus musculus]	27	26851	8.1	4.84	0.12	0.77
71	gil6671682	caspase 11 [Mus musculus]	25	43356	2.7	6.61	0.08	0.51
							15.57	100

P80 2nd replicate MS analysis Wildtype oocytes								
prot_hit_num	**prot_acc**	**prot_desc**	**prot_score**	**prot_mass**	**prot_cover**	**prot_pi**	**emPAI**	**molar %**
1	gil33859506	albumin [Mus musculus]	841	70730	9.9	5.75	0.31	4.03
2	gil119372294	peptidyl arginine deiminase, egg and embryo abundant [Mus musculus]	626	77755	30.5	5.36	1.02	13.26
3	gil112983636	keratin complex 1, acidic, gene 10 [Mus musculus]	322	57178	10.9	5	0.4	5.20
4	gil29244176	hypothetical protein 4732456N10 [Mus musculus]	235	58629	5.6	8.47	0.24	3.12

5	gil16716569	protease, serine, 1 [Mus musculus]	227	26802	8.1	4.75	1.02	13.26
6	gil7106335	keratin 17 [Mus musculus]	217	48417	9	5	0.49	6.37
7	gil126116585	keratin complex 2, basic, gene 1 [Mus musculus]	215	66079	4.9	8.39	0.34	4.42
8	gil54607171	keratin 6A [Mus musculus]	179	59641	9	8.04	0.31	4.03
9	gil20911031	keratin 5 [Mus musculus]	178	61957	6.7	7.59	0.3	3.90
10	gil134288917	dynein, cytoplasmic, heavy chain 1 [Mus musculus]	168	534447	0.3	6.03	0.01	0.13

11	gil51921343	hypothetical protein LOC432987 [Mus musculus]	150	35315	9.3	5.09	0.43	5.59
12	gil31981690	heat shock protein 8 [Mus musculus]	150	71055	16.1	5.37	0.25	3.25
13	gil124487419	keratin complex 2, basic, gene 17 [Mus musculus]	142	71336	4.2	8.26	0.14	1.82
14	gil47679095	keratin 42 [Mus musculus]	133	50488	6.4	5.05	0.37	4.81
15	gil51092293	keratin 77 [Mus musculus]	127	61379	5.4	7.74	0.23	2.99
16	gil6680604	keratin 16 [Mus musculus]	124	51973	4.7	5.13	0.28	3.64

17	gil71043961	trypsinogen 7 [Mus musculus]	123	27089	4.9	8.22	0.12	1.56
18	gil145580629	keratin Kb40 [Mus musculus]	121	114018	1.3	8.36	0.06	0.78
19	gil22164776	keratin 6L [Mus musculus]	108	57802	3.6	7.55	0.12	1.56
20	gil82933144	PREDICTED: coiled-coil domain containing 6 isoform 1 [Mus musculus]	103	53077	10.7	6.87	0.2	2.60
21	gil6680606	keratin 19 [Mus musculus]	100	44515	9.2	5.28	0.15	1.95
22	gil28395018	junction plakoglobin [Mus musculus]	96	82490	2.7	5.75	0.08	1.04

23	gil40556608	heat shock protein 1, beta [Mus musculus]	92	83571	2.2	4.97	0.08	1.04
24	gil84781771	trypsin 10 [Mus musculus]	70	26888	10.6	5.5	0.26	3.38
25	gil94367594	PREDICTED: similar to orthologue of H. sapiens chromosome 20 open reading frame 119 (C20orf119) [Mus musculus]	65	64975	4.3	8.32	0.1	1.30
26	gil16716583	transducin-like enhancer protein 6 [Mus musculus]	43	65930	5.3	5.67	0.05	0.65

27	gil30410752	hypothetical protein LOC241943 [Mus musculus]	36	62199	1.5	8.95	0.05	0.65
28	gil30520043	hypothetical protein LOC210757 [Mus musculus]	34	73362	1.6	5.77	0.04	0.52
29	gil58037397	zinc finger protein 509 [Mus musculus]	32	84862	0.7	7.99	0.04	0.52
30	gil134948762	protein tyrosine phosphatase, non-receptor type 13 [Mus musculus]	32	271947	0.5	5.93	0.01	0.13
31	gil30424697	genethonin 1 [Mus musculus]	30	36219	5.3	5.62	0.09	1.17

32	gil23510259	a disintegrin and metallopeptidase domain 32 [Mus musculus]	30	86035	1.1	6.77	0.04	0.52
33	gil31981842	3-hydroxy-3-methylglutaryl-Coenzyme A synthase 1 [Mus musculus]	30	58160	5.8	5.65	0.06	0.78
							7.69	100